

THE STUDY OF A MAGNESIUM WIRE FEEDING
TECHNIQUE FOR THE DESULPHURIZATION OF
MOLTEN IRON AND LIQUID STEEL

by

ENZO A. PALUMBO

A Thesis Submitted to the Faculty of Graduate Studies and Research
in Partial Fulfilment of the Requirements for the Degree of
Master of Engineering

Department of Mining and Metallurgical Engineering
McGill University
- Montreal, Canada

©September 1985

1

ABSTRACT

The present study was divided into two parts. In the first part, 3.2mm diameter magnesium wires, insulated with powdered glass and enclosed in metallic sheaths, were immersed in molten metal baths at 1400°C and 1600°C. When the magnesium wires were immersed, violent and periodic eruptions were encountered. The study revealed that the primary cause of the eruptions was the inability of the glass powder to remain intact as the wires were immersed. In the second part, magnesium wires were insulated by wrapping them with glass tape. Relationships between penetration depths and insulation thicknesses for magnesium and aluminum cores were obtained for two types of glass tape. It was found that the penetration depth increased with increasing insulation thickness while the degree of pyrothermic display decreased. The study also showed that, with the appropriate insulation thickness and immersion speed, the eruptions could be totally eliminated.

A simple mathematical model simulating the radial heat flow to a composite cored wire was developed. It was used to predict the melting times of magnesium wires with various insulation thicknesses. The results of the experimental investigations were found to be in good agreement with those predicted by the model.

Furthermore, magnesium tests showed that recoveries of over 65 percent were consistently obtained with thicknesses greater than 2.65 mm, provided that the bath was stirred.

RESUME

L'étude a été effectuée en deux étapes. Dans la première étape, des fils de magnésium d'un diamètre de 3.2 mm isolés avec du verre en poudre et enveloppés dans une gaine métallique ont été immergés dans des bains métalliques en fusion à des températures de 1400° C et 1600°C. Lors de l'immersion de ces fils, des éruptions périodiques et violentes ont été observées. L'étude a montré que l'incapacité du verre en poudre de demeurer intact lors de l'immersion, était la cause principale des éruptions. Dans la deuxième étape, les fils de magnésium ont été isolés en les enveloppant avec du ruban de verre. Des relations entre la profondeur de pénétration et l'épaisseur de l'isolation pour des fils de magnésium et aluminium ont été développées pour deux types de ruban de verre. Les résultats ont montré que la profondeur de pénétration du fil augmente avec une augmentation de l'épaisseur de l'isolation alors que la sévérité des éruptions diminue. L'étude a également démontré qu'avec une épaisseur d'isolation et vitesse d'immersion adéquates, les éruptions peuvent être complètement éliminées.

Un modèle mathématique simple a été développé afin de simuler le transfert radial de chaleur dans un fil composite. Les temps de fusion des fils de magnésium en fonction des épaisseurs d'isolation ont été calculés à partir du modèle.

Les résultats expérimentaux de l'étude concordent avec les résultats du modèle mathématique. Finalement, les essais avec le magnésium ont montré qu'une récupération de plus de 65 pourcent du magnésium est possible avec une épaisseur d'isolation d'au moins 2.65 mm et lorsque le bain est agité.

ACKNOWLEDGEMENTS

The author wishes to extend his sincere gratitude to Dr. F.A. Mucciardi, director of this research project, for his guidance, helpful suggestions, and the countless hours of discussions on the present work.

The author would also like to thank Mr. R. Paquette for his assistance in conducting the experiments, Mr. M. Knoepfel for his aid in the preparation of the samples, and the staff and graduate students of the department of Mining and Metallurgical Engineering for making my two years at McGill University enjoyable.

Finally, the author wishes to thank the Natural Sciences and Engineering Council of Canada and Stelco Inc. for their financial support.

v

TABLE OF CONTENTS

<u>Contents</u>	<u>Page</u>
ABSTRACT	i
RESUME	ii
ACKNOWLEDGEMENTS	iv
LIST OF FIGURES	vii
LIST OF TABLES	xiii
LIST OF APPENDICES	xiv
CHAPTER 1. INTRODUCTION	1
1.1 Preliminary Remarks	2
1.2 External Desulphurization	2
1.2.1 Advantages of External Desulphurization	2
1.2.2 Prerequisites for External Desulphurization	4
1.3 Commercially Used External Desulphurization Techniques	6
1.3.1 Desulphurization with Soda Ash	6
1.3.2 Desulphurization with Calcium Based Reagents	9
1.3.2a Powder Injection	9
1.3.2b Wire Feeding	16
1.3.3 Magnesium Based Reagents	19
1.3.3a Bulk Additions	21
1.3.3b Dispersed Injection	24
1.3.3c Wire Feeding	31
1.4 Present Work	35
CHAPTER 2. PREVIOUS WORK	41
2.1 Paper Tape Insulation	41
2.2 Polyethylene Tubing Insulation	42
2.3 Pyrex Tubing Insulation	43
2.4 Soda-lime Insulation	44
CHAPTER 3. GLASS	49
3.1 Structure	49
3.2 Broad Classification of Glass Types	57
3.2.1 Chemical Composition	57
3.2.2 Physical Forms	60
3.2.2a Flat Glass	60
3.2.2b Holloware and Glass Tubing	60
3.2.2c Glass Foam	61
3.2.2d Glass Fibers	61
3.2.2e Glass Powders	65

<u>Contents</u>	<u>Page</u>
3.3 Viscosity	67
3.4 Thermal Properties	70
3.4.1 Thermal Conductivity	70
3.4.2 Heat Capacity	70
CHAPTER 4. EXPERIMENTAL	73
4.1 Apparatus	73
4.1.1 Induction Furnace	73
4.1.2 Wire Feeder	73
4.1.3 Data Acquisition System and Transducers	77
4.2 Materials	79
4.2.1 Core Wires	79
4.2.2 Insulating Materials	79
4.2.3 Metal Sheathing	82
4.2.4 Thermocouples	82
4.2.5 Molten Baths	86
4.2.6 'Dummy' Bars	86
4.3 Procedure	87
4.3.1 Preparation of Glass Powder Insulated Samples	87
4.3.1a Preparation of Glass Powders	90
4.3.2 Preparation of Glass Tape Insulated Samples	92
4.3.3 Hand-Dipping Experiments	92
4.3.3a Qualitative Tests	94
4.3.3b Heat Transfer Tests	94
4.3.4 Temperature Profile and Pyrotechnic Tests	96
4.3.5 Pyrotechnic and Volatility Experiments	97
4.3.6 Desulphurization and Recovery Experiments	98
CHAPTER 5. RESULTS AND DISCUSSION	99
5.1 Part 1- Glass Powder Insulation	99
5.1.1 Dipping Experiments	99
5.1.2 Heat Transfer Tests	108
5.1.3 Temperature and Pyrotechnic Tests	122
5.2 Part 2- Glass Tape Insulation	138
5.2.1 Heat Transfer Tests	138
5.2.1a Aluminum Core	138
5.2.1b Magnesium Core	147
5.2.2 Temperature and Pyrotechnic Tests	153
5.2.3 Pyrotechnic and Volatility Tests	166
5.2.4 Desulphurization and Recovery Tests	174
5.2.4a Desulphurization	174
5.2.4b Magnesium Recovery Tests	180
CHAPTER 6. SUMMARY AND CONCLUSIONS	181

LIST OF FIGURES

<u>Figures</u>	<u>Page</u>
1.1 Schematic of KR Reactor (1. hot metal ladle, 2. impeller, 3. dust collecting hood, 4. chute for desulphurizing agent, 5. dust catcher.)	12
1.2 Schematic of plunger bell assembly.	22
1.3 Schematic of IRSID injection lance equipped with double-flow circuit. a.) outside view, b.) schematic view of the double-flow circuit arrangement.	27
1.4 Schematic representation of a torpedo car with splash plug.	30
1.5 T-shaped lance that was developed for the injection of magnesium granules.	32
1.6 Schematic of ladle and orifice.	34
1.7 Schematic of wire feeding process.	36
2.1 Conceptual illustration of how the soda-lime insulated magnesium wire system was expected to work.	46
2.2 Viscosity-temperature curve of a typical soda-lime silicate glass.	48
3.1a- Two-dimensional representation of a metal oxide in 3.1b a.) the crystalline form b.) the glassy form.	52
3.2 Aluminum in a silicate network. (The structure is shown in a simplified form; the true structure is three-dimensional.)	53
3.3 Reaction between sodium oxide and silica tetrahedra. (For simplicity, a two-dimensional representation of the SiO_4 groups is given.)	55
3.4 Two-dimensional representation of the structure of soda-silica glass.	55
3.5 The effect of adding CaF_2 to silicate glass.	56

<u>Figures</u>	<u>Page</u>	
3.6	Typical viscosity-temperature curves for soda-lime glass and some commercial mold fluxes.	68
4.1a- 4.1b	Photographs of a.) furnace controls, b.) induction furnace.	74
4.2a	Photograph of wire feeder.	75
4.2b	Schematic drawing of wire feeder.	76
4.3	Schematic drawing of a compression type accelerometer.	78
4.4	Photograph of a roll of Mudge, Watson tape.	84
4.5	Schematic of a metal sheathed composite magnesium wire sample showing the dimensions of the various sections.	88
4.6	Schematic of the centering device.	89
4.7	Photograph of a typical glass powder insulated sample.	91
4.8	Photograph of typical glass tape insulated samples.	93
5.1	Typical dipping samples used for qualitative experiments.	100
5.2	Soda-lime powder samples. Sample 1A was immersed for a period of 30 seconds at a temperature of 1350°C while sample 1B was immersed for 40 seconds at 1400°C.	102
5.3	Photograph of a soda-lime powder sample showing that the molten aluminum had been contained within the glass framework.	103
5.4	Photograph of samples containing no.3 insulating powder. Sample 3A was immersed for a period of 30 seconds at 1400°C while sample 3B was immersed for 25 seconds.	104
5.5	This photograph shows sample 3A after the glass shell was broken off.	105

<u>Figures</u>	<u>Page</u>
5.6 Photograph of samples containing powder FM408 after they were immersed for 25-30 seconds at 1400°C.	106
5.7 Photograph of samples containing powder FM914 after they were immersed for 25-30 seconds at 1400°C.	107
5.8 Photograph of a sample containing powder no.5 after it was immersed for 30 seconds at 1400°C.	109
5.9 Typical temperature trace for a sample containing powder FM907 that was immersed in a bath at 1350°C.	111
5.10 Typical temperature trace for a sample containing soda-lime powder that was immersed in a bath at 1350°C.	112
5.11 Typical trace for a sample containing powder FM907.	113
5.12 This photograph shows the remains of a typical sample containing soda-lime powder.	115
5.13 Two typical temperature traces for soda-lime powder.	116
5.14 Photograph of a typical sample containing powder FM938 after it was immersed for 60 seconds.	117
5.15 Typical temperature trace for a sample containing powder FM938.	119
5.16 Photograph of the remains of a composite sample containing powder 1693.	120
5.17 Typical temperature trace for a sample containing powder 1693.	121
5.18 The effect of a 5 second immersion on a sample containing powder 1693.	123
5.19a Typical temperature traces for a sample containing powder 1693. The powder was dried in a drying furnace prior to being packed in the metal sheathing.	124
5.19b Typical temperature traces for a sample containing powder 1693. The powder was not dried prior to being packed in the metal sheathing.	125

<u>Figures</u>	<u>Page</u>
5.20a- Photographs of typical eruptions. 5.20b	127
5.21 Temperature and photocell traces for sample MG1693.	128
5.22 Temperature and photocell traces for sample LMF3/8.	130
5.23 Temperature and photocell traces for sample M81963.	131
5.24 Temperature traces for sample 1AF3/8.	132
5.25 Temperature and photocell traces for sample 34MS2.	135
5.26 Temperature and photocell traces for sample 34MS1.	136
5.27a Typical temperature traces for a composite aluminum sample insulated with Ajax tape. The bath temperature was 1600°C.	139
5.27b Typical temperature traces for a composite aluminum sample insulated with Mudge, Watson tape. The bath temperature was 1400°C.	140
5.28 A photograph of typical glass tape insulated samples.	141
5.29 A plot of aluminum melting times versus insulation thickness for both Ajax and Mudge, Watson tapes.	142
5.30 Theoretical aluminum melting times versus . insulation thickness for bath temperatures of 1400°C and 1600°C.	144
5.31a- These photographs show two typical aluminum 5.31b composite samples that bent upwards when they were immersed in a pig iron bath.	146
5.32 A plot of melting times versus insulation thickness for samples containing Mg cores.	148
5.33 Comparison of melting times between magnesium and aluminum samples insulated with Mudge, Watson tape.	149

<u>Figures</u>	<u>Page</u>
5.34 Comparison of melting times between magnesium and aluminum samples insulated with Ajax tape.	150
5.35 Melting time results for Mg composite samples that were immersed in a bath at 1600°C. The samples were insulated with Ajax tape.	152
5.36- Typical traces for tests conducted at 1400°C with 5.39 various thicknesses of Ajax tape.	154
5.40 Typical temperature and photocell traces for a Mg composite sample tested at 1600°C.	159
5.41 Typical temperature and photocell traces for an Al composite sample tested at 1600°C.	160
5.42 Temperature and photocell traces for a Mg composite sample that bent upwards and released Mg close to the bath surface.	161
5.43- Temperature and photocell traces of Mg composite 5.45 samples that were insulated with various thicknesses of Mudge, Watson tape. All were fed at different speeds.	163
5.46 A typical accelerometer and photocell trace showing violent and periodic explosions. These traces were obtained from work conducted previously.	167
5.47 Typical accelerometer and photocell traces for a sample insulated with 4,6mm of Mudge, Watson tape.	170
5.48 Traces for the case when two composite samples were simultaneously fed into a pig iron bath.	172
5.49 Typical photocell and accelerometer traces for a bare magnesium wire.	173
5.50 Typical photocell and accelerometer traces for a sample that had 1.45mm of Ajax tape insulation.	175
5.51 Dependence of the sulphur partition coefficient on the slag basicity.	179

<u>Figures</u>		<u>Page</u>
A.1	Plot of magnesium melting times versus insulation thickness for bath temperatures of 1400°C and 1600°C. These curves were calculated using a heat transfer model. The diameter of the magnesium core was 3.2mm.	191
A.2	Plot of magnesium melting times versus insulation thickness for a 15.9mm diameter magnesium rod.	193
A.3	Schematic of composite sample with temperature profiles. The composite sample consisted of a 3.2mm diameter Mg wire insulated with 3.0mm of glass tape.	194
A.4	Schematic of composite sample with temperature profiles. The composite sample consisted of a 15.9mm diameter Mg rod insulated with 3.0mm of glass tape.	195
A.5	Temperature traces of a 15.9mm Al rod insulated with 3.0mm of glass tape.	197

LIST OF TABLES

<u>Table</u>		<u>Page</u>
3.1	CHEMICAL COMPOSITIONS OF COMMON COMMERCIAL GLASSES	60
3.2	CHEMICAL COMPOSITIONS OF GLASS FIBERS	64
3.3	COMPOSITIONS AND VISCOSITIES OF TYPICAL MOLD POWDERS	66
3.4	OXIDE FACTORS FOR CALCULATION OF MEAN SPECIFIC HEAT	72
4.1	COMPOSITIONS AND VISCOSITIES OF EXPERIMENTAL POWDERS	81
4.2	CHEMICAL COMPOSITIONS OF TAPES	83
4.3	SHEATHING DIMENSIONS	85
5.1	DESULPHURIZATION RESULTS	177
5.2	RECOVERY RESULTS WITHOUT STIRRING	181
5.3	RECOVERY RESULTS WITH STIRRING	182

LIST OF APPENDICES

APPENDIX

Page

APPENDIX A
APPENDIX B

190
205

CHAPTER 1
INTRODUCTION

1.1 Preliminary Remarks

In the steel industry, the quality of a steel product is improved by eliminating or minimizing the concentration of harmful impurities such as sulphur. The trend in recent years has been towards more stringent sulphur specifications.

Nowadays, steels must be produced to sulphur levels of 0.02% or lower, and for very demanding applications, such as seamless tubes for oil drilling, the required sulphur levels can be as low as 0.005-0.008%.

Much of the sulphur can be removed in the blast furnace operation. The blast furnace operates under high temperature and highly reducing conditions. Under these conditions the blast furnace slag is an effective desulphurizer. However, the blast furnace operation becomes increasingly expensive if required to produce very low sulphur contents in the pig iron. Moreover, obtaining pig iron with sulphur contents lower than 0.01% is generally considered impossible. Furthermore, in recent years many countries have experienced a deterioration in the quality of raw materials, particularly in the content of sulphur and alkalis in the coke. Lowering the sulphur content of pig iron under these constraints has led many steel producers to desulphurize the hot metal externally (i.e. outside the blast furnace) in order to meet the stringent requirements.

Another factor which led to the increased importance of

external desulphurization was the replacement of the open hearth process by the basic oxygen furnace (B.O.F.) process which occurred in the same time frame as the trend toward progressively more stringent sulphur specifications. The B.O.F. removed much of the flexibility in hot metal/scrap ratios that existed under the open hearth practice. In addition, the large reduction in heating time and the more highly oxidized slags made the B.O.F. process more sensitive to hot metal sulphurs.

The external desulphurization of pig iron is not a recent development. It had been used for many years, but only selectively for reducing the hot metal sulphur content to 0.02-0.03%. The cheapest and most readily available reagents such as sodium carbonate and lime were used. The methods of adding the reagents into the metal were primitive (i.e. manually adding the reagents to the iron runners and/or the ladle), the degree of utilization was low, and the specific consumption was very high. But as the importance of external desulphurization has increased, the search for new reagents and the development of new and more efficient methods of introducing them into hot metal has become of major interest to many steel producers.

1.2 External Desulphurization

1.2.1 Advantages of External Desulphurization

Although many steel producers have adopted external desulphurization because of raw material constraints and restrictive steel sulphur specifications, external desulphurization can also result in substantial economic and

operational benefits.

By relieving the blast furnace of a portion of its sulphur removal task, external desulphurization allows the blast furnace to operate at a lower slag basicity. It has been known for many years that burdening for a less basic slag increases productivity and a leaner flux rate results in an increased solubility of bosh alkalis (mainly K_2O and Na_2O). A furnace operating at a high slag basicity tends to accumulate solid sodium and potassium compounds in the cooler section of the furnace which results in a restriction of gas flow through the burden and an erratic descent of the charge⁵³. In other words, lower basicity slags result in a more permeable burden and a smoother operating furnace.

In 1974, Dofasco conducted a fundamental investigation to determine the effects of operating a blast furnace with a less basic slag coupled with external desulphurization⁵⁴. This investigation was conducted over a two week period. The slag basicity was lowered to 1.02 from the usual 1.17. The major furnace parameters such as silicon, manganese, and carbon were held constant at 1.02%, 1.42%, and 4.75%, respectively. The thermal condition of the furnace was controlled by adjusting the pellet consumption and the silicon content was kept constant by adjusting the hot blast humidity. The manganese content was maintained by controlling the consumption of Wabush pellets.

The lower slag basicity was achieved by reducing the flux rate which resulted in an increased solubility of bosh alkali. Eighty percent of the alkali (K_2O) was removed with the slag

compared to 58% during normal furnace operation. To eliminate the accumulation of alkalis in the furnace, over 60% of the alkalis should be removed in the slag.

Other operating parameters that were affected are as follows:

- 1.) The blast pressure decreased, thus increasing gas permeability.
- 2.) The blast consumption increased by 7%.
- 3.) The blast furnace productivity increased by 13%.
- 4.) The consumption of coke decreased by 8.8 %.
- 5.) The slag volume decreased as a result of a 27% decrease in flux consumption.
- 6.) The temperature of the pig iron dropped from 1510⁰C to 1490⁰C.

The 13% increase in furnace productivity was attributed to the increased blast consumption and the reduced coke rate. Furthermore, the investigation indicated that operating with a lower slag basicity may make it possible to use cheaper raw materials that contain previously unacceptable sulphur and alkali contents. Finally, the investigation concluded that the cost of desulphurization amounted to 69% of the savings to the blast furnace. Investigations conducted at other steel plant installations have shown similar results².

1.2.2 Prerequisites for External Desulphurization

When a steelmaker decides to desulphurize externally, there are several factors which must be considered. These factors include the choice of reagents and the methods of introducing the reagents, the cost of the various methods, the environmental problems the methods may create, and the material handling procedures that may be required.

The ideal reagent should be soluble in molten iron or steel and have a strong affinity for sulphur. It should be low in cost, however, the cost of the addition practice, slag handling practice, and fume collection system should be kept in mind. Furthermore, the reagent should react in a non-violent manner and should not yield any objectionable fumes, dust, and vapors.

In order to obtain high desulphurization efficiencies and more importantly reproducible results, certain criteria must be fulfilled for any particular desulphurization method. These are outlined below.

- 1.) There must be a rapid rate of reaction between the desulphurizing reagent and the sulphur bearing iron or steel. This may require the use of appropriate stirring techniques.

- 2.) The oxygen potential of the slag/metal system must be as low as possible. In the case of blast furnace hot metal, this is not a problem as the hot metal is saturated with respect to carbon. However, in the case of steel, strong deoxidizers often have to be used.

- 3.) The desulphurizer reaction slag should be fluid, highly basic, low in volume, and of low iron oxide content.

- 4.) When desulphurized hot metal is transferred to the steelmaking vessel, it is essential that a minimum amount of sulphur containing slag be transferred along with the hot metal. Otherwise, the oxidizing conditions generated during steelmaking will cause the sulphur to revert to the metal phase.

To date, none of the existing desulphurizing methods offer a good solution to all the production, metallurgical, and economic factors raised by the iron-sulphur problem. As a result, there is no uniformity in desulphurization technology amongst the steel producers around the world.

1.3 Commercially used External Desulphurization Techniques

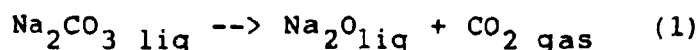
The most commonly used reagents for external desulphurization of hot metal are calcium and magnesium based reagents. However, for many years soda ash (Na_2CO_3) was used because of its easy accessibility and low cost. Although there are many problems associated with the use of soda ash, it is still being used to some degree in such countries as the United States, France, Belgium, and Japan.

In the following sections, the various desulphurizing reagents and methods of introducing them into the hot metal will be presented.

1.3.1 Desulphurization with Soda Ash

For many years iron was desulphurized by the addition of soda ash in the blast furnace runners or in the hot metal stream during tapping from the torpedo cars into the hot metal charging ladle. Now, lance injection methods are used.

At high temperatures, sodium carbonate decomposes as follows:



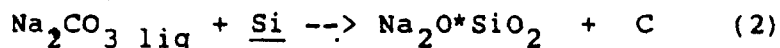
The sodium oxide that is generated has a high chemical affinity for sulphur and the gases produced contribute to the mixing of the hot metal with the slag. Desulphurization of the hot metal is essentially finished when dense smoke begins to form. This indicates a significant chemical reduction of the sodium oxide. The desulphurizing effectiveness of soda ash decreases with increasing temperature. Consequently, it is preferred that the temperature be kept low, and at the same time, it must be ensured that the temperature is not too low for subsequent processing.

Although sodium carbonate (soda ash) is quite cheap, the trend in the past decade towards lower sulphur requirements in steels and the deteriorating quality of raw materials has caused soda ash to lose popularity to calcium and magnesium based reagents for the following reasons. First, sulphur removal with soda ash is more sensitive to temperature than any other method, making desulphurization efficiencies unpredictable. Second, the alkaline slags emanating from the use of soda ash are extremely corrosive with respect to most types of refractories. Third, the consumption of soda ash increases dramatically with decreasing sulphur levels. This increasing specific consumption is a shortcoming of all reagents. However with soda ash, the consumption can increase to unacceptable levels. For example, to lower the sulphur content of molten metal to 0.01% S, approximately 2.5-3.0 kg of calcium carbide per 0.01% drop in sulphur may be required whereas with soda ash more than 6 kg may be required. The high consumption results in the production of a large quantity of slag. This is undesirable because the higher the slag volume the higher the hot metal losses. Moreover, it also creates slag handling problems. Fourth, the fine particles of Na_2O that are released into the surrounding area during the treatment process can cause considerable irritation to the skin, especially during hot humid days. Finally, the large volume of carbon monoxide gas that is produced during the soda ash treatment can burn within the dust collection system, causing considerable damage. The waste gases often have to be cooled before entering the bag filters, and, as a precautionary

measure, restrictions are imposed on the amount of soda ash that can be used per treatment.

In Japan, soda ash is still extensively used for hot metal treatment. A major concern of Japanese steelmakers is their dependence on relatively high phosphorous iron ores. The recent stringent restrictions on both sulphur and phosphorous contents in steel has forced the Japanese to develop processes to treat both sulphur and phosphorous. With the present state of technology, it appears that sodium carbonate is the only reagent that is known to be effective in the simultaneous dephosphorization and desulphurization of hot metal.

The Japanese steel producers inject powdered soda ash into the hot metal through a submerged lance. Prior to the soda ash treatment, the hot metal is desiliconized. Studies have shown that the degree of dephosphorization increases as the initial dissolved silicon content decreases⁵⁵. The reaction of soda ash with dissolved silicon and silica takes precedence when the dissolved silicon is high. The silicon in the hot metal reduces the available sodium carbonate for dephosphorization as follows:



The dissolved silicon can be reduced by the injection of oxygen or powdered iron oxide.

Other advantages of desiliconization include decreased slag volumes, increased iron yields, reduced converter lining damage from silica rich slags, and increased converter productivity due to reduced slopping. Hence, soda ash treatment becomes more attractive when preceded by desiliconization. However, since

North American steel producers do not have a phosphorous problem, they have opted for alternative desulphurizing reagents rather than desiliconizing prior to using soda ash. Nonetheless, it should be noted that the desiliconization of hot metal is now being given serious consideration by North American producers for the alternative advantages outlined above.

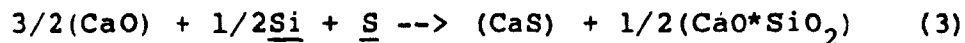
1.3.2 Desulphurization with Calcium Based Reagents

1.3.2.a Powder Injection

Lime Injection

Lime has long been used for the desulphurization of iron due to its unlimited supply and relatively low cost just as sodium carbonate. However, because of its slow reaction rate, it is seldomly used alone as a desulphurizer.

The removal of sulphur in hot metal by lime (CaO) is considered to take place according to either of the two following reactions:



At temperatures greater than 1500°C, carbon is a stronger reducer than silicon, whereas at temperatures lower than 1400°C, silicon is the stronger reducer in iron. Therefore, reaction (3) is considered to make a greater contribution to the desulphurization of the molten iron.

The slow reaction rate is considered to be attributable, on the one hand, to the solid-liquid phase reaction involved, and, on the other, to the fact that the sulphur removal reaction releases oxygen, which is fixed by silicon in the hot metal as

silica. This silica may lead to the formation of a layer of calcium silicate on the lime particles which adversely affects the diffusion of sulphur into the lime particles.

It is evident that in order to use lime as a desulphurizer, measures have to be taken to enhance the kinetics for its effective utilization. The obvious first step would be to ensure that the lime is finely crushed and uniformly dispersed in the molten iron bath. The lime can be uniformly dispersed by blowing powdered lime through a submerged lance with a carrier gas. The reason the lime should be finely crushed is that since the desulphurization reaction is a liquid-solid diffusion process, one would want to increase the reaction interface area. However, the lime should not be ground excessively fine. The reason for this is twofold; firstly, some of the smaller lime particles tend to be swallowed up by the dust collection system, thereby reducing the effective amount of reagent added, and secondly, a portion of the finest particles tend to agglomerate prior to injection, thus reducing the specific reaction area.

Other measures that have been taken to improve the efficiency of lime utilization include adding other compounds or elements with the lime that would either destroy or prevent the formation of the calcium silicate layer. One process developed by the Hoesch Company (FGR) involves the injection of powdered lime along with a hydrocarbon gas, usually methane². The oxygen released during the desulphurization process is thought to be reduced by the decomposition product (i.e. carbon) of the

hydrocarbon gas. Along the same lines, the Nippon Steel Corporation began using a lime-fluorspar-carbon (90% CaO, 5% CaF₂, and 5% coke) reagent in 1976 at their Hirohata Works¹¹. The desulphurization process was carried out in an impeller-stirred 100 ton 'KR' reactor as shown in Figure 1.1. The reagent was added by means of a chute located above the reactor, and the sulphur removal reaction was accelerated by impeller stirring. The role of the carbon, which was added in the form of coke breeze or oil coke, was to provide a reducing atmosphere at the reaction interface, while the function of the fluorspar was to increase the transport rate of the reaction products. A low purity fluorspar was used because it was believed that the presence of SiO₂ and Al₂O₃ lowers the melting point and viscosity of the reaction products, thus accelerating the separation rate of the reaction products and the reaction interface.

Prior to shifting to the lime-fluorspar-carbon reagent, the Hirohata Works used calcium carbide as the reagent. It was found that the cost of desulphurization with lime was less than half that of calcium carbide, but, the consumption of reagent more than doubled.

Yet another approach taken to improve the utilization of lime involves the addition of a deoxidizing agent that is stronger than silicon (such as Al, Mg, Ti, etc..) to the bath to prevent the formation of calcium silicate. This has led to the development of the lime-Al process. The lime-Al process is being used at the Aliquippa Works of the J&L Steel Corporation and the

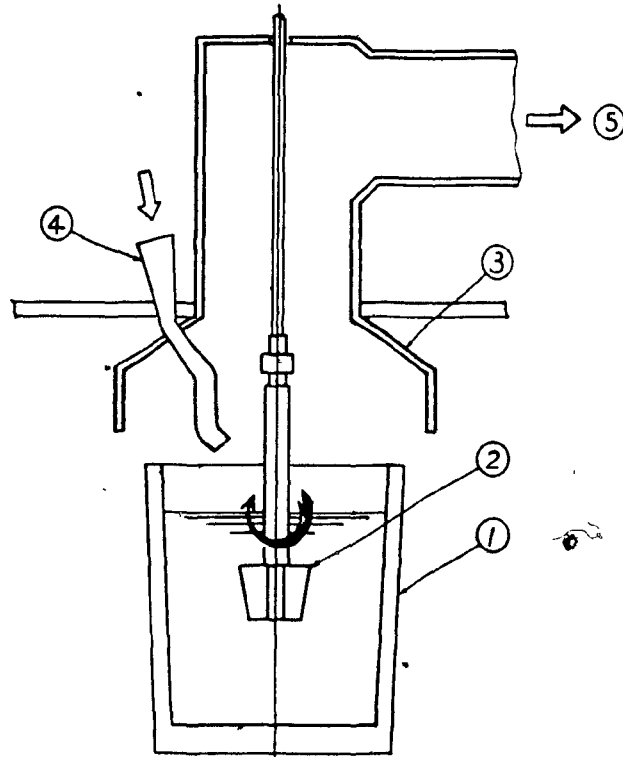


Figure 1.1. Schematic of KR Reactor (1. hot metal ladle, 2. impeller, 3. dust collecting hood, 4. chute for desulphurizing agent, 5. dust catcher.)

Solmer plant in France. In the lime-Al process, aluminum is added either before the injection of lime or simultaneously with the injection of lime. At the Solmer plant, aluminum is added at the casthouse during filling of the torpedo cars. At the Solmer plant, the hot metal can be desulphurized from 0.05% S to about 0.005% S with 6 kg/t of lime. Prior to using the lime-aluminum process the Solmer plant used calcium carbide. It was found that, all other factors being equal, the same sulphur removal ratio was obtained by replacing calcium carbide with the equivalent amount of lime (after adding aluminum to the hot metal). Thus using the lime-aluminum process is advantageous in terms of reagent cost. However, it was also found at the Solmer plant that the lime-aluminum process also contributes to a higher degree of skulling of the torpedo ladle pouring mouths. Therefore, the Solmer plant alternated between lime-Al and calcium carbide to minimize the degree of skulling and at the same time minimize costs⁵⁶.

Calcium Carbide

The use of calcium carbide for desulphurization of pig iron has been well established in the foundry industry since the 1950's. By the 1970's, the demand for low sulphur steel increased significantly. Since reproducible and reliable techniques for calcium carbide treatment had been already developed by the foundry industry, many steel producers adopted these techniques. Today, calcium carbide is still one of the most widely used desulphurizing reagents. The earliest applications of calcium carbide were lance injection techniques.

Calcium carbide has a high chemical affinity for sulphur and it reacts with sulphur in hot metal as follows:



Although the thermodynamic conditions for sulphur removal are favorable, the kinetics are not. Since calcium carbide is solid at molten iron temperatures (i.e. 1350°C), the reaction with sulphur can only take place on the surface of the calcium carbide particles. Moreover, the diffusion of sulphur into a calcium carbide particle is slow. In order to obtain efficient use of calcium carbide, the particles should be ground to a fine powder, not unlike lime, and they should be dispersed uniformly throughout the molten bath.

The effectiveness can be further enhanced if a mixture of calcium carbide and a gas generating compound such as calcium carbonate (CaCO₃) is injected into the molten iron. The release of gas should result in a gentle localized stirring within the bath. Studies have shown that the consumption of calcium carbide can be significantly reduced using this method¹².

Another method is to mechanically mix the calcium carbide with the molten iron. One such method is the 'KR' process developed by the Nippon Steel Corporation. In the 'KR' process, the calcium carbide is added to the surface of the molten iron in the transfer ladle after the slag is skimmed, then the calcium carbide is mixed with the iron with the aid of a refractory coated mixer-impeller. Studies have shown that the 'KR' process achieves a higher degree of reagent utilization than the injection of calcium carbide, with or without the

addition of calcium carbonate. The KR process would require about 2.75 kg/t of calcium carbide to decrease the sulphur level from 0.05% to 0.01% S, whereas the injection of carbide alone, and the injection of carbide with CaCO_3 would require about 7.5 kg/t and 4.0 kg/t respectively. Despite this fact, the KR process has not been adopted by other concerns. The reason for this is twofold; first, the KR process can only be carried out in the absence of blast furnace slag, and secondly, the impellers wear out quickly and cool the bath to a greater degree than the other methods.

An alternative method to the KR process is the 'Porous Plug' method. This method promotes desulphurization by rapidly changing the slag/metal interface. In this method, calcium carbide is added to the melt in a similar fashion to that of the KR method. However, instead of using an impeller to promote stirring, an inert gas such as nitrogen is injected through a porous heat resistant plug built into the bottom of the transfer ladle. This method appears to be more effective than the KR process, but, it also has not received wide acceptance.

Although calcium carbide has been extensively used as a desulphurizing reagent, it does have its shortcomings. First, when calcium carbide comes in contact with water or humidity it generates acetylene gas, which is highly explosive. Consequently, extreme care must be exercised when storing or handling it in order to avoid inadvertent exposure to moisture. Second, the carbide reaction slag must be skimmed after desulphurization since the slag often contains unreacted calcium

carbide. This can pose a major problem at the wet deking station. Third, the treatment with calcium carbide generates a large volume of slag with correspondingly high metal losses. And finally, the carbide particles that are emitted into the air during the loading of dispensers, or the desulphurization treatment itself, are particularly annoying. Not only does it have a putrid smell, it can also irritate the skin especially during periods of high atmospheric humidity.

1.3.2.b Wire Feeding

At present, calcium based wire feeding techniques for the desulphurization of molten iron are non-existent mainly because the available calcium based reagents are not suitable for wire feeding. First, the solubility of metallic calcium is less than 1 ppm at 1773 K²⁹, making it a poor desulphurizer. Second, reagents such as lime and calcium carbide, which are effective desulphurizers, require that the reaction surface area be maximized and that they be uniformly distributed throughout the bath. This can only be effectively accomplished by powder injection methods. Third, wires containing reagents such as calcium silicide (CaSi) are generally very expensive and cannot compete with existing powder injection techniques.

The main interest in the calcium wire feeding techniques has been in their excellent ability to modify non-metallic inclusions in steel^{20,21,57}. Powder injection methods, such as the TN process, are still the preferred methods when very low sulphur steels and high volume steel desulphurization is required.

Since calcium is a volatile metal (normal boiling point is 1492°C) having a low solubility and a density one-fifth that of steel, it is not possible to feed a pure calcium wire into a steel bath without it vaporizing and oxidizing close to the bath surface producing fumes of CaO particles. Consequently, the various calcium based wire feeding techniques in use at the present time use calcium wires that are covered by a thin steel sheath. This allows calcium to penetrate to such a depth that the pressure of the liquid steel suppresses the vaporization of the calcium, and, any vapor that does form will have sufficient time to react fully as it rises through the steel bath.

The advantages of using cored wires versus powder injection methods for steel treatment are as follows: 57,61,20

- 1.) Flexibility: Additions can be made at any location of the steel plant as only a relatively compact feeder is required. The wires can be fed into tundishes, ingot moulds, and ladles. Whereas, powder injection techniques can only be readily implemented when the ladles are large enough.
- 2.) Less agitation: This minimizes the possibility of contamination by hydrogen, nitrogen, and oxygen from the atmosphere.
- 3.) Better injection efficiency: In powder injection some of the particles become entrapped in gas bubbles, and rise to the surface without coming into contact with the liquid steel. This results in higher reagent consumption.
- 4.) Lower heat loss: Since no inert gases are used to homogenize the bath, the temperature losses are lower. Even if it is required, the inert gas flow rate would be independent of the quantity of reagent, and therefore, it would generally be lower for wire feeding.

5.) Lower investment cost: The investment for a coil loader and wire feeder is considerably lower than that for powder injection equipment and the problem of storing the powder is eliminated.

6.) Lower operating cost: The wire feeding equipment requires only one operator. Maintenance cost is lower as no costly injection lances are required and wear of ladle lining is lower.

The most commonly used calcium based wires are the AFFIVAL wire which was developed at the Saint Saulve steel works in Saint Saulve, France, the Pfizer Pferrocal wire which was developed by Pfizer Calcium Metal Products, and the Ferrokal wire which was developed in Japan.

Ferrokal is a composite wire consisting of a monolithic calcium or calcium-aluminum core. The sheath thickness is 0.2mm and the standard core diameters are 4.8 and 7.0mm. The Pfizer Pferrocal wire can consist of metallic calcium, CaSi, or Ca-Al cores with diameters of 5.4 and 8.0mm. The sheath thickness is 0.2mm for the 5.4mm diameter wire and 0.25 for the 8.0mm diameter wire. The AFFIVAL wires are rectangular in shape and come in various sizes. The sheath thicknesses range from 0.2mm to 0.4mm. The core material is usually CaSi, however, cores of other alloy additions are also produced. The reason the AFFIVAL wires are rectangular is that the time required to melt the wire is determined by its smallest dimension, this being its thickness. In other words, if a wire had a width that is twice that of another and had the same thickness, the time to melt them would be the same, provided that the width is larger than the thickness. Theoretically, one can feed twice as much reagent

to an equivalent depth simply by doubling the width while keeping all other parameters constant. In practice one would probably not double the feed rate by doubling the width because of the increased turbulence, nonetheless, one can increase the feed rate by increasing the width of the wire.

One problem with cored wires is that it is difficult to predict the actual behavior of the wire, especially the depth to which the wire penetrates the bath. When a wire is fed into a steel melt it is subjected to friction and buoyancy forces which tend to deflect it from the vertical. Consequently, knowing the time it takes the wire to melt, which in itself is difficult to determine, and the speed at which the wire is fed is not sufficient to determine the depth of penetration.

1.3.3 Magnesium Based Reagents

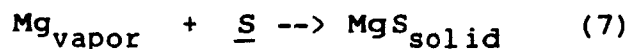
Magnesium has a strong affinity for both sulphur and oxygen and has been known to be an excellent desulphurizer for many years. From a thermodynamic point of view, magnesium has a higher desulphurizing ability than calcium oxide, but, slightly lower than that of calcium carbide in the temperature range of 1200-1550°C². However, since lime and calcium carbide are solid at molten iron temperatures, the desulphurization kinetics are relatively slow as compared to that of magnesium. This makes magnesium a more attractive desulphurizer.

Although the solubility of magnesium is relatively low, it is significantly higher than that of calcium. It is estimated that the maximum solubility of magnesium in carbon saturated

iron at 1773 K is about 0.26 wt%. This is based on the solubility data from Trojan and Flinn^{29,28,63}. Magnesium is also characterized by a low boiling point(1107°C) and a low density(1.74 g/cm³). Because of this, magnesium tends to vaporize when immersed in molten iron causing violent agitation of the melt as the vapor bubbles rise through the melt. At times, the violent agitation can result in ejection of hot metal from the vessel.

Magnesium is never added to the melt in pure form because of its volatile behavior. The violence of the reaction is often controlled by either diluting the magnesium with other agents or by applying a protective coating to the magnesium, which allows the magnesium to penetrate deep into the molten iron bath before any reaction can occur.

There is no common consensus as to what the predominant mechanism of magnesium desulphurization is. However, it is believed that it occurs in two modes. One is the homogeneous reaction of dissolved magnesium in the hot metal with dissolved sulphur (Eq.6) and the other mode is the interaction of magnesium vapor with sulphur at the bubble interfaces as the bubbles rise through the melt (Eq.7).



1.3.3a Bulk Additions

Mag-coke

The mag-coke process was developed by the American Cast Iron Company to be used in the foundry industry in the production of nodular cast iron. By the 1970's, the mag-coke process became the most widely used process for desulphurizing pig iron in the steel industry.

In the mag-coke process, a cylindrical can containing coke impregnated with 45% magnesium is loaded into a bell-shaped plunger assembly as shown in Figure 1.2. The plunger assembly is then fed into liquid iron, usually contained in a torpedo car, and kept there until all the magnesium is consumed.

The vaporization of magnesium provides good mixing of the metal and improves the desulphurization process. However, the vigorous agitation of the melt proceeds for only a few minutes and then it retards to a steady boil of the metal².

The widespread use of mag-coke in the 1970's can be attributed to several attractive features of the process:

- 1.) The low specific consumption of magnesium, which was considerably lower than lime, CaC_2 , and NaCO_3 , contributed to much lower slag volumes.
- 2.) Very little capital expenditure was required.
- 3.) Mag-coke was supplied in packages convenient for application.

In spite of these attractive features, mag-coke had several shortcomings which eventually led to the abandonment of the process. First, the high cost of mag-coke outweighed the cost

PLUNGER BELL ASSEMBLY

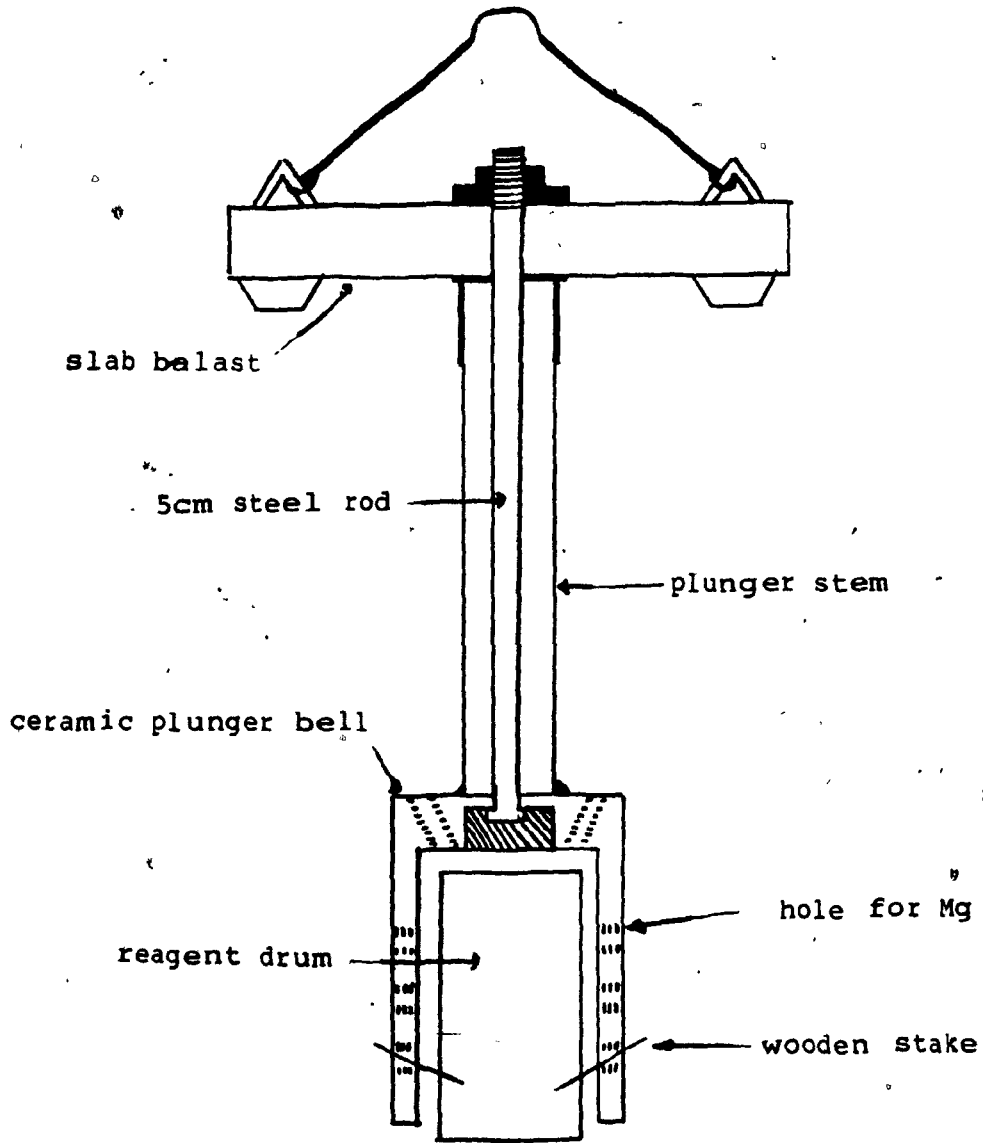


Figure 1.2. Schematic of plunger bell assembly.

savings due to the lower consumption. Second, because of the relatively low durability of the plunger bell assembly (about 17-20 plunges), maintenance costs were quite high. Third, since a constant quantity of mag-coke was charged into the bell, it was not always possible to consume the calculated amount of mag-coke required for a particular torpedo car. This often led to an excess consumption of mag-coke. Finally, as the demand for desulphurized iron increased, it became apparent that its use for volume production was limited on account of it being a batch process. Since the hot metal treatment was carried out in torpedo cars, the dimensions of the bell assembly were dependent on the small diameter of the torpedo car's neck. In many instances the torpedo car could not be desulphurized to the desired level with one 'dunk'. At times as many as five 'dunks' were required which resulted in treatment times in excess of two hours.

Numerous other bulk addition reagents had been tried, but none of them were effective or received widespread use. The most notable reagents were magnesium-dolomite briquettes and pure magnesium ingots coated with a heat resistant material^{9,2,64}.

Another bulk addition reagent called MAGFAX has been recently developed by Foseco. MAGFAX is applied in the form of a magnesium impregnated non-consumable refractory sleeve which slides over a dummy stopper rod. MAGFAX has been used for the treatment of steel to reduce the number of inclusions and to alter their distribution²⁸.

1.3.3.b Dispersed Injection

Magnesium Powder

The Soviet Union began experimenting with magnesium powder injection in 1965. In these experiments, powdered magnesium was introduced into liquid iron by a stream of compressed air blown through an immersed lance. Initial tests indicated that nozzle clogging was a major problem². It was found that the problem was eliminated when lime was injected along with the magnesium in a ratio of 2:1. The purpose of the lime was to shield the powdered magnesium from the thermal radiation of the liquid iron and to clean out the lance outlet if any magnesium accumulated there. The magnesium-lime mixture was premixed in a mixer bin. Compressed air was blown through the bottom of the bin to mix the magnesium and lime thoroughly. The mixture was then pneumatically charged into the feed bins. With this type of system it was difficult to maintain a homogeneous mixture, and, it was found that the homogeneity of the mixture strongly affected the success of the hot metal treatment. Inhomogeneous mixtures led to lance vibration, nozzle clogging, and surges of metal splashing.

A variation of the magnesium-lime injection techniques is the Lime-Mag process, which was developed by Jones and Laughlin Steel. The process differs from the Soviet method in that the lime and magnesium are fed separately from the feed bins to the transport line. This allows for better control of the lime-magnesium mixture. The magnesium content of the lime-magnesium mixture is about 30%.

According to Voronova², the sulphur removal reaction can be described as follows:



Both lime and magnesium act as desulphurizers, with magnesium playing a dual role of desulphurizer and deoxidizer. Since magnesium is a stronger deoxidizer than silicon, it prevents the lime from being consumed to form calcium silicate. Furthermore, the lime particles contribute to the efficiency of the process by breaking down the magnesium bubbles in the melt, allowing them to dissolve much faster. The main disadvantage of the lime-mag process is that it produces a large volume of slag. Along with the large slag volume is a high loss of metal in the slag. This is common to all calcium based reagent processes.

Prior to the lime-mag process, Jones and Laughlin had used the magnesium-aluminum system. The reagent consisted of 75% Mg and 25% Al. The purpose for the aluminum was to reduce nozzle clogging, however, the aluminum significantly increased the cost of the contained magnesium. Although its variability in chemical efficiency was less than with other injection techniques, its reaction violence was more vigorous than any process in use. As a result, the mouths of the torpedo cars had to be protected with an inexpensive gunning refractory which prevented the hot metal splashes from contacting the steel shell of the torpedo car. Moreover, the injection lances had to be replaced frequently due to breakage caused by the vigorous action of the vaporizing magnesium.¹⁰

Another magnesium powder injection method is the USIRMAG 2 process which is used at the Usinor Dunkirk works. The desulphurizer for this process consists of magnesium powder mixed with a granulated basic slag, with magnesium forming 90 percent of the mixture. This granulated basic slag has been patented by Usinor-Sofrem. The USIRMAG 2 process utilizes the IRSID 'double flow' lance shown in Figure 1.3. The inner circuit, which consists of the powdered desulphurizer and 30 percent of the injected gas, flows at a low speed through a central tube while the outer circuit, consisting of the remaining 70 percent of the injected gas, acts as a thermal shield for the powder injected through the central tube. The gas speed of the outer circuit ranges from 100-200 m/s. The two circuits are combined just before they enter the hot metal. At the point of merger, the gas is squeezed. This prevents the magnesium powder from contacting the hot nozzle walls, thus avoiding nozzle clogging.

The USIRMAG 2 process has allowed the Usinor Dunkirk plant to obtain highly predictable end sulphurs with relatively low reagent consumption. For instance, to lower the sulphur content of the hot metal from 0.025% to 0.005% S requires 0.46 kg/t of magnesium.

Given the fact that the desulphurizing powder contains 90% magnesium, the amount of slag produced during a treatment process is minimal compared to that produced by the lime-mag process. However this process has not spread to other plants probably because of the cost and availability of the premixed reagent and the fact that a modified lance has to be used.

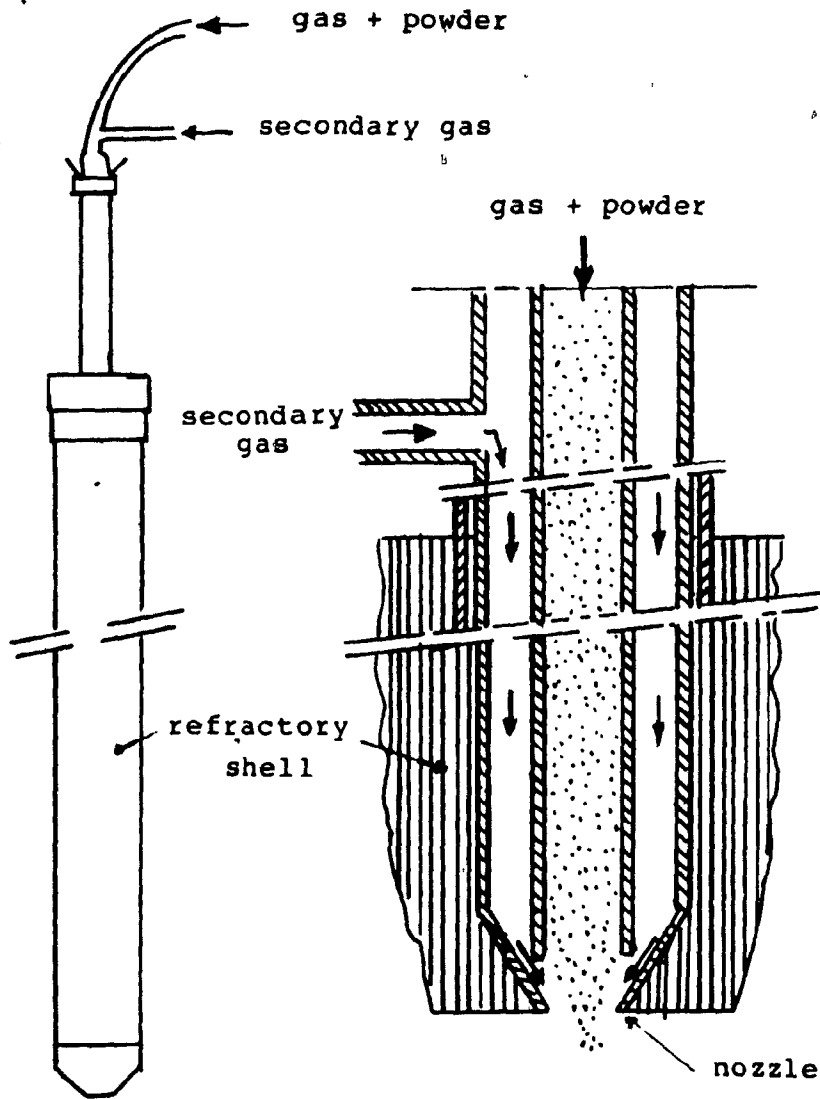


Figure 1.3. Schematic of IRSID injection lance equipped with double-flow circuit. a.) outside view, b.) schematic view of the double-flow circuit arrangement.

Salt Coated Magnesium Granules

Salt coated magnesium granules have become one of the more popular magnesium based reagents over the past few years. They are produced by the Dow Chemical Company and are marketed by Foseco International Ltd. They are also produced in the Soviet Union.^{2,16}

Salt coated magnesium granules were originally produced in electrolytic cells during the refining of magnesium, which made them cheaper than pure magnesium. The granules have a magnesium content of approximately 90% and the coating is a mixture of sodium, calcium, potassium, and magnesium chlorides. The salt coating keeps the granules separated, preventing lance blockage from partial melting or magnesium nitride formation. In addition, these granules can be heated in air to above their melting point (650°C) without spontaneous ignition, making them relatively safe with respect to fire and explosion hazards.

Salt coated magnesium granules can be injected, with nitrogen as the carrier gas, into torpedo cars or transfer ladles. For most applications, approximately 0.5 kg per tonne of hot metal is required to lower the sulphur content from 0.04% to 0.01% S, with injection rates of about 6.5 kg/min.^{9,5} For calcium based reagents such as calcium carbide, the consumption can be as much as ten times higher. The low consumption rate of salt coated magnesium granules can provide significant economic and operational benefits. Some of these benefits are:

- 1.) Lower reagent cost: Even if the cost per kilogram is more for salt coated magnesium granules, its lower consumption results in lower overall costs.

2.) Lower treatment times: Treatment times of about eight minutes are considered normal.

3.) Minimal slag generation: The lower slag volume minimizes metal losses in the slag and makes deslagging easier. Slag handling and disposal costs are significantly reduced.

4.) Lower gas costs: Shorter treatment times result in lower gas consumption.

Like all the other reagents, salt coated magnesium granules also have their disadvantages. First, the desulphurization efficiency is dependent on the hot metal temperature. This is due to the fact that the magnesium vapor pressure increases and the solubility decreases with increasing hot metal temperature. Secondly and more importantly, the desulphurization efficiency and reaction violence is greatly dependent on lance immersion depth. For shallow torpedo cars, as most torpedo cars are, the reaction violence can be quite severe causing skulling problems and considerable damage to the refractories.

The Algoma steel Corporation experienced skulling problems when they used salt coated magnesium granules. They eliminated the skulling problem by developing a ceramic splash plug. The ceramic plug fitted into the ladle mouth as shown in Figure 1.4. The ceramic plug suppressed hot metal splashing completely.⁹ Furthermore, the plug allowed the injection rate to be increased from 6.8 to 13.6 kg/min. The service life of the plug was about 25 injections. This added substantially to the cost of the process.

Armco Inc. had a similar problem which they overcame by developing an injection system that utilized a lance that was

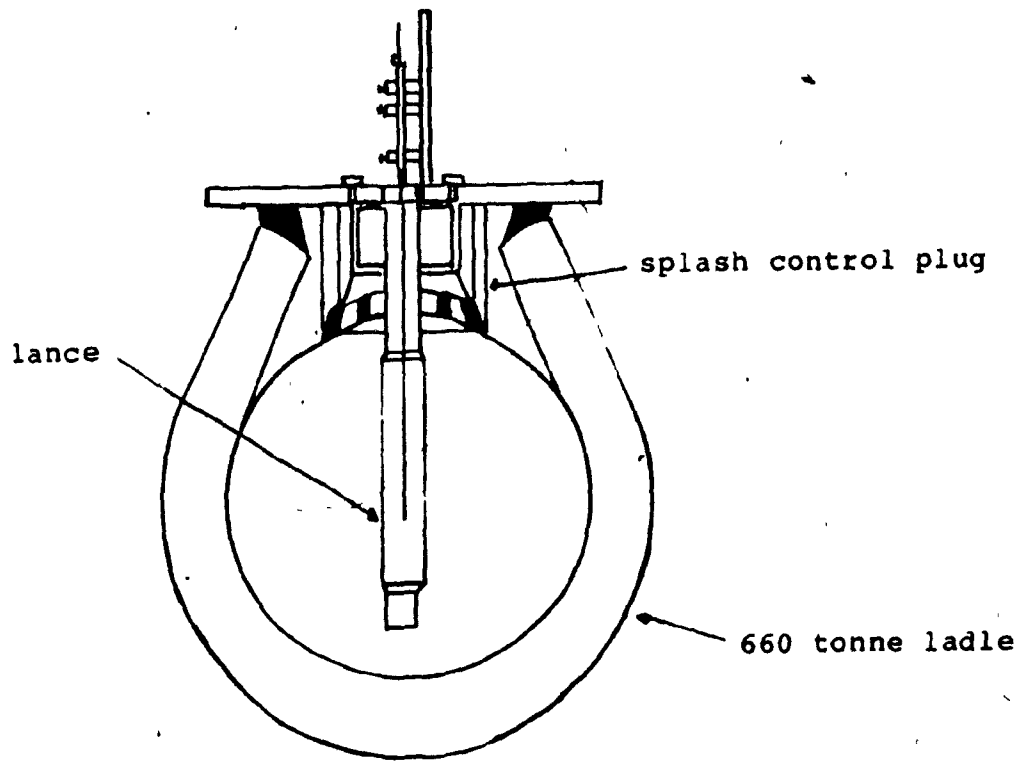


Figure 1.4. Schematic representation of a torpedo car with splash plug.

angled at 15 to 25 degrees from the vertical and positioned about one foot from the bottom of the torpedo car. This permitted an injection rate of approximately 13.6 kg/min without a significant amount of hot metal being ejected from the torpedo cars when filled to 95% capacity.⁵ Prior to using salt coated magnesium granules, Armco used the lime-mag process. With the lime-mag process, they experienced severe skulling problems because of the large volume of slag generated during the treatment process. The switch over to magnesium granules resulted in a dramatic decrease in skulling and the torpedo car capacity increased from an average of 136 tonnes/car to 164 tonnes/car.

Other steel plants have used T-shaped lances, as shown in Figure 1.5, to inject magnesium granules in torpedo cars. This design resulted in better distribution of the reagent to the extremities of the torpedo car, thus, reducing the reaction violence.

1.3.3.c. Wire Feeding

In recent years, there has been considerable interest and research in the area of wire feeding of treating agents to the hot metal and steel. At present, numerous plants are using various forms of calcium wire feeding techniques for the treatment of steel and wire feeding of aluminum has been widely accepted. However, commercial magnesium wire feeding techniques for the treatment of hot metal and steel are non-existent, although a search of the patent literature will show that numerous patents on magnesium wire feeding have been issued. The majority of these methods were developed for use in the foundry

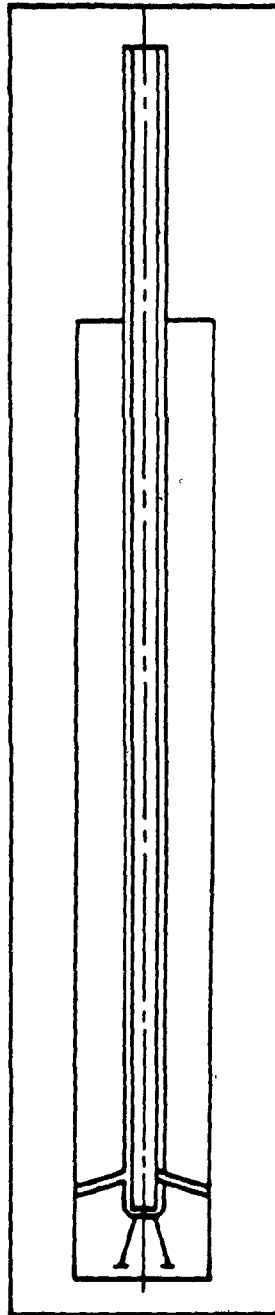


Figure 1.5 T-shaped lance that was developed for the injection of magnesium granules.

industry for the production of nodular iron, however, very few of them have actually been used.

One typical technique, which was developed by Dr. Ashton et al., involves the injection of a 3.2mm diameter magnesium wire through an orifice in a removable plug at the base of a specially constructed ladle.^{14,15} In order to prevent molten iron from running back into the orifice, a high nitrogen gas pressure is applied at the mouth of the orifice. A schematic of the ladle and the orifice is shown in Figure 1.6. The plug consists of a 4.8mm inner diameter mullite tube set in rammed magnesite of 50.8mm thickness. The nitrogen gas enters at a T-junction in the copper tubing near the plug. The pressure tightness of the system is ensured by passing the wire through Teflon seals at the T-junction.

This method was originally intended for the production of nodular iron, however, laboratory scale desulphurization experiments were performed with this method and the results were compared to similar experiments conducted using mag-coke. It was found that the efficiency of the wire injection method was comparable to that of mag-coke.

The disadvantage of this wire feeding technique is that the use of a gas stream can produce excessive agitation of the molten iron which contributes to excessive heat losses. In the laboratory scale tests, the temperature drops were approximately 150°C per run for a bath size of 250 kg and treatment times of one minute. Furthermore, this method requires the utilization of a specially constructed vessel.

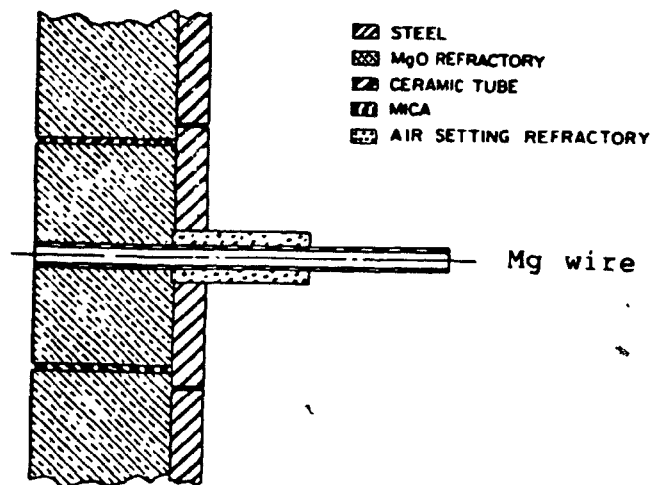
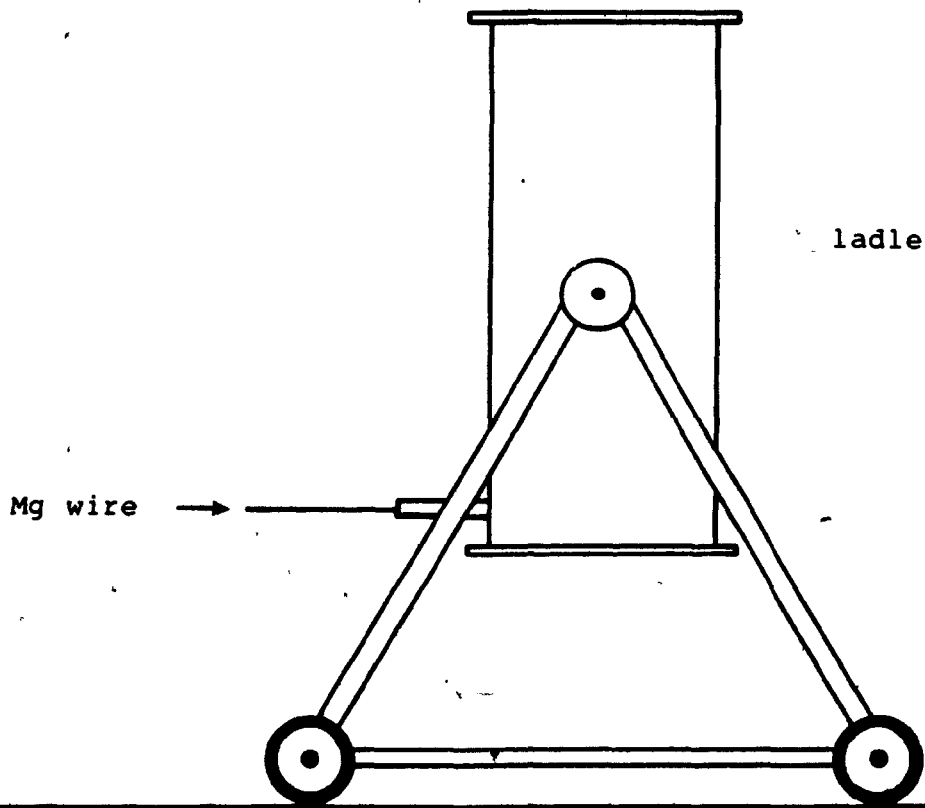


Figure 1.6. Schematic of ladle and orifice.

Another method, which was developed by the International Harvester Company (U.S. patent 4205981), utilizes a protective steel-sheathed magnesium wire that is fed at a high speed into the molten metal from the upper surface of the iron. The purpose of the steel sheath is to provide enough protection to allow the magnesium to penetrate deep into the bath where it will volatilize at a controlled rate. A schematic diagram of the wire feeding process is shown in Figure 1.7.

In the development stage of the wire feeding process various magnesium wire diameters and sheathing thicknesses were tested to determine the optimum combination for maximum magnesium recovery. The magnesium wire diameters used were 3.2, 4.8, and 6.4mm and the sheathing thicknesses were 0.6, 0.8, 1.0, and 1.4mm. It was found that magnesium recoveries increased with increasing sheathing thickness and decreasing wire diameter, with 3.2mm diameter magnesium wire sheathed with 1.0mm of steel being the optimum combination. Furthermore it was reported that the feed rate appeared to have little influence on magnesium recovery.²²

When the optimum combination of magnesium wire and sheathing thickness was employed, there was a complete absence of violence with minimal fumes. Yet this process has not been used commercially.

1.4 Present Work

With the rapid increase in the demand for low sulphur steels, it has become necessary for many steel producers to install external hot metal desulphurization stations. Although

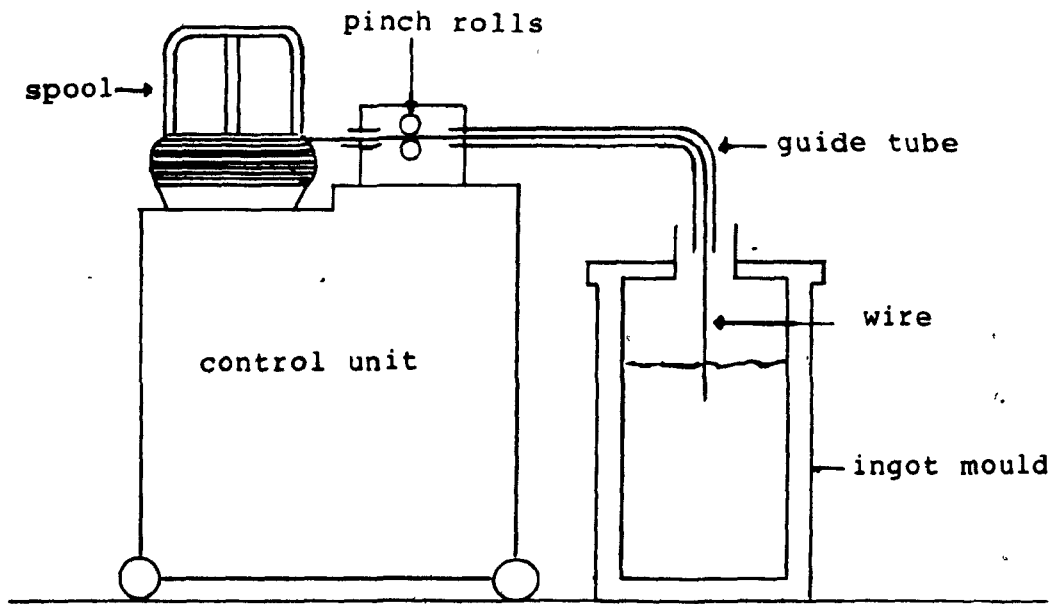


Figure 1.7. Schematic of wire feeding process.

very low sulphur can be attained with hot metal desulphurization, the restrictions for certain applications have become so stringent that further desulphurization of the steel is required. Steel is desulphurized for two basic reasons: 1) to reduce the sulphur level in the steel, and 2) to modify the shape of the sulphide inclusions.

At the present time, the most popular desulphurizers and inclusion shape modifiers are calcium silicide (CaSi), calcium metal (Ca), rare earth metals (REM) and rare earth silicides (ReSi). Of these, the most commonly utilized reagent is CaSi . The most widely used method of adding these reagents has been powder injection through submerged lances. The drawback of powder injection techniques for steel treatment is that the capital cost can be quite high, and, the operating and maintenance costs are significantly higher than that for hot metal treatment. As a result, steel is treated only when it is absolutely necessary.

In recent years, there has been considerable interest in wire feeding techniques of volatile and non-volatile reagents, mainly because of their low capital cost and flexibility. To date, wire feeding methods for the desulphurization and treatment of steel consist mainly of steel clad calcium based wires. Its widespread acceptance has been curtailed by the cost of the wire, relatively low desulphurization efficiency, and the fact that for high volume desulphurization of steel, lance injection techniques are still more practical. Nevertheless, calcium wire feeding methods are becoming increasingly popular

for inclusion modification in ladles and tundishes.

Magnesium has been known for many years to be an effective desulphurizer of molten iron. Consequently, there have been numerous desulphurization processes developed that use magnesium as a reagent, despite its volatile nature at molten iron temperature. The situation is quite different for the treatment of steel with magnesium. The reason for this is quite simply that it is known that the solubility of magnesium decreases with increasing temperature and that its vapor pressure is quite high at steelmaking temperatures. This has led to a reluctance on the part of steel producers and researchers to experiment with magnesium at steelmaking temperatures. As a result, little direct data of magnesium solubility has been reported. However, indirect estimates reveal that the solubility of magnesium, although low, is not low enough to preclude some dissolution during treatment. The solubility of magnesium may be greater than that of calcium, and therefore, due to its great affinity for sulphur and oxygen, one might expect it also to act as an inclusion modifier in steel. In fact, independent work by S.K. Saxena²⁷ and W. Moore²⁸ has shown that magnesium does modify and reduce the number of non-metallic inclusions in steel. The reason for the interest in magnesium is that magnesium is much cheaper than calcium, and on a theoretical basis, less magnesium is required to remove the equivalent amount of sulphur removed by calcium since the molecular weight of calcium is almost twice that of magnesium.

What is required at this point is an inexpensive, safe, and reliable method for introducing magnesium into a molten iron or steel bath. It is felt by the author that because of the low capital, maintenance, and operating costs of wire feeding methods, the greatest potential for developing a desulphurization technique that utilizes magnesium is in the wire feeding field.

One thing that must be kept in mind when developing a wire feeding technique for magnesium is that magnesium vaporizes at typical hot metal temperatures (i.e. magnesium boils at 1107°C), and therefore, in order to utilize magnesium effectively it must be fed deep into the bath before the magnesium begins to vaporize. This can be achieved by applying a 'thermal resistance' on the surface of the magnesium wire. The thermal resistance will allow the magnesium to penetrate deeply into the bath. The depth of penetration can be varied by changing the thickness of the thermal resistance, the wire velocity or a combination of both.

The present research work was undertaken in an effort to find an appropriate 'thermal resistance' and a viable method of applying it to the magnesium surface. Moreover, various process parameters such as immersion speed and insulation thickness were analysed with respect to volatility, pyrotechnic display, and depth of penetration.

The first part of the present study dealt with the testing of glass powder insulators of various chemical compositions and viscosities, while the second part dealt with the testing of

glass woven tape as an insulator. The magnesium composite samples used in the experiments consisted of 3.2mm diameter magnesium wire insulated with various thicknesses of glass powders or glass tape. Furthermore, dynamic systems for monitoring internal temperatures, pyrotechnic displays, and the volatility of the magnesium immersions were implemented with the aid of a process control HP microcomputer. Desulphurization and recovery data was also obtained concurrently with some of the temperature, pyrotechnic and volatility experiments.

CHAPTER 2 PREVIOUS WORK

Prior to the present study, work had been conducted at McGill University on desulphurization by magnesium wire feeding. The work consisted mainly of investigating the effectiveness of various insulating materials. The materials used were paper tape, polyethylene tubing, Pyrex tubing, and soda-lime powder.

The findings of the previous work are briefly outlined in this chapter.

2.1 Paper Tape Insulation

Initial tests were conducted using adhesive paper tape (i.e. masking tape) as an insulator. The paper tape was wrapped around the magnesium wire until a thickness of about 2mm or greater was attained. The idea here was that as the magnesium wire was fed into the molten metal bath the tape would decompose and vaporize. The vapor produced by the tape would provide a thermal barrier between the molten metal and the magnesium thus allowing the magnesium to penetrate deep below the bath surface. All the preliminary tests were conducted in pig iron at 1400°C.

The paper tape, however, proved to be ineffective. Several factors prevented the attainment of any degree of desulphurization of the melt. First, the paper tape was primarily composed of cellulose, $(C_6H_{10}O_5)_n$. As the wire was injected into a pig iron bath, the cellulose decomposed to produce CO gas. A thermodynamic analysis of the system showed that magnesium vapor would preferentially react with carbon monoxide to form magnesium oxide rather than react with the

dissolved sulphur. Hence, even if the wire was made to penetrate deep into the bath, its desulphurization efficiency would still be strongly influenced by the relative amount of CO gas within the melt.

Another problem with paper tape was that for slow speeds (i.e. 1 cm/s - 2 cm/s), the paper tended to burn prior to entering the bath. Even when the magnesium wire was made to penetrate the bath by using a larger thickness of tape, the amount of gas produced by the combination of magnesium and tape was so excessive that a large quantity of metal was ejected from the crucible.

2.2 Polyethylene Tubing Insulation

Since paper could not be used because of the contained oxygen, it was decided that a hydrocarbon such as polyethylene, $(CH_2)_n$, would be more effective. Polyethylene was obtained in the form of tubing with a wall thickness of 1.5mm. The 3.2mm diameter wire was inserted into the polyethylene tubing.

Even though polyethylene contains no oxygen, no desulphurization was achieved when the polyethylene coated magnesium wire was fed into the bath. It was found that the polyethylene never actually penetrated the melt surface. Therefore, the magnesium wire was, in effect, bare as it contacted the melt surface. Consequently, no sulphur removal was achieved.

2.3 Pyrex Tubing Insulation

After the unsuccessful attempts of using paper tape and polyethylene tubing it was decided that it would be best to abandon the idea of using an insulating material which decomposed into a gaseous phase and instead use a material that has the following properties:

- 1.) a very low thermal conductivity.
- 2.) does not produce a gaseous phase.
- 3.) will protect the magnesium wire for a sufficient length of time to enable it to penetrate deep into the melt.
- 4.) is molten or at least 'soft' at the boiling point of magnesium (1107°C), and
- 5.) does not react with magnesium.

It was found that 'glass', in general, met these requirements. Because of its availability, the initial test with glass focussed on the use of Pyrex tubing. Pyrex glass (Corning Glass-7740) contains about 81% SiO_2 , 13% B_2O_3 , 4% Na_2O , and 2% Al_2O_3 . It belongs to the borosilicate family of glasses. Glass does not exhibit a unique melting point but softens as it is heated. For this reason, the viscosity of glass is of vital importance when describing the state of the glass. By definition, the 'softening point' of glass is 10^{6-6} Pa-s. The softening point of Pyrex glass occurs at 821°C. The 'working point' of glass is associated with a viscosity of 10^3 Pa-s. For Pyrex the working point occurs at 1252°C. Further details of the composition, structure and properties of glasses are presented in Chapter 3.

In the majority of tests, two layers of Pyrex tubing having

a total thickness of 1.7mm were fitted over the 3.2mm diameter magnesium wire. The experimental results indicated that there was a substantial degree of desulphurization especially when the initial sulphur content was relatively high (i.e. 0.07% S).³⁴ At times the desulphurization efficiencies were as high as 60%, but normally they were in the 20-40% range. During these experiments, it was evident from the absence of pyrotechnics that the magnesium wires were penetrating deep into the melt. In fact, subsequent tests showed, with the aid of a microphone attached to the furnace structure, that the magnesium wires were actually striking the bottom of the crucible.

2.4 Soda-lime Insulation

The Pyrex tubing experiments showed that glass was a viable insulator, however, it was obvious that for large scale desulphurization where long lengths of wire would be required, the use of glass tubing would be impractical. After considering numerous possibilities, it was decided that a more feasible and practical method of applying the insulation would be to center the magnesium wire in glass powder and encase the two in a metallic sheath. This would make the composite magnesium wire more flexible, and in turn, it could be made in coil form. In the preliminary tests, rigid metallic tubes were used as the sheathing material. The reason for this was that it facilitated the manual construction of the samples. Furthermore, since the working point of Pyrex was substantially higher than the boiling

point of magnesium, it was decided that a lower melting point glass would be more beneficial. One such glass was 'soda-lime' glass. This glass contains 73% SiO_2 , 17% Na_2O , 5% CaO , 4% MgO , and 1% Al_2O_3 . It has a softening point of 696°C and a working point of 1005°C .

Numerous tests were conducted with the above described sample configuration in molten pig iron and it appeared that a significant degree of sulphur removal was attained. However, some problems were encountered during the experiments. One of the more significant problems encountered was that when a magnesium composite sample was fed into the molten pig iron, the sample exhibited periodic eruptions which at times resulted in some metal being ejected from the crucible.

The core of a typical magnesium composite sample consisted of a 3.2mm diameter magnesium wire 36cm in length. The glass insulation thickness varied from 1.5mm to 7.0mm, depending on the feeding velocity. The bath depth was normally 22cm. Figure 2.1 illustrates conceptually how the 'soda-lime' insulated magnesium wire system was expected to work. As the composite magnesium wire is fed into the bath, the glass at the vicinity of the leading end of the sample begins to be consumed until such time that the magnesium, most likely in the liquid state, is exposed to the liquid iron. At this point, the magnesium vaporizes and rises through the bath as it dissolves. Ideally, it is preferable that the magnesium be released as soon as it

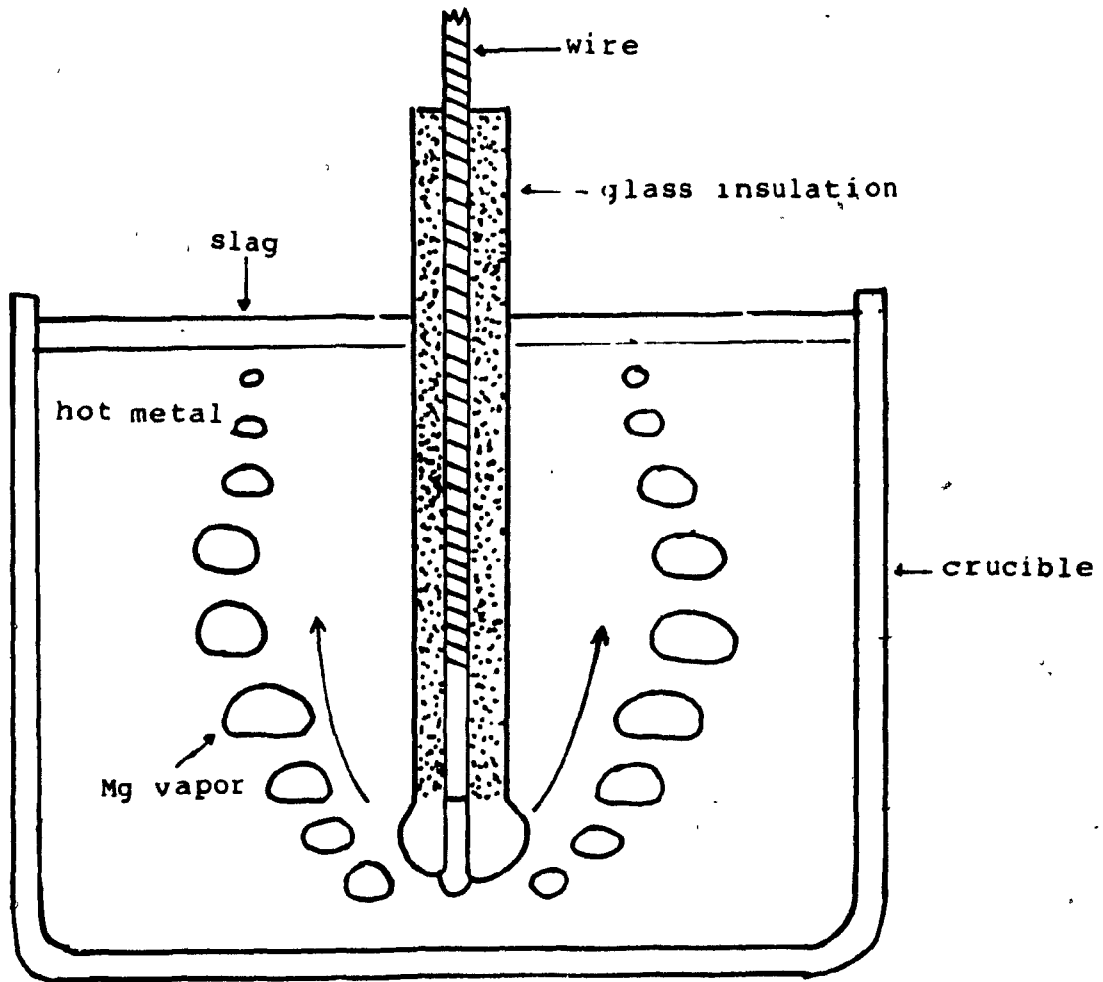


Figure 2.1. Conceptual illustration of how the soda-lime insulated magnesium wire system was expected to work.

becomes liquid in order to attain a controlled and consistent release of magnesium.

However, it was thought that it was conceivable, due to the relatively high viscosity of the glass and the small diameter of the magnesium used in the experiments, that the leading end of the composite sample 'clogged up'. As a result, a liquid column of magnesium accumulated until such time that the leading end of the composite sample either struck the bottom of the crucible or the molten magnesium that was contained within the glass framework blew a hole through a weak portion of the glass, thus releasing a packet of magnesium. The sudden release of a packet of magnesium resulted in an eruption.

Since the viscosity of glass is greatly dependent on temperature (see Figure 2.2), it was decided that increasing the bath temperature would probably reduce the violence of the eruptions or eliminate them altogether. Tests were conducted using pig iron at steelmaking temperatures (i.e. about 1600°C) and it was found that the eruptions were almost completely eliminated. Hence, it was logical to assume that soda-lime glass was too viscous at a temperature of 1400°C. Therefore the present study was undertaken to find a glass material with a suitable viscosity.

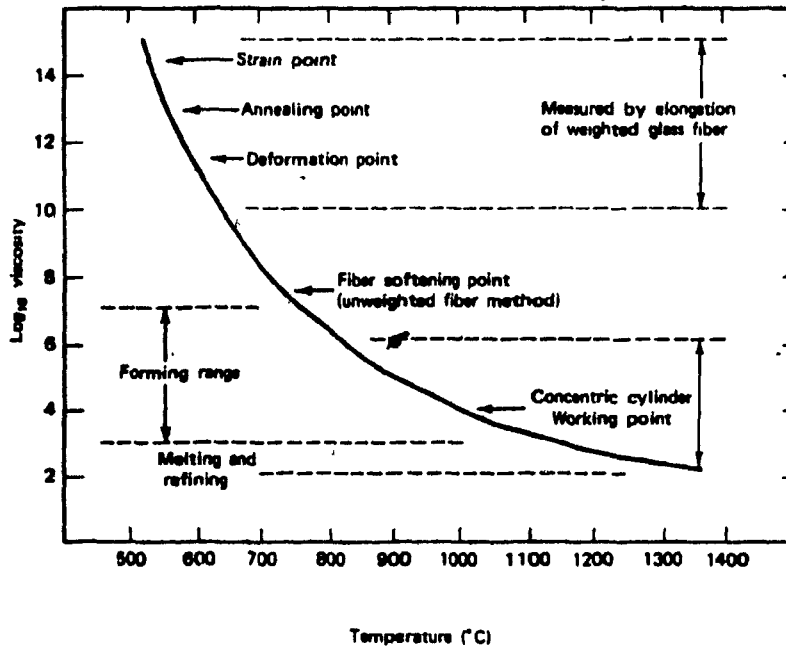


Figure 2.2. Viscosity-temperature curve of a typical soda-lime silicate glass.

CHAPTER 3
GLASS

Glass materials play a major role in this study, and therefore, it is important at this point to present a chapter on glasses to provide a basic understanding of its molecular structure, properties, and the effects of various components. In addition, a description of glass applications and the physical forms in which they can be obtained will give a better insight as to the reason glass was chosen as a suitable insulating material in the present investigative work.

3.1 Structure

Traditionally, glasses are defined as supercooled liquids. This is due to the fact that glasses do not behave like metals, ceramics, or plastics on cooling from the molten state. When ceramics and metals undergo a transformation from molten state to the crystalline state, heat is released (i.e. heat of solidification) and an inflection point can be observed in the temperature of the material. Similarly, volume changes on crystallization can be detected. However, glasses do not display any of these indicators of structural changes on cooling from the molten state, thus it is often considered simply to be a very viscous liquid when it is in a solid form. The most widely accepted definition for glass is that proposed by the

A.S.T.M.:⁴⁸

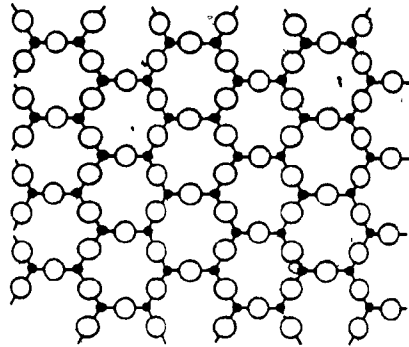
'Glass is an inorganic product of fusion which has cooled to a rigid condition without crystallizing.'

In order to understand the reason glass is often considered to be a very viscous liquid at room temperature, it is essential at this point to consider the relationship between the solid and liquid states. From X-ray diffraction measurements, it is observed that a certain degree of regularity exists in a liquid since the diffraction patterns consist of one or more diffuse halos. This implies that a liquid is not structureless like a gas but it has some type of grouping or arrangement of molecules that is related to that which exists in the solid. The units of structure are the same in a liquid as in a crystalline solid except that these units are not arranged in a regular manner. Consequently the liquid possesses short-range order but not long-range order whereas a crystalline solid possesses both long and short-range order which leads to complete regularity throughout the solid.

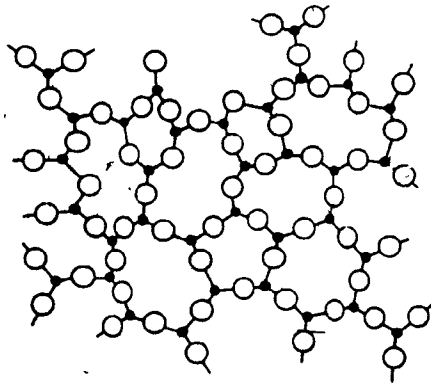
The basic ingredient for most glasses is silicon dioxide (silica), although, there are other oxides capable of forming glasses such as B_2O_3 , P_2O_5 , GeO_2 , and As_2O_5 . The molecular building block of silicate glasses is SiO_4 in a tetrahedral configuration. In a crystal, the SiO_4 tetrahedra are built up to give a regular lattice whereas in the glassy state there is enough distortion of the bond angles to permit the structural units to be arranged in a non-periodic fashion giving a random network. The difference between the regular crystalline lattice and the random network of silicate glasses

is illustrated in Figures 3.1a and b. Hence to recap, the figures show that glass possesses short-ranged order since the oxygen molecules are arranged in a fairly regular polyhedra but long-range order is absent.

Oxides which form glasses when melted and cooled are often called network forming oxides because of their ability to build up continuous three-dimensional random networks. When considering glass structures, it is also necessary to distinguish two other types of oxides in terms of their functions in the glass structure. There are network modifying oxides and intermediate oxides. A modifying oxide is one that is incapable of forming a continuous network and the effect of such an oxide is usually to weaken the glass network. An intermediate oxide is one which is normally incapable of forming a glass by itself but can take part in the glass network. Aluminum oxide is a good example of an intermediate oxide. In crystals, the aluminum ion can be co-ordinated with four or six oxygen ions, this gives rise to tetrahedral AlO_4 or octahedral AlO_6 configurations. The AlO_4 tetrahedral groups can replace SiO_4 tetrahedra in silicate lattices to impart the configuration illustrated in Figure 3.2. Since each aluminum ion has a charge of +3 as compared to a charge of +4 for each silicon ion, an additional unit positive charge must be present to ensure electroneutrality. This requirement can be satisfied by the presence of an alkali metal ion per AlO_4 tetrahedron. The



(a)



(b)

○ — oxygen ion
• — metal ion

Figure 3.1. Two-dimensional representation of a metal oxide in a.) the crystalline form b.) the glassy form.

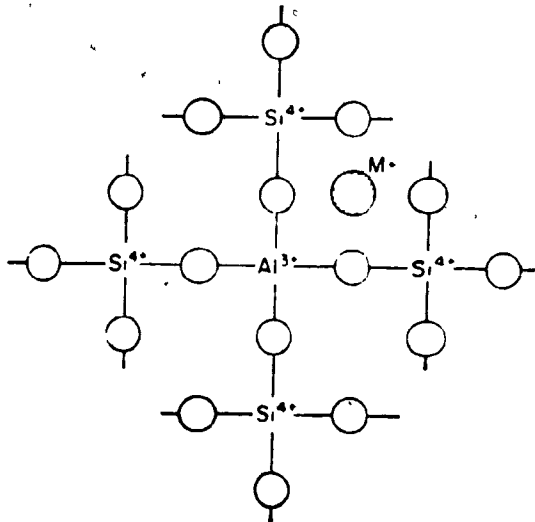


Figure 3.2. Aluminum in a silicate network. (The structure is shown in a simplified form; the true structure is three-dimensional.)

alkali metal ion can be accommodated in the interstices between tetrahedral groups. This type of structural configuration is found for many aluminosilicates such as feldspar where the crystals are built up of linked SiO_4 and AlO_4 groups.

A good example of a modifying oxide is sodium oxide. When sodium oxide is added to silica glass to form sodium silicate glasses, certain structural changes occur as illustrated in Figure 3.3. Prior to the addition of Na_2O , there is one oxygen ion bridging the two SiO_4 tetrahedra. After the addition of Na_2O there are two non-bridging oxygens, one of which has been contributed by the sodium oxide. Thus the introduction of Na_2O produces a gap in the continuous network structure. The sodium ions are accommodated by the interspaces in the random network structure as shown in Figure 3.4.⁴⁸ These structural changes result in property changes such as reduction of viscosity and increase in thermal expansion coefficient.

Other alkali metal oxides, such as lithium or potassium oxide, behave in the same fashion as sodium oxide when added to silicate glasses. The alkaline earth oxides such as MgO , CaO , and BaO also act as modifying oxides. Fluorides such as NaF and CaF_2 (fluorspar) can also be used as modifying agents. Since the ionic radii of oxygen and fluorine are quite similar (i.e. 1.32\AA for oxygen as compared to 1.33\AA for fluorine) their mutual substitution is possible at high temperatures. The effect of adding CaF_2 is shown in Figure 3.5. The Si-O-Si is broken

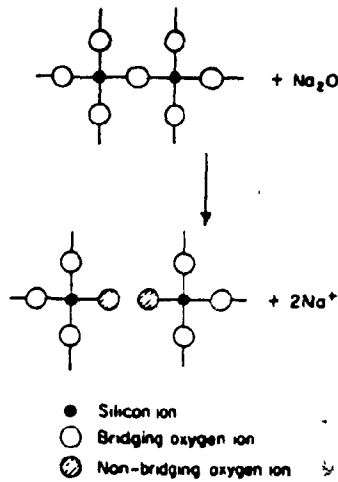


Figure 3.3. Reaction between sodium oxide and silica tetrahedra. (For simplicity, a two-dimensional representation of the SiO_4 groups is given.)

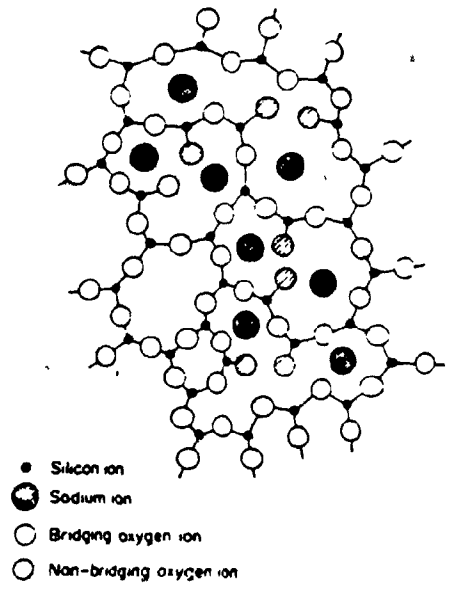


Figure 3.4. Two-dimensional representation of the structure of soda-silica glass.

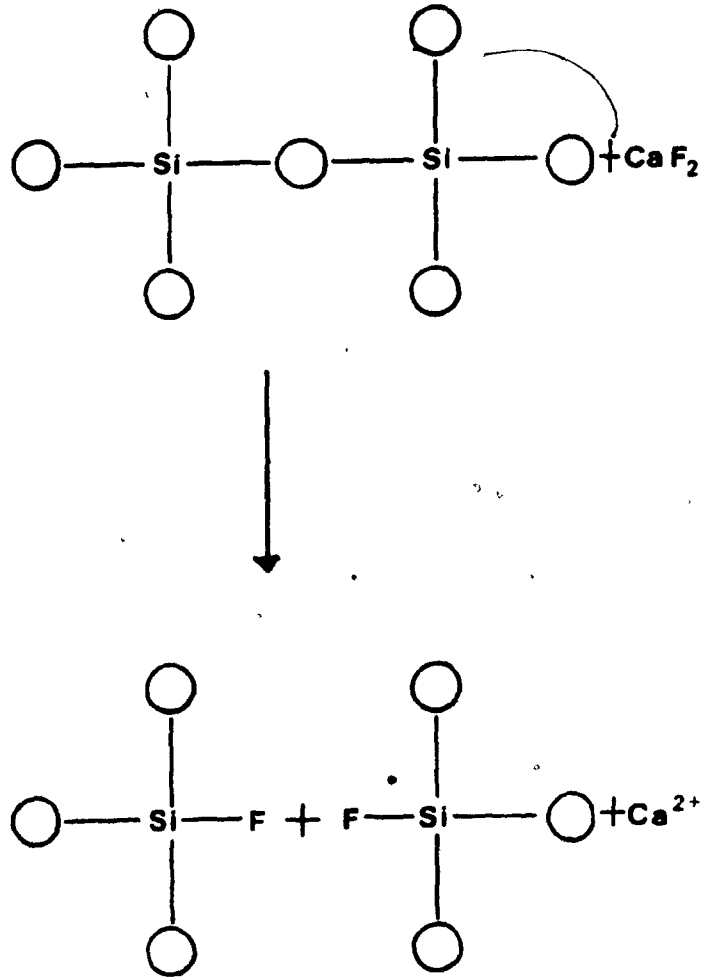


Figure 3.5. The effect of adding CaF_2 to silicate glass.

and the oxygen bridging ion is replaced by two fluorine ions. The Ca^{2+} ions occupy the interstitial positions. CaF_2 is often used to lower the viscosity of glasses or slags.

3.2 Broad Classification of Glass Types

Glasses can be classified in several ways. For example, classifications can be based on chemical composition, physical form and application. The most widely used classification is chemical composition.

3.2.1 Chemical Composition

The majority of glasses can be classified in three main groups: soda-lime glass, lead glass, and borosilicate glass. These glasses account for at least 95% of all glass types. The remaining 5% are special glasses manufactured in small quantities. Thousands of special glass types have been developed, and many of them have special applications.

As previously mentioned, most glasses are silicate based glasses, the chief component of which is silicon dioxide (SiO_2).

Soda-Lime Glass

By far the largest number of industrially produced glasses belong to the 'soda-lime' family. As the name indicates, soda (Na_2O) and lime play a major role along with the main component silica.

The wide use of soda-lime glass is attributed to its chemical and physical properties. Among the most important properties is its light transmission which makes it suitable for use as flatglass in windows. Furthermore, the relatively high alkali content of the glass imparts a lower melting point as compared to pure SiO_2 glass, and also causes an increase in the thermal expansion coefficient. Due to its high thermal expansion, the resistance of soda-lime glass to sudden temperature changes is comparatively poor.

Lead Glass

As the name indicates, lead plays a major role in this type of glass. Lead glasses are composed of 54-65% SiO_2 , 18-38% lead oxide (PbO), 13-15% soda or potash (K_2O). Varying amounts of barium oxide, zinc oxide, and potassium oxide can be added to the composition to partially replace some of the lead oxide. Glasses containing lead exhibit a high refractive index and are especially suited for decorating by grinding.

Borosilicate Glass

This glass has a higher percentage of silica (i.e. 70-80%) than soda-lime and lead glass. In addition to the SiO_2 , borosilicate glass contains 7-13% boric oxide (B_2O_3), 4-8% Na_2O and K_2O , and 2-7% Al_2O_3 .

Borosilicate glasses possess a high resistance to chemical corrosion and temperature change. For this reason, they are used in process plants in the chemical industry and in

laboratories. This glass also has domestic applications for such items as baking and casserole dishes and other heat-resistant cookware.

The chemical compositions of some of the more common commercial glasses are shown in Table 3.1.

3.2.2 Physical Forms

Glasses come in forms too numerous to mention, however, the majority of glasses can be categorized in one of the following groups: flat glass, holloware and tube glass, fibers, foam, and powders.

A detailed discussion of all the various forms of glass is beyond the scope of this study, therefore, a brief description of the some forms will be presented with emphasis placed on the forms pertinent to the present work.

3.2.2a Flat Glass

The term 'flat glass' pertains to all glasses produced in a flat form, regardless of the method of manufacture. By far the greatest amount of flat glass consists of soda-lime glass. All manufacturers use basically the same formula.

3.2.2b Holloware and Glass Tubing

The most widely distributed glass products belong to the holloware family. These products are mainly consumer goods such as bottles, drinking glasses, or glass lamps. Most holloware is made of soda lime glass.

Glass tubing is usually made of soda-lime glass or

TABLE 3.1
CHEMICAL COMPOSITIONS OF COMMON COMMERCIAL GLASSES

TYPE	SiO ₂	Al ₂ O ₃	CaO	Na ₂ O	B ₂ O ₃	MgO	PbO	Others
Fused silica	99							
96% silica (vycor)	96				4			
Pyrex	81	2		4	12			
Soda-lime	74	1	5	15		4		
Fibers	54	14	16		10	4		
Lead glass (Tableware)	67			6			17	K ₂ O-10
Optical flint	50			1			19	B ₂ O-13

borosilicate glass. Soda-lime is suitable for fluorescent light tubing, whereas, borosilicate glass is used for glass tubing in the chemical industry.

3.2.2c Glass Foam

Glass foam is a porous glassy material which is suitable for thermal and acoustic insulation in the construction of buildings. Foam glass has a high compressive strength and dimensional stability with a density of 0.13-0.3 g/cm³. The cellular structure of the foam glass imparts a thermal conductivity that is about 10 times less than that of a compact glass. Due to its low density and water impermeability, it is also used in flotation devices.

3.2.2d Glass Fibers

'Glass fiber' is a collective term for glass processed into fibers which have diameters between 0.1mm and a few thousandths of a millimeter. Glass fibers can be subdivided into three groups; insulating fiberglass, textile fiberglass, and lightguide fibers or optical fibers. Optical fibers are a recent development and are not pertinent to the present study.

Insulating Fiberglass

Insulating fiberglass is often referred to as glass wool. These fibers are normally made of soda-lime glass by the centrifugal process using a rotating disk. The fibers cool in air and are hardened. The individual fibers immediately mat together. This is sometimes called glass wadding. The actual

weight of loosely piled insulating glass fibers is between 30 and 200 kg/m³. Thus glass wool is well suited for building insulation, since it does not add a significant load to the structure.

Fiberglass Textiles

Fiberglass textiles are made from continuous filaments produced from molten glass. The filaments are uniform, usually have a circular cross section, and can be further processed into threads. Continuous filaments are produced by mechanically drawing, at high speed, a stream of molten glass vertically downwards from a special furnace to a suitable package for subsequent processing into yarn, cords, mat, or fabrics. The diameters of continuous filaments range from 3-16 micrometers.

Continuous filaments in the form of chopped strands are widely used for plastic reinforcement. The high tensile strength of up to 10^3 N/mm² and low expansion are the properties which render fiberglass suitable for improving the mechanical qualities of plastics.

Glass fibers in the form of woven tape and fabric are almost exclusively used for electrical and thermal insulation. Fiberglass cloth is also used as welding curtains and fire blankets.

Over 95% of all continuous glass fibers produced are of the so-called 'E-glass' composition. They are essentially free of alkalis (i.e. sodium and potassium content is less than 0.8%) and

are characterized by water resistance and high softening and melting points (i.e. softens at 732-800°C and melts at 1120-1182°C). E-glass is an alumino-borosilicate glass by composition.

Until recently, significant quantities of fibers were made from soda-lime glass (A-glass) since patents covering E-glass prevented producers from using it, or, because a local source of cheap sheet-glass was available. For certain applications, A-glass can adequately replace E-glass and it can be cheaper to produce. One particular disadvantage of E-glass is that it is susceptible to attack by dilute acids. For applications where chemical resistance to acids is required, C-glass is used. C-glass is a soda-lime based glass. D-glass is used if good dielectric qualities are important. There are other fiber glass textiles which are used in conjunction with thermosetting adhesives or resins that harden in sun or u-v light. Two such glass textiles are made of G-glass and B-glass compositions and can resist temperatures of 121°C and 130°C respectively.

Another glass worthy of mention is the high strength glass fiber known as S-glass, which was developed for use in such specialized applications as rocket motor cases. This glass is difficult and expensive to make and has a very limited application. The typical composition of some the glass fibers mentioned are presented in Table 3.2.

TABLE 3.2

CHEMICAL COMPOSITION OF GLASS FIBERS

Constituent	E-glass	C-glass	A-glass	S-glass
SiO ₂	55.2	6.5	72.0	65.0
Al ₂ O ₃	14.8	4.0	2.5	25.0
B ₂ O ₃	7.3	5.0	0.5	-
MgO	3.3	3.0	0.9	10.0
CaO	18.7	14.0	9.0	-
Na ₂ O	0.3	8.5	12.5	-
K ₂ O	0.2	-	1.5	-
Fe ₂ O ₃	0.3	0.5	0.5	-
F ₂	0.3	-	-	-

3.2.2e Glass Powders

The major group of commercially used glass powders are continuous casting mold fluxes or mold powders. These powders are primarily used to cover the liquid steel meniscus in continuous casting molds to protect the liquid metal surface from reoxidation and excessive heat loss. Moreover, they are used to eliminate entrapped scum and provide lubrication to facilitate withdrawal of the steel strand from the mold.

Mold flux compositions are generally based on the $\text{SiO}_2\text{-CaO-Al}_2\text{O}_3$ system with alkali oxides (e.g. Na_2O) and fluorides (e.g. CaF_2) added as fluidizers. Three to six percent graphite is usually added to effect the melting characteristics of the flux and to improve the thermal insulating properties of the fluxes. The properties of a flux which can be controlled are melting temperature, melting rate, viscosity, surface tension, and chemical activity. These properties can be controlled by flux chemistry, the physical form of the flux (i.e. a raw material blend or a prefused homogeneous material) and by the addition of free carbon in the form of coke or graphite.

The silica content and viscosity of mold fluxes is generally much lower than that of conventional soda-lime glass. Some typical compositions and viscosities are exhibited in Table 3.3. The viscosity-temperature-composition relationships for glasses will be discussed in greater detail in the following section.

TABLE 3.3
COMPOSITION AND VISCOSITIES OF TYPICAL MOLD POWDERS

POWDERS	SiO ₂	Na ₂ O +K ₂ O	CaO	MgO	Al ₂ O ₃	Fe	F	Viscosity (1573 K)* (dPa-s)
soda-lime	73	17	5	4	1			300
A	31	3.1	28		6.5	0.5	3.7	10
B	29.6	4	29		10.7	0.8	2.7	16
C	31.3	5.6	24.2		14.7	4.0	3.2	17
D	23.5	13.7	18.4		9.3	1.4	6.8	1.0
E	25.8	14.4	22		7.7	0.8	6.2	1.0
F	22.1	11.2	30.4		8.8	0.6	4.0	1.2
G	22.3	8.6	27.0		5.6	3.5	6.2	0.7

* 1 dPa-s = 1 poise = 1 dyne-second/cm²

3.3 Viscosity

All fluids possess a definite resistance to change of form. This property, a sort of internal friction, is called viscosity and is expressed in dyne-s/cm² or Pa-s.

The viscosity of a glass depends on both temperature and composition. For a given glass composition, the change in viscosity with temperature can be described as a first approximation by the equation:³⁷

$$\eta = A \exp(-E/RT) \quad (10)$$

where η = viscosity in dyne-s/cm²
 E = activation energy for viscous flow
 T = temperature in K
 R = gas constant

Figure 3.6 shows typical viscosity-temperature curves for soda-lime glass and some commercial mold fluxes. Note that the viscosity range for the mold powders is significantly lower than that of soda-lime.

Since the viscosity of glasses is dependent not only on temperature but on composition as well, a more useful expression for viscosity would be one that includes the effect of composition. The development of such quantitative relations requires data obtained on systematically arranged experimental compositions. Relatively few data of this type are found in the literature. Large glass manufacturers maintain research laboratories in which viscosity-composition-temperature relations are developed, however, these relations are often held

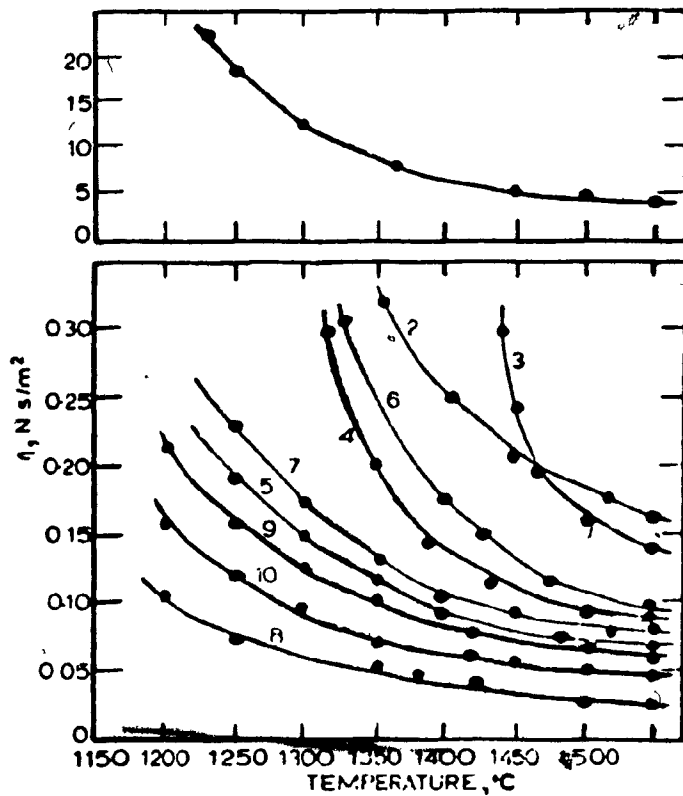


Figure 3.6. Typical viscosity-temperature curves for soda-lime glass and some commercial mold fluxes.

to be proprietary. For continuous casting mold fluxes, these relationships appear to be more readily available mainly because viscosity is one of the most important properties of mold fluxes. One such empirical relationship was developed by Ribaud et al. for mold powder compositions belonging to the $\text{CaO-SiO}_2\text{-Na}_2\text{O-CaF}_2\text{-Al}_2\text{O}_3$.^{35,36} The relationship is expressed as follows:

$$n = A \exp(B/T) \quad (11)$$

where T = temperature in K
n = viscosity in Pa-s

$$\ln A = -19.81 - 35.75X_{\text{Al}_2\text{O}_3} + 1.72X_{\text{CaO}} + 5.82X_{\text{CaF}_2} + 7.02X_{\text{Na}_2\text{O}}$$

$$B = 31140 + 68833X_{\text{Al}_2\text{O}_3} - 23896X_{\text{CaO}} - 46351X_{\text{CaF}_2} - 39519X_{\text{Na}_2\text{O}}$$

X = mole fraction

Equation (11) is valid for fluxes in the following composition range:

$$\begin{array}{l} 33 < \text{SiO}_2 < 56\% \\ 12 < \text{CaO} < 45\% \\ 0 < \text{Al}_2\text{O}_3 < 11\% \\ 0 < \text{Na}_2\text{O} < 20\% \\ 0 < \text{CaF}_2 < 20\% \end{array}$$

The effect of composition on viscosity can be understood qualitatively by taking into account the following facts. First, viscosity is determined by the degree of polymerization of silico-alumino oxygen ions, and second, the degree of polymerization decreases with increasing amounts of oxides and fluorides such as CaO , Na_2O , MgO , and CaF_2 as was mentioned

in section 3.1 of this Chapter. Therefore, it is expected that equation (11) exhibits an increase in viscosity with increasing quantities of SiO_2 and Al_2O_3 and a decrease in viscosity with increasing amounts of CaO , Na_2O , and CaF_2 .

3.4 Thermal Properties

3.4.1 Thermal Conductivity

The thermal conductivity coefficient of a material relates the amount of heat, in joules/s, that is conducted through a centimeter cube of the substance for a temperature difference of 1°C between two of its opposite faces. The thermal conductivity of silicate glasses at room temperature ranges from 4.7×10^{-4} to 7.2×10^{-4} J/s-cm- $^\circ\text{C}$. This coefficient increases with temperature and is dependent on glass composition. The thermal conductivities of glasses are difficult to determine experimentally, and their quantitative relationship with composition is not well known. There has been little systematic study of the thermal conductivity of glasses and its dependence on composition.

3.4.2 Heat Capacity

Heat capacity (i.e. specific heat) represents the heat energy required to raise the temperature of a unit mass of a material by one degree. It is usually expressed in joules. The specific heat at constant pressure, c_p , applies to a single temperature, while the mean specific heat, c_m , is the average specific heat taken over a temperature interval, such as 0° to 500°C .

The mean specific heat is usually determined by the method of mixtures, which involves measuring the difference in heat content between some elevated temperature and that of a calorimeter. Mean specific heat is more convenient to use when performing a rough heat transfer analysis of a material, since only one specific heat value is required for a given temperature range.

As with viscosity and thermal conductivity, the specific heat is affected by both temperature and composition. Sharp and Ginther (1951) developed the following empirical equation to represent the mean specific heat for a multicomponent glass.⁵⁰

$$c_m = aT + c_0 / 0.00146T + 1 \quad (12)$$

where a and c_0 are constants given in Table 3.4, and T is in $^{\circ}\text{C}$.

For a multicomponent system, the a and c_0 is determined by adding all the a 's and c_0 's of the individual components on a weighted basis.

TABLE 3.4
OXIDE FACTORS FOR CALCULATION OF MEAN SPECIFIC HEAT

OXIDE	a	C ₂
SiO ₂	0.000468	0.1657
Al ₂ O ₃	0.000453	0.1765
CaO	0.000410	0.1709
MgO	0.000514	0.2142
K ₂ O	0.000335	0.2019
Na ₂ O	0.000829	0.2229
B ₂ O ₃	0.000635	0.198
SO ₃	0.00083	0.189
PbO	0.000013	0.049

CHAPTER 4
EXPERIMENTAL

4.1 Apparatus

4.1.1 Induction Furnace

A Tocco Meltmaster induction furnace was used to melt and hold the pig iron baths for both the aluminum hand-dipping and Mg wire feeding experiments. The furnace operated at 3000 Hz and had a maximum power input of 150 kVA at 400 volts. The internal diameter of the coil was 38cm and had 10 turns in a 30cm length. Photographs of the induction furnace and the control panel are shown in Figures 4.1 a and b.

The molten pig iron baths were held in alumina crucibles 14cm in internal diameter and 28cm in height. Alumina crucibles measuring 20cm in internal diameter and 36cm in height were used for some experiments.

4.1.2 Wire Feeder

The composite magnesium and Al samples were fed into pig iron baths with the aid of a 'batch type' wire feeder. A photograph and a schematic diagram of the wire feeder are shown in Figures 4.2a and 4.2b respectively. The feeding mechanism was driven by a 1/3 HP variable speed DC motor which was controlled by a remote unit. The desired immersion speed was attained by adjusting the electrical resistance of the potentiometer, which controlled the rotational speed of the motor. The immersion velocities varied between 0.5 to 2.5cm/s, with 1.0cm/s being the most commonly used speed.

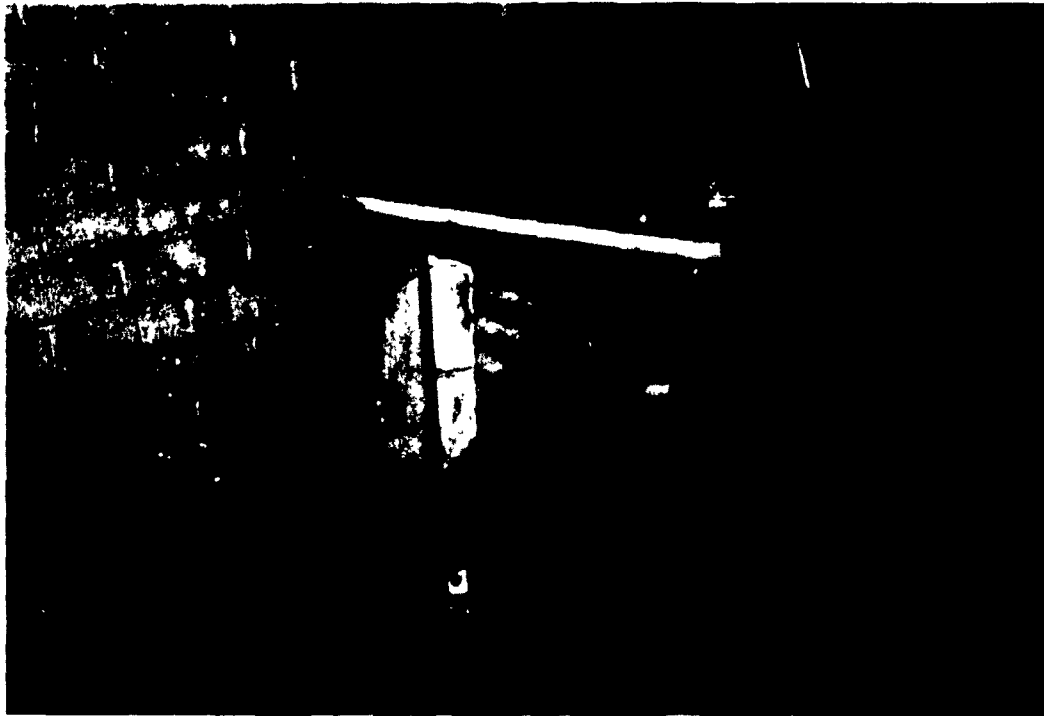
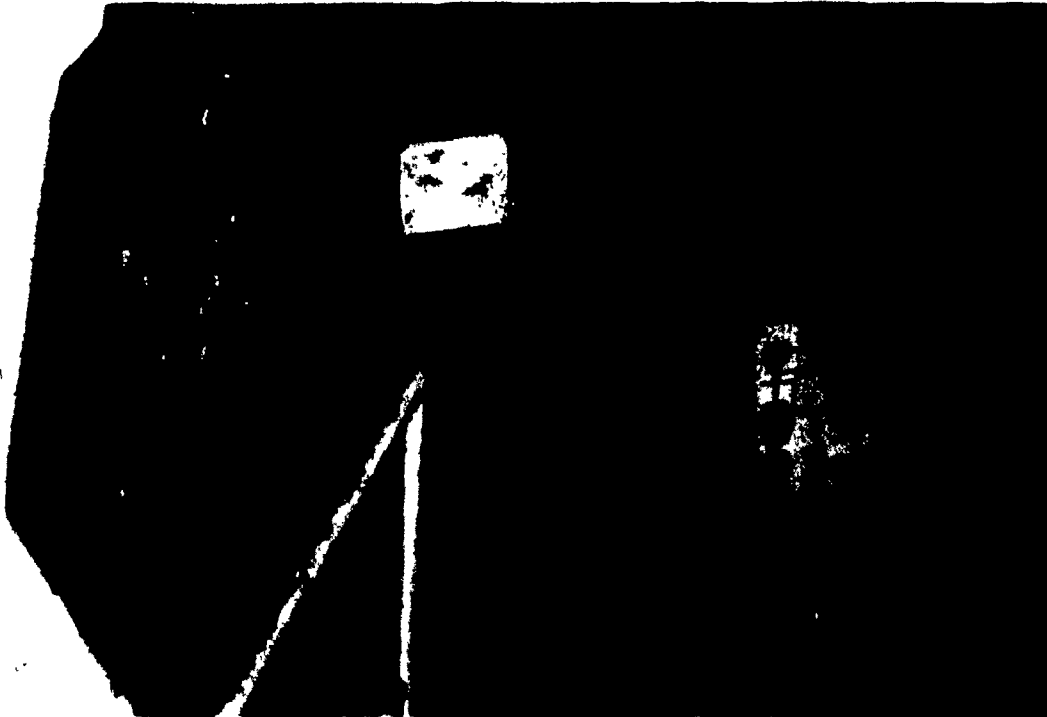


Figure 4.1. Photographs of a.) furnace controls, b.) induction furnace.

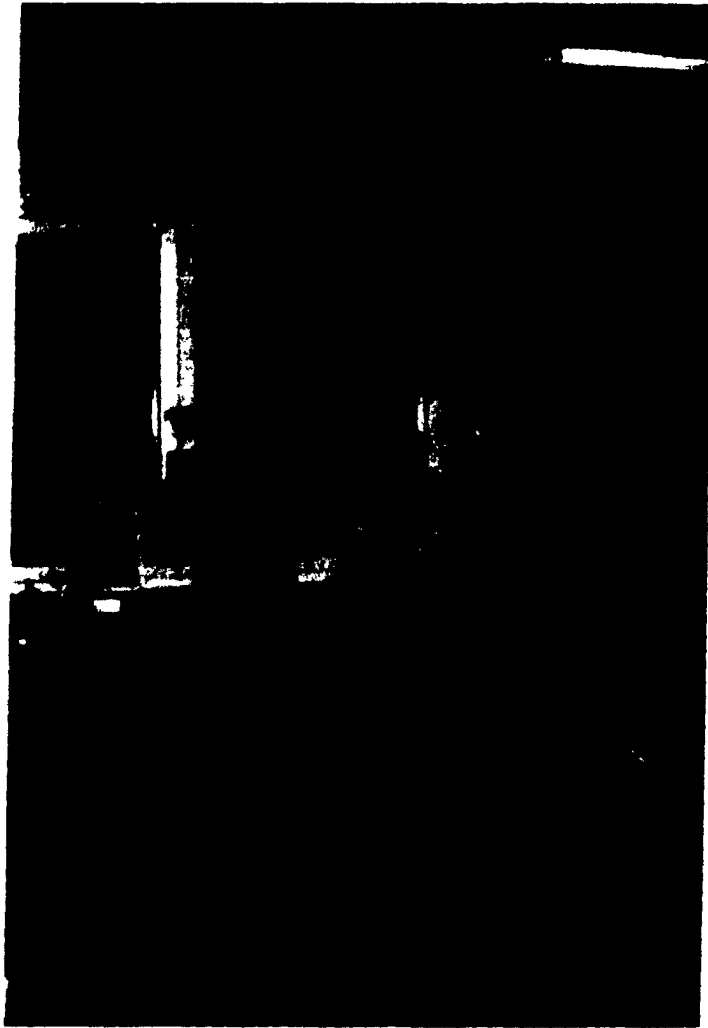


Figure 4.2a Photograph of wire feeder.

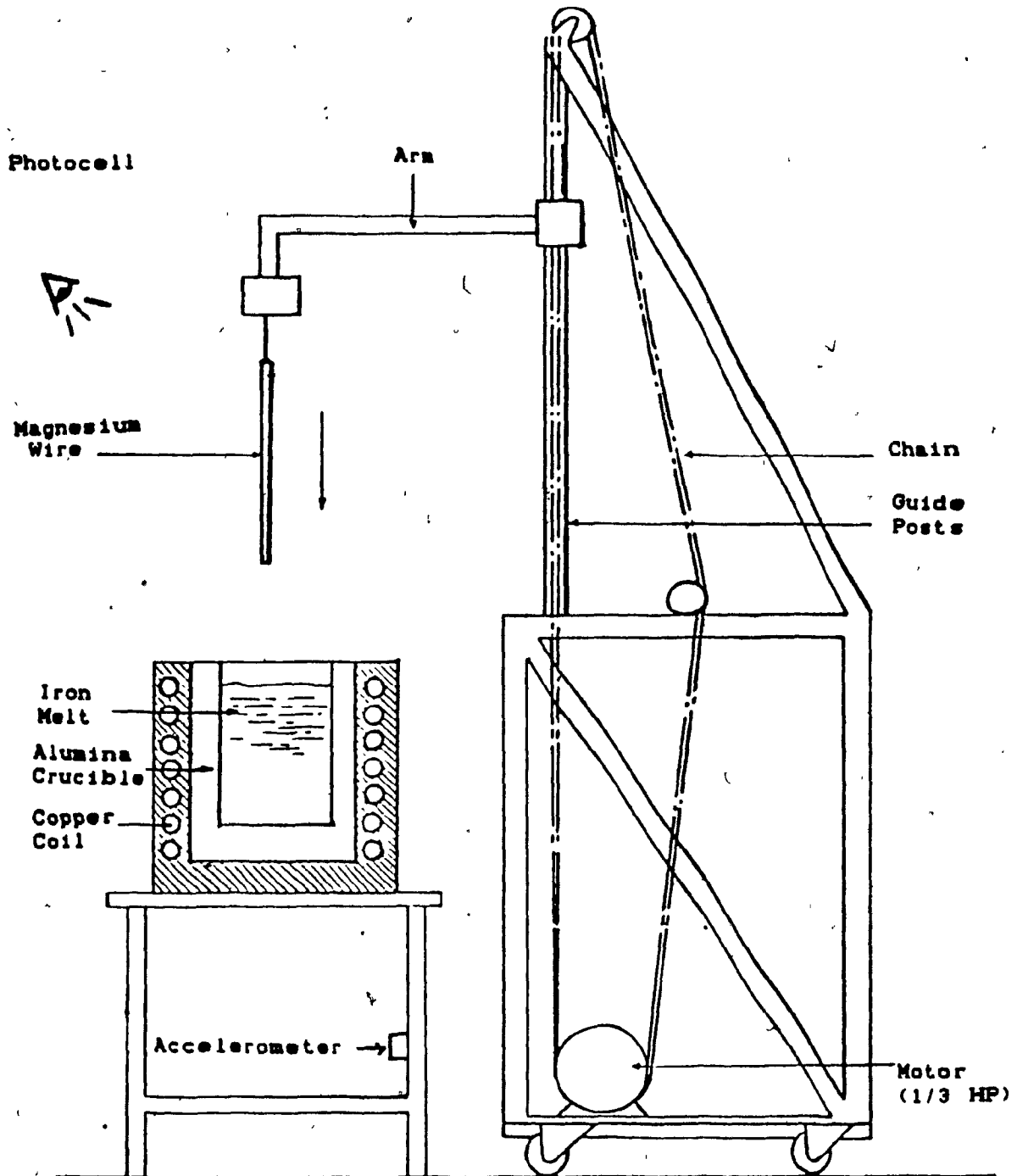


Figure 4.2b Schematic drawing of wire feeder.

4.1.3 Data Acquisition System and Transducers

An HP 3497 data acquisition unit and an HP 85 microcomputer were used to record the readings produced by the transducers utilized for the experiments. The transducers or sensors included thermocouples, an accelerometer, and a photocell. Thermocouples were used to evaluate the thermal characteristics of the composite wires while the accelerometer and photocell were used to evaluate the volatility and pyrotechnic behavior of the Mg samples.

An accelerometer is an electromechanical transducer that generates an electrical output when subjected to mechanical shock or vibration. The electrical output is directly proportional to the acceleration of the vibration applied at its base. The active element of the accelerometer consists of a number of piezoelectric discs that produce an emf when subjected to compressive forces on which rests a relatively heavy mass. The mass is preloaded by a stiff spring and the whole assembly is sealed in a metal housing with a thick base as shown in Figure 4.3. When the accelerometer is subjected to vibration, the mass exerts a variable force on the discs which in turn develops a variable charge that is proportional to the force and therefore the acceleration of the mass.

For the volatility and pyrotechnic tests of the present study, the accelerometer was mounted on the housing of the induction furnace to detect any movement of the pig iron bath caused by the volatilization of the immersed magnesium. The

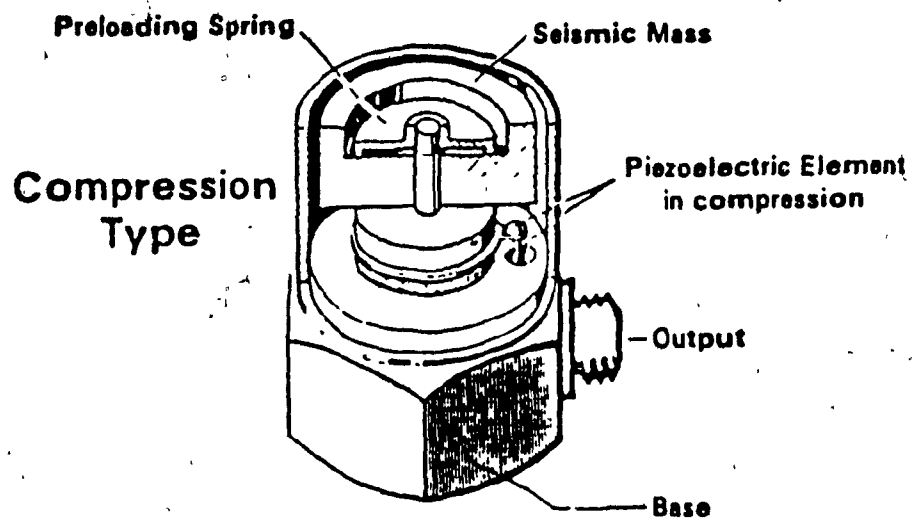


Figure 4.3. Schematic drawing of a compression type accelerometer.

photocell was mounted onto the fume hood, directly above the melt, and focused on the mouth of the crucible.

The composite samples that were used to assess the thermal behavior of the insulation had thermocouples implanted at various locations along the core wire/insulation interface. Those wires used for volatility and pyrotechnic testing did not contain thermocouples.

4.2 Materials

4.2.1 Core Wires

Magnesium was the only volatile reagent tested. The magnesium was produced by Chromasco Inc. and came in the form of extruded wires measuring 3.2mm in diameter and had a purity of 99.9%. In addition to the magnesium cores, aluminum cores were also used for some thermal tests. Since magnesium and aluminum have similar thermal diffusivities and melting points, aluminum cores were used to determine the effect of Mg volatilization on the thermal behavior of the insulation. The aluminum wires were supplied by Alcan in the form of extruded rods (4043 grade) 3.2mm in diameter and 1m in length. Both the magnesium and aluminum wires were cut into 30 or 36cm lengths in order to make the composite samples.

4.2.2 Insulating Materials

The insulating materials used in the first part of the present study were made of powdered glass of various compositions and viscosities. The powdered glasses were of the following three types:

1.) Soda-lime glass powder: This powder was produced by crushing and grinding soda-lime window glass and soda-lime glass tubes obtained from Fisher.

2.) Modified glass powders: These powders were made by melting mixtures of soda-lime powders and various amounts of other compounds such as CaO , CaF_2 , and Na_2CO_3 . The glasses produced were then reground to a fine powder with the aid of a miniature ball mill. The powders were subsequently analyzed for their approximate compositions.

3.) Continuous casting mold fluxes: These powders were acquired from the Mobay Chemical Company. They are marketed under the 'Pemco' trade name and are used specifically for lubrication in the continuous casting of steel. The powders are prefused fluxes of homogeneous composition and are considerably less viscous than soda-lime glass powder.

The powders used in this present study are listed in Table 4.1 along with their approximate compositions and viscosities. The compositions of some of the Pemco powders are not available because they are proprietary.

In the second part of the present study, glass woven tape was used as the insulating material. Supplies of the glass tape were purchased from Mudge, Watson Canada Inc. and Ajax Magnethermic. Both tapes were 0.25mm in thickness. The 'Mudge, Watson' tape was 3.8cm in width and was supplied in rolls of 33m in length while the 'Ajax' tape was 5.1cm in width and was supplied in 45m rolls. The glass tapes are exceptionally flexible, non-flammable and quite strong and durable. The Mudge, Watson tape retains 75% of its strength at 343°C , softens at $732-800^\circ\text{C}$, and melts at $1121-1182^\circ\text{C}$. Its thermal

TABLE 4.1
COMPOSITION AND VISCOSITIES OF EXPERIMENTAL POWDERS

POWDERS	SiO ₂	Na ₂ O	CaO	MgO	Al ₂ O ₃	CaF ₂	Other	Viscosity (1573 K)* (dPa-s)
Soda-lime (1)	73	17	5	4	1	0	0	300
2	40.5	8.7	39.1	1.91	1.0	8.2		1.9
3	51.2	4.5	28.2	2.5	1.1	11.9		8.0
4	52.7	6.8	34.2	2.7	0.8	2.0		9.4
5	57.3	6.1	23.3	2.5	1.2	9.0		21.8
FM408	33	13	30	2	tr		F-12	
FM914	48	15			12		K ₂ O-5 ZrO-1 B ₂ O ₃ -17 F-2	
FM907								
FM938								
1693								

* 1 dPa-s = 1 dyne-second/cm²

conductivity is $0.87 \text{ W/m}^\circ\text{C}$. The specifications for the Ajax tape are not available. Both glass tapes are from the 'E-glass' family of tapes and their chemical compositions are shown in Table 4.2. A photograph of a roll of tape is shown in Figure 4.4.

4.2.3 Metal Sheathing

In the first part of this study, copper and steel tubes were used to contain the powdered glass insulation. The dimensions of the tubes used are shown in Table 4.3. The steel tubes were cold-rolled electrically welded tubes of SAE 1010/1015 grade. The copper tubes consisted of the standard plumbing pipes.

4.2.4 Thermocouples

In order to assess the thermal behavior of the composite samples used in the study, chromel-alumel thermocouples were implanted at various locations along the core wire/insulation interface. The thermocouples were flexible and very inexpensive (i.e. about \$0.60 per foot) and were insulated by a coating of braided glass. The thermocouples were approximately oval in cross-section ($0.9\text{mm} \times 1.4\text{mm}$) and were supplied by Thermo-Kinetics (Montreal) in 6m rolls. The thermocouples were cut to the desired length and the chromel-alumel wires were fused together at one end.

For the hand-dipping experiments, the thermocouples were placed 3.0cm from the leading end of the core wires, whereas for the samples that were fed into the bath by the wire feeder, one

TABLE 4.2
CHEMICAL COMPOSITIONS OF TAPES

Component	Mudge, Watson	Ajax
Na ₂ O	0.61	0.67
K ₂ O	0.19	0.25
CaO	21.7	21.87
MgO	1.0	0.57
SiO ₂	55.4	53.44
Al ₂ O ₃	15.6	14.61
B ₂ O ₃	4.2	5.0
Fe ₂ O ₃	0.56	0.4
MnO	0.03	0.04
P ₂ O ₅	0.06	0.064
Cr ₂ O ₃	0.1	0.1
V ₂ O ₅	0.01	0.01
ZnO	0.01	0.01
TiO ₂	0.63	0.58

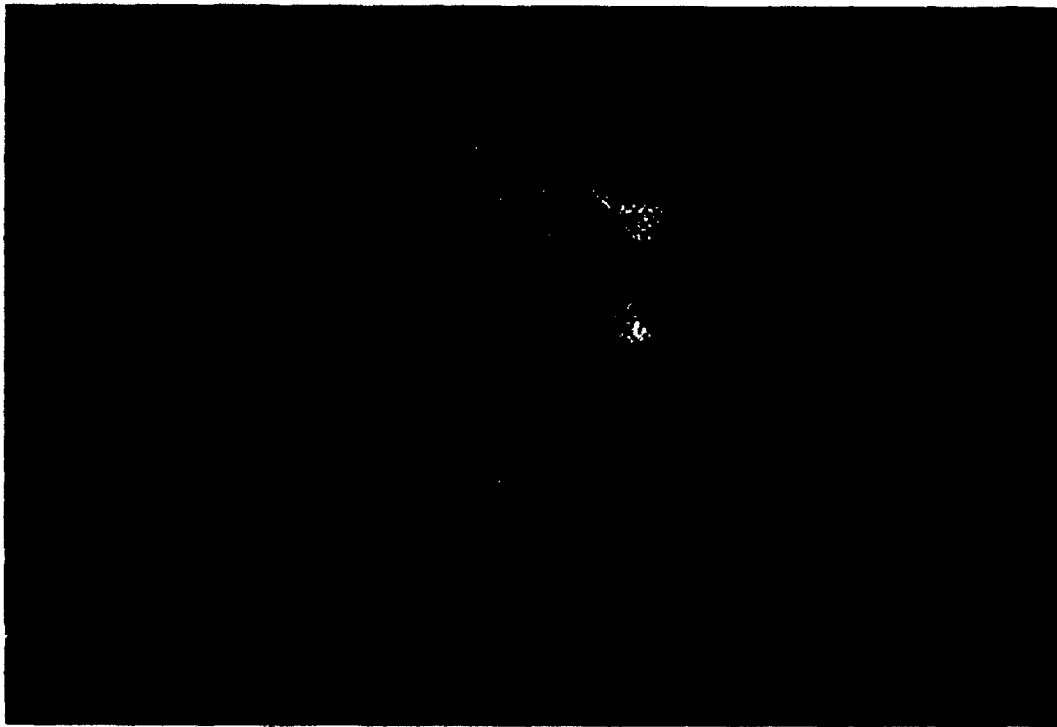


Figure 4.4. Photograph of a roll of Mudge, Watson tape.

TABLE 4.3
SHEATHING DIMENSIONS

<u>Tube</u>	<u>O.D. (mm)</u>	<u>Wall Thickness (mm)</u>
copper	9.5	1.0
"	12.7	1.0
"	22.0	1.0
steel	15.9	1.5
"	19.1	0.9

thermocouple was placed 10cm from the leading end while another was placed 20cm from the leading end.

4.2.5 Molten Baths

Molten baths of pig iron were used for all experiments in this present study. The pig iron baths were prepared from ingots of 'Sorel' pig iron which was produced and supplied by Quebec Fer et Titane Inc.(Q.I.T.). The carbon and sulphur content of the pig iron was 3.9% and 0.024% respectively. In the case of the desulphurization experiments, additional sulphur was introduced into each melt with a graphite bell plunger containing pyrite (FeS_2) powder wrapped in aluminum foil. The sulphur content was normally increased to about 0.10%S.

4.2.6 'Dummy' Bars

In order to determine the 'zero time' of each test, 'dummy' bars were used. Zero time refers to the instant the leading end of the composite wire made contact with the melt surface. This time was determined by measuring the electrical resistance between the dummy bar and the actual test sample as they were simultaneously fed into the molten bath. As the dummy bar and the test sample made contact with the bath surface the electrical resistance decreased thus pin-pointing the zero time. The dummy bar was a 3.2mm diameter aluminum rod.

For the samples that were hand-dipped into the molten bath, the same principle was used to determine the zero time, however, instead of using an aluminum rod, an open ended thermocouple of

the type described in section 4.2.4 was attached to the outer surface of the composite wire. In this case the resistance between the two thermocouple leads was measured.

4.3 Procedure

4.3.1 Preparation of Glass Powder Insulated Samples

The glass powder insulated samples comprised of an inner core of magnesium or aluminum, packed in glass powder and contained within a steel or copper tube. Basically, the purpose for the metal tube was to contain the glass powder long enough to allow the outer surface of the powder to fuse. This fused portion would support the remaining unfused glass. A description of the construction of the sample will be outlined below.

A piece of core wire measuring 3.2mm in diameter was cut to length, pointed at one end and threaded on the other. The threaded end was then screwed into a 6.35mm threaded steel handle measuring 35.5cm in length. The handle was screwed into an aluminum cap which was subsequently fitted into one end of the metal tube (see Figure 4.5). Glass powder was then funnelled into the tube/wire assembly and compacted with a vibrator. A centering device was inserted into the metal tube during compacting to ensure that the magnesium wire remained centered as the tube was being filled. This centering device consisted of a pair of concentric glass tubes held together with a Teflon seal as shown in Figure 4.6. After the tube was filled with the powdered glass the open end was sealed with an aluminum cap. For

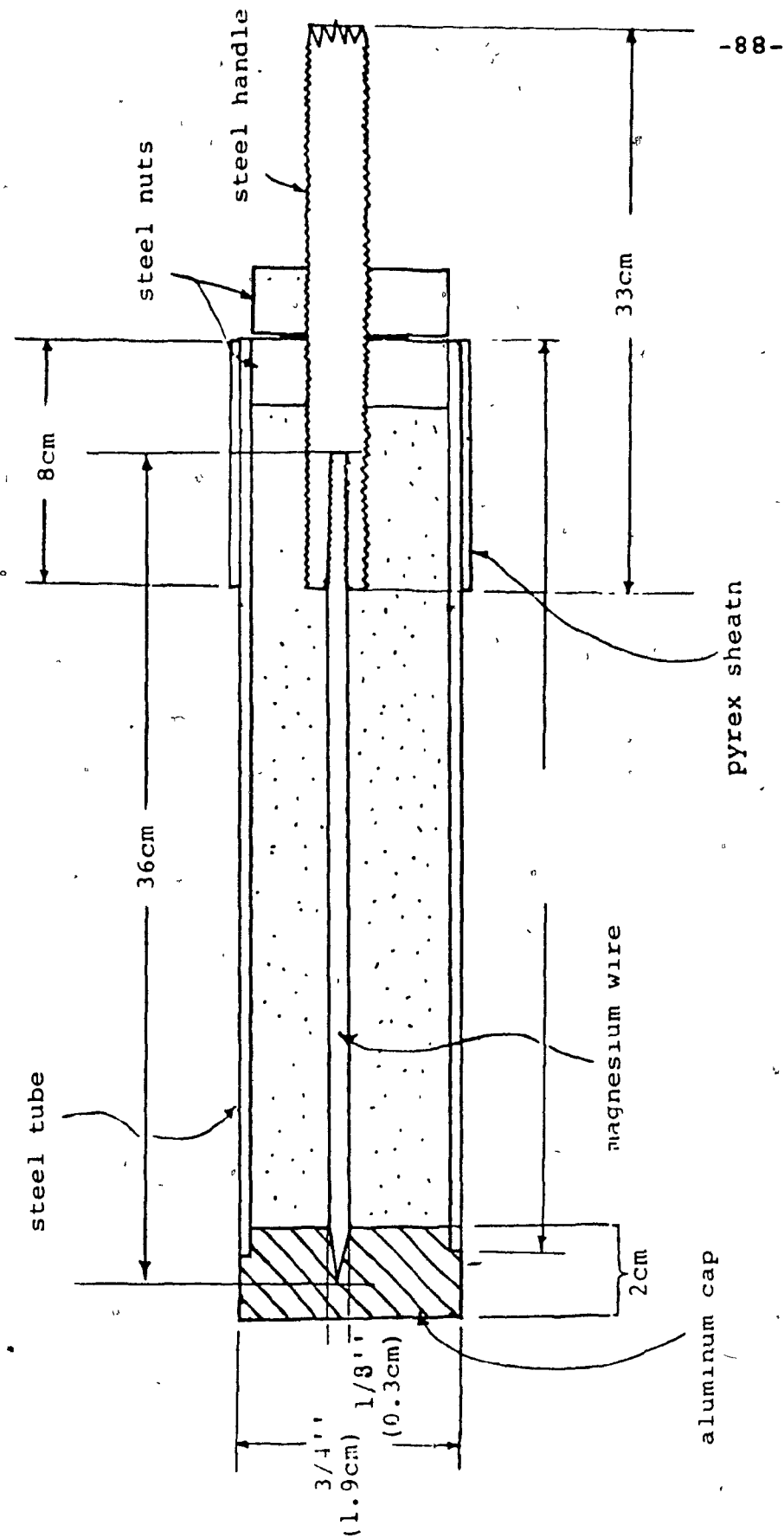


Figure 4.5. Schematic of a metal sheathed composite magnesium wire sample showing the dimensions of the various sections.

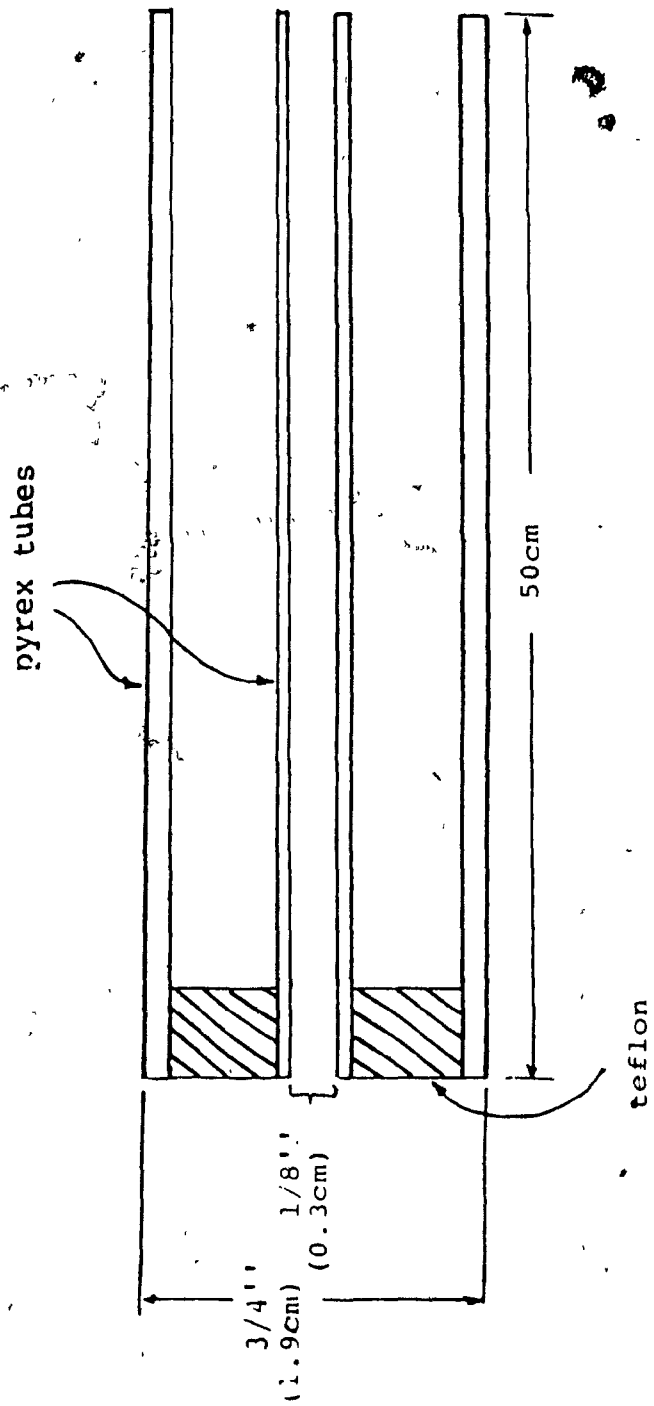


Figure 4. Schematic of the centering device.

the case where thermocouples were used, the tips of the thermocouples were tied to the core wires with thin metal wires while the trailing ends of the thermocouples were passed through 1.5mm holes bored through the aluminum cap at the handle end of the sample so that they could be connected to the data acquisition unit. A photograph of a typical sample is shown in Figure 4.7.

The steel handles, core wires, metal tubes and Al caps were given a thorough washing in acetone (to remove any grease and dirt that may have accumulated during their preparation) prior to assembly.

4.3.1.a Preparation of Glass Powders

As was pointed out in section 4.2.2., three groups of glass powders were utilized in this study: 1) soda-lime glass powder, 2) modified soda-lime glass powders, and 3) continuous casting mold fluxes. The continuous casting mold fluxes were acquired from the Mobay Chemical Company, while the other two groups were prepared at McGill University by the author. The soda-lime was produced by crushing and grinding soda-lime glass windows and/or soda-lime glass tubes in a miniature ball mill. The glass was ground to 100% -32 mesh.

It was believed in the early stages of this present study that the soda-lime powder was too viscous when immersed into the metal, consequently it was decided to test less viscous glass powders. This was accomplished by acquiring continuous casting

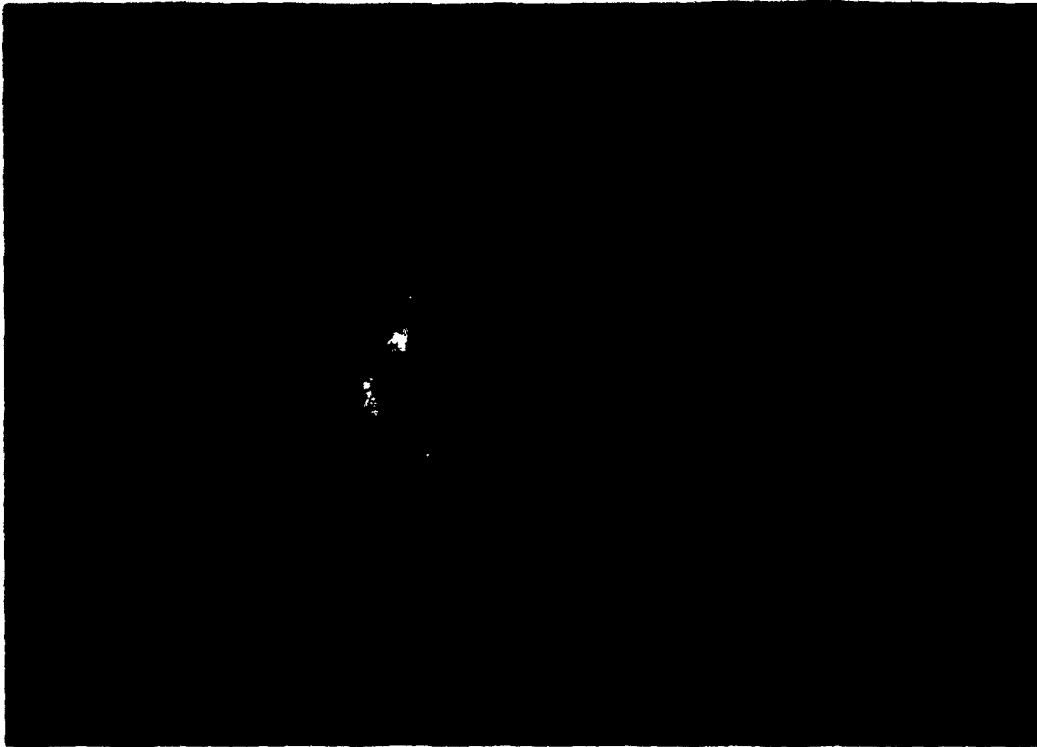


Figure 4.7. Photograph of a typical glass powder insulated sample.

mold fluxes and lowering the viscosity of the soda-lime glass by adding various amounts of lime and fluorspar to it. Mixtures of soda-lime powder, CaO , and CaF_2 were melted in a graphite crucible by induction heating. When the glass was completely molten it was poured into a metal container to cool. Afterwards, the glass was crushed and ground in a ball mill to 100% -32 mesh. Four different powders were obtained in this fashion. The compositions of the powders that were produced were presented in section 4.2.2. of this chapter.

4.3.2 Preparation of Glass Tape Insulated Samples

The core wires and steel handles were prepared in a similar fashion to those of the glass powder insulated samples. In the case where thermocouples were required, they were tied onto the core wires at the desired locations. The samples were then wrapped with the glass tape until the desired insulation thickness was attained. It is important to note that approximately 25cm of the steel handles were also wrapped to allow the last portion of magnesium to be fed deep into the molten bath. A photograph of typical glass tape insulated samples is shown in Figure 4.8.

4.3.3. Hand-Dipping Experiments

Two types of dipping experiments were conducted in this study. The first type was qualitative in nature whereas the other was conducted to assess the heat transfer characteristics of the insulating materials.

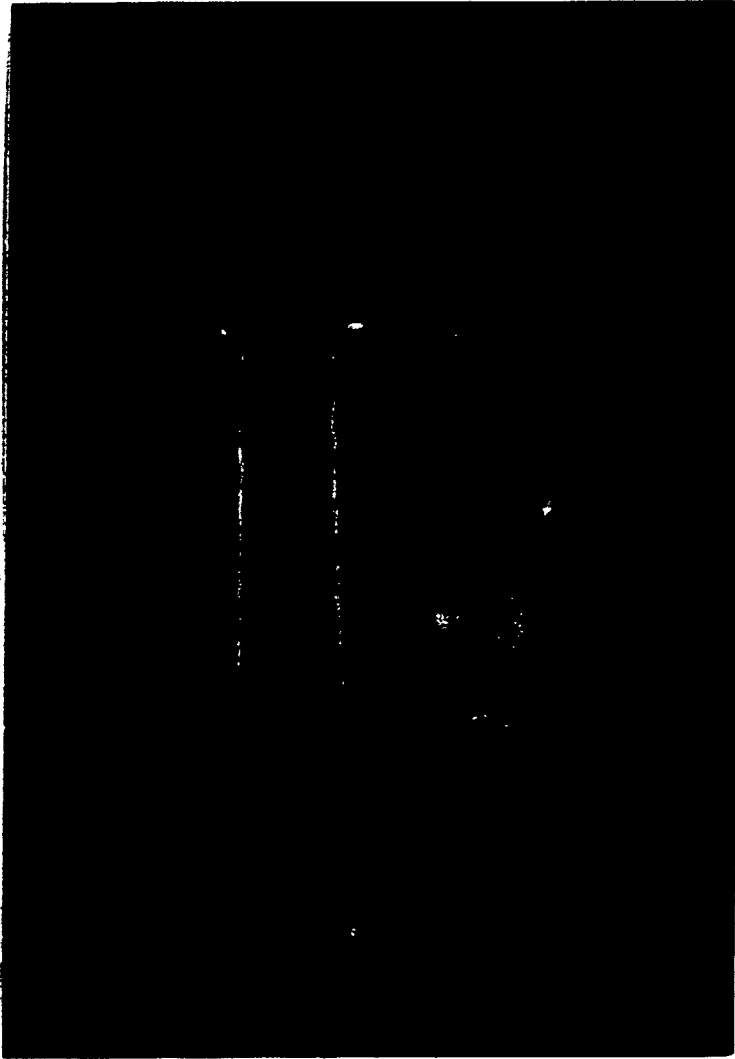


Figure 4.8. Photograph of typical glass tape insulated samples.

4.3.3.a. Qualitative Tests

The initial tests of this study were qualitative in nature and were conducted to develop an appreciation for the manner in which the various glass powders fused or were consumed. The composite samples were approximately 15cm in length and the steel sheathing measured 1.9cm in diameter. The core consisted of a 3.2mm Al core. The tests were conducted in a 22 kg molten pig iron bath. The bath temperature was raised to about 1400°C and the power was turned off prior to the manual immersion of the samples. The samples were then held in position for approximately 45 seconds. After the samples were withdrawn from the bath, they were left to cool. Photographs of the samples were then taken. Some samples were broken apart to assess the 'integrity' of the Al core.

4.3.3.b. Heat Transfer Tests

Heat transfer experiments were conducted on two types of composite sample configurations. The first configuration consisted of an aluminum core surrounded by glass powder. These samples had thermocouples embedded at various locations along the core wire/glass powder interface. The second configuration consisted of an aluminum core insulated with glass tape. The samples measured 15cm or 30cm in length and the aluminum core diameter was 3.2mm. The insulation thickness varied from 1.5 to 5.5mm. All tests were conducted in 22kg molten pig iron baths at 1400°C.

A data acquisition program was used to monitor the temperatures at various locations along the core wire. One channel of the data acquisition unit was used to measure the resistance between the two leads of an open-ended thermocouple while one or two other channels, depending on the number of thermocouples, were used to monitor internal temperatures. When a composite sample made contact with the bath surface, the chromel alumel circuit was closed thus changing the resistance of the circuit. This change in resistance triggered the internal clock to start measuring the immersion time.

At the start of each test, the program was provided with the desired immersion time. At this point the program went into a delay mode. The bath temperature was measured to ensure that it was maintained at 1400°C , the induction furnace power was turned off, and the program was reactivated. At this point, the program began scanning all the channels. When the sample was immersed, the change in resistance activated the internal clock. Once the clock was activated, only the channels monitoring temperatures were scanned. As the desired immersion time was reached the terminal 'beeper' was sounded three times. All the pertinent data was then stored on cassette. The temperatures were stored as millivoltage readings. Another software package was used to retrieve the stored data and convert the voltage readings to temperatures. The results were then plotted on a Hewlett Packard plotter. All programs were written in BASIC.

4.3.4 Temperature Profiles and Pyrotechnic Tests

Two composite sample configurations were tested in these experiments. The two configurations were similar to those described in section 4.3.3.b. except that the aluminum cores were replaced by magnesium cores, and the samples were 30cm in length.

A pyrotechnic evaluation for each sample was based on the readings obtained from a photocell which was located above the bath surface. If magnesium was exposed at the bath surface it rapidly oxidized producing a bright flash.

A data acquisition program was used to monitor temperatures, pyrotechnic displays, and immersion times. One channel was used to find the zero time. The zero time was determined in a slightly different manner as described in section 4.3.3.b., however the same principle was used. Instead of measuring the resistance between the chromel and alumel wires, the resistance between the magnesium wire and a 3.2mm diameter aluminum dummy rod that was suspended beside the composite sample was measured. One lead from the channel measuring resistance was attached to the handle of the magnesium wire while the other was attached to the handle of the aluminum rod.

At the start of each test, the feeding mechanism was set to the desired feed rate by adjusting the resistance of the potentiometer on the remote control unit, the bath temperature was measured, and the program was provided with the desired

immersion time. At this point the program went into a delay mode. The wire feeder was then pushed up against the induction furnace and feeding of the sample was commenced. The program was reactivated when the sample made contact with the bath. After the sample was fully immersed, it was held in position for a few seconds to ensure that the magnesium was completely consumed before it was pulled out. The data was recorded and stored in the same fashion as described in section 4.3.3.b. The flash intensities in these experiments were also stored as voltage readings:

In order to contain any metal that was splashed out of the crucible, a ring of high temperature cement was placed around the mouth of the crucible.

4.3.5 Pyrotechnic and Volatility Experiments

These experiments were conducted in the same fashion as the temperature and pyrotechnic experiments except that the volatility of the immersed magnesium was measured instead of the temperature. The volatility was measured by means of an accelerometer attached to the frame of the furnace. Its function was to detect the extent of bubbling and explosions that occurred within the melt during the feeding. Hence for these experiments, three channels of the data acquisition unit were used to measure the contact resistance, volatility, and flash intensity.

4.3.6 Desulphurization and Recovery Experiments

The desulphurization and recovery experiments were conducted using the glass tape insulated samples only. For the recovery experiments the sulphur content of the pig iron was about 0.024%, while for the desulphurization experiments the sulphur level was raised to approximately 0.1% by plunging pyrite powder into the melt. Temperature, pyrotechnic, and volatility information was obtained from some of these experiments. In these experiments a slag cover was used to prevent the sulphur from reverting back into the bath or to prevent the dissolved magnesium from being oxidized.

Prior to the commencement of an experiment, steps were taken to ensure that the desired bath temperature and a fluid slag were attained. Furthermore, the feeding apparatus was set to the desired feed rate (usually 1.0cm/s). Before the immersion of each sample, a pin sample of the bath was taken with a glass vacuum tube for subsequent sulphur and magnesium analysis. The induction furnace power was then turned off and the magnesium sample was fed into the bath. When the magnesium was fully immersed, it was held in position to ensure that the magnesium was totally consumed. Then the sample was pulled out and the furnace power was turned back on for about 30 seconds to induce stirring within the bath. This ensured a homogeneous bath composition. At this point, another bath sample was taken. After the experiments, the samples were analysed with a Leco analyzer. The magnesium contents were analyzed by atomic absorption techniques.

CHAPTER 5
RESULTS AND DISCUSSION

The results section is divided into two parts. The first part deals with the experiments conducted with glass powder insulated samples, and the second part deals with the experiments conducted with glass tape insulated samples.

5.1 PART 1- Glass Powder Insulation

5.1.1 Dipping Experiments

The initial dipping experiments were qualitative in nature. In these experiments seven glass powders were tested. Five of these were produced at McGill University, while the other two were obtained from the Mobay Chemical Company. The five powders produced at McGill were powders 1 through 5, and the other two powders were FM408 and FM914. Their respective compositions and viscosities were presented in Table 4.1.

The dipping samples measured approximately 10cm in length. The steel sheathing was 8.6mm O.D. and the core measured 3.2mm in diameter. The thickness of the glass powder insulation was approximately 6.5mm. The core material was an aluminum rod. Aluminum was used because it has approximately the same melting point and thermal diffusivity as magnesium. Furthermore, since the samples were dipped by hand, it was safer to use aluminum. Typical dipping samples are shown in Figure 5.1.

Fourteen samples, two of each powder, were manually immersed into a pig iron bath at 1400°C. The immersion times varied between 25 and 40 seconds. Figure 5.2 shows a photograph of two



Figure 5.1. Typical dipping samples used for qualitative experiments.

samples that contained soda-lime glass. Sample 1A was immersed for a period of 30 seconds at an initial temperature of 1350°C while sample 1B was immersed for 40 seconds at 1400°C. There are two points worth noting about the two samples. First, the dissolution of the steel tube was relatively slow at 1350°C, and second, since the soda-lime remained quite viscous, it was not buoyed to the melt surface. As the aluminum core melted, the composite sample lost its rigidity causing it to bend upwards towards the melt surface with the molten aluminum still contained within the glass framework as shown in Figure 5.3.

Now consider the two samples shown in Figure 5.4. These samples were prepared with the no.3 insulating powder that was produced at McGill. This powder was considerably less viscous than soda-lime. Sample 3A was immersed for a period of 30 seconds at 1400°C while sample 3B was immersed for 25 seconds at the same bath temperature. Note the integrity of the aluminum core of sample 3B. Figure 5.5 shows sample 3A after the glass shell had been broken off. This picture shows that the thickness of the glass insulation had decreased substantially, however, the aluminum core was still relatively 'cool and rigid'. This is significantly different from the soda-lime sample shown in Figure 5.3 where the aluminum was completely molten but still contained within a significant amount of glass insulation.

The two Pemco powders, FM914 and FM408, furnished by the Mobay Chemical Company were tested in the same manner, however, these powders seemed too fluid for the present application. Figure 5.6 and 5.7 show pictures of samples containing powders



Figure 5.2. Soda-lime powder samples. Sample 1A was immersed for a period of 30 seconds at a temperature of 1350 °C while sample 1B was immersed for 40 seconds at 1400 °C.

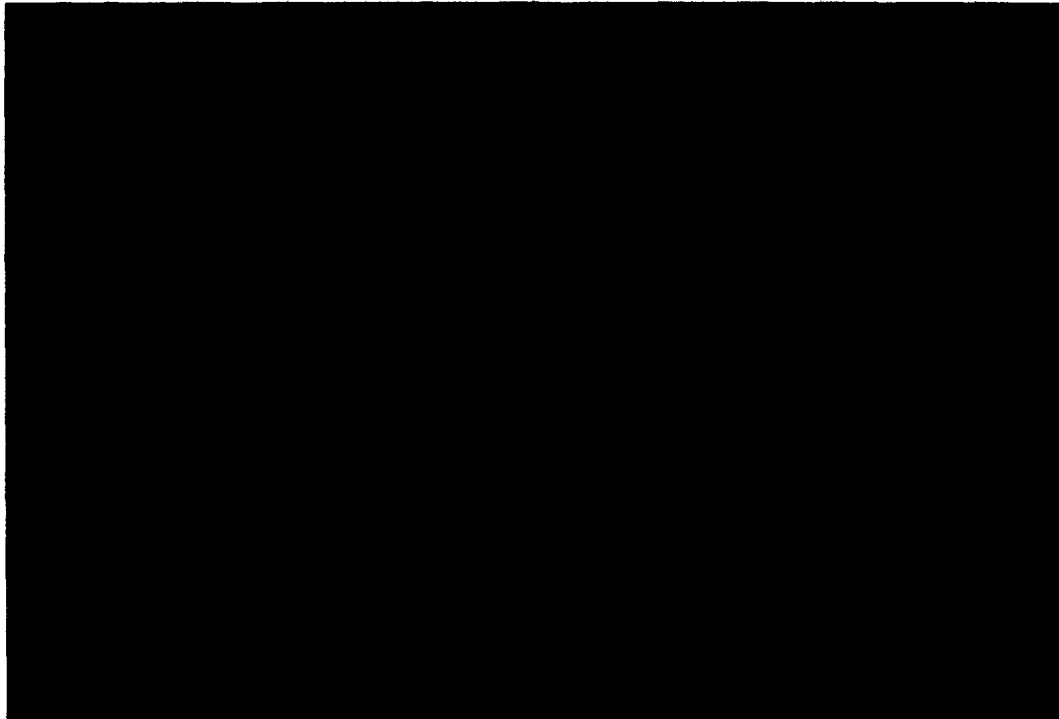


Figure 5.3 . Photograph of a soda-lime powder sample showing that the molten aluminum had been contained within the glass framework.

7

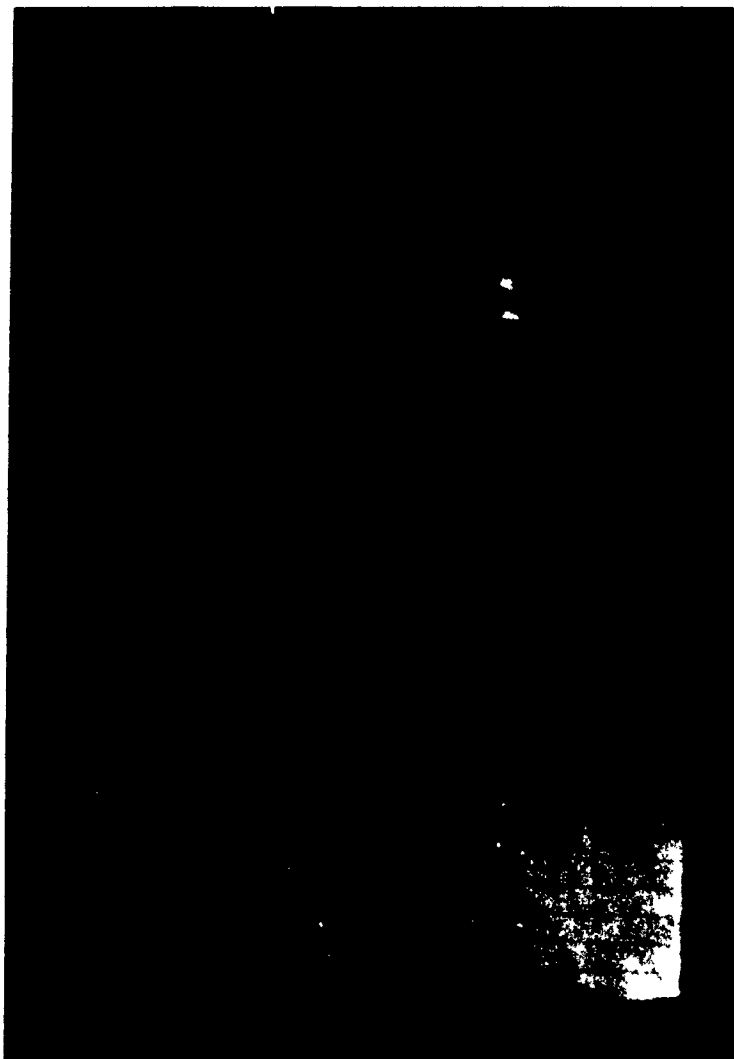


Figure 5.4. Photograph of samples containing no.3 insulating powder. Sample 3A was immersed for a period of 30 seconds at 1400°C while sample 3B was immersed for 25 seconds.

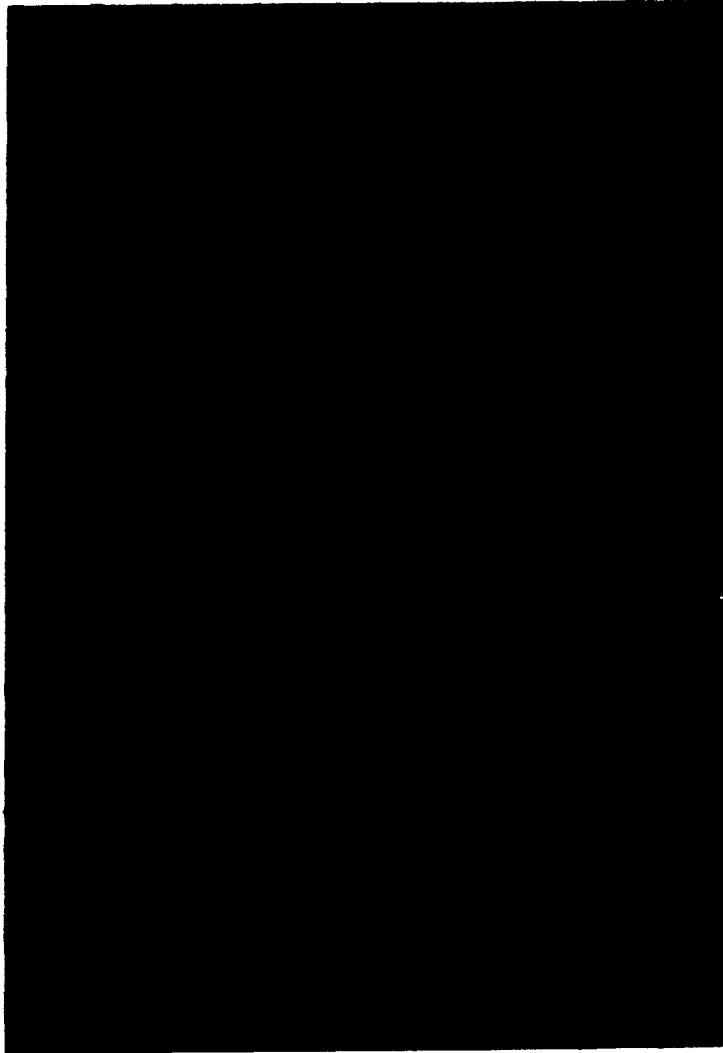


Figure 5.5. This photograph shows sample 3A after the glass shell was broken off.

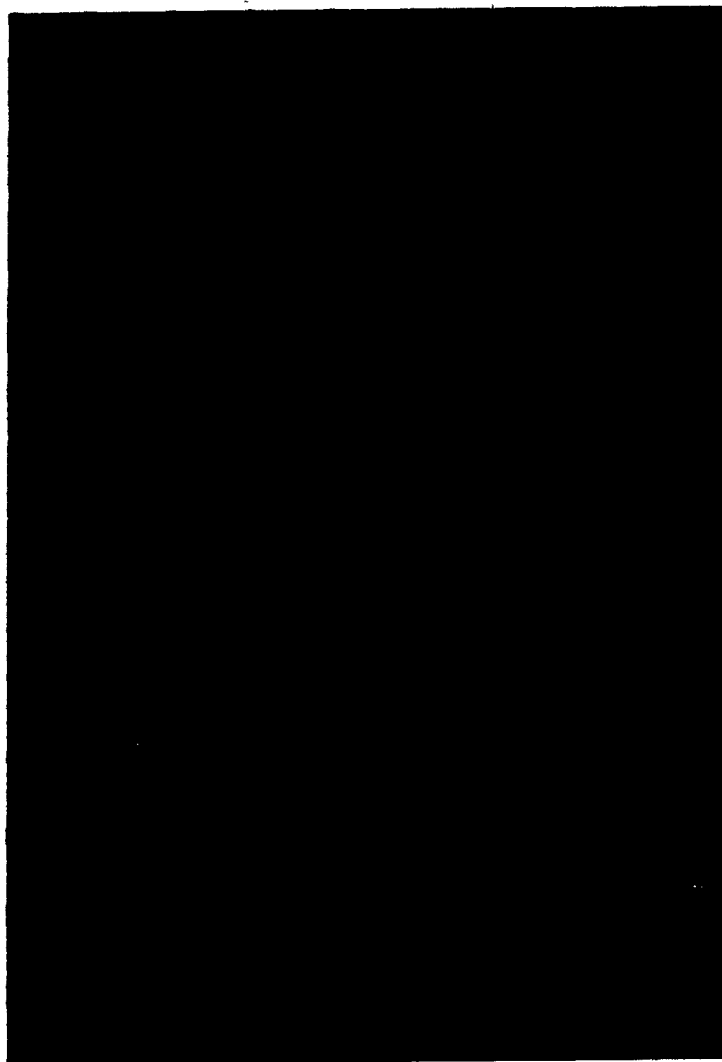


Figure 5.6. Photograph of samples containing powder FM408 after they were immersed for 25-30 seconds at 1400°C.



Figure 5.7. Photograph of samples containing powder FM914 after they were immersed for 25-30 seconds at 1400°C.

FM408 and FM914 after they were immersed for approximately 25 to 30 seconds at 1400°C. As can be seen, the glass powders and the aluminum cores were completely consumed, thus indicating that the powders would not provide sufficient protection. Powders 2, 4, and 5 showed similar results as powder 3, however powder 2 was consumed at a slightly quicker rate than 3 while 5 was consumed at a slightly slower rate as shown in Figure 5.8.

In summary, it was gathered from these experiments that the core wire can be effectively insulated so that it remains rigid, and that the wire can be made to be exposed to the bath as it begins to melt (or shortly thereafter), provided that the appropriate powder is used.

5.1.2 Heat Transfer Tests

From the qualitative experiments, it was decided that powder 3 was the most suitable powder. The Mobay Chemical Company was contacted to ascertain whether powders that exhibited characteristics similar to those of powders 2, 3, and 4 were commercially available. Pemco powders FM938 and 1693 were subsequently obtained. The compositions of these powders were not available as they are proprietary.

Rather than carrying out qualitative evaluations of the powders, as was done in the initial set of tests, it was decided that it would be better to evaluate their relative performance by assessing their heat transfer characteristics. This was achieved by embedding a thermocouple in each sample. The main objective of the initial thermocouple experiments was to

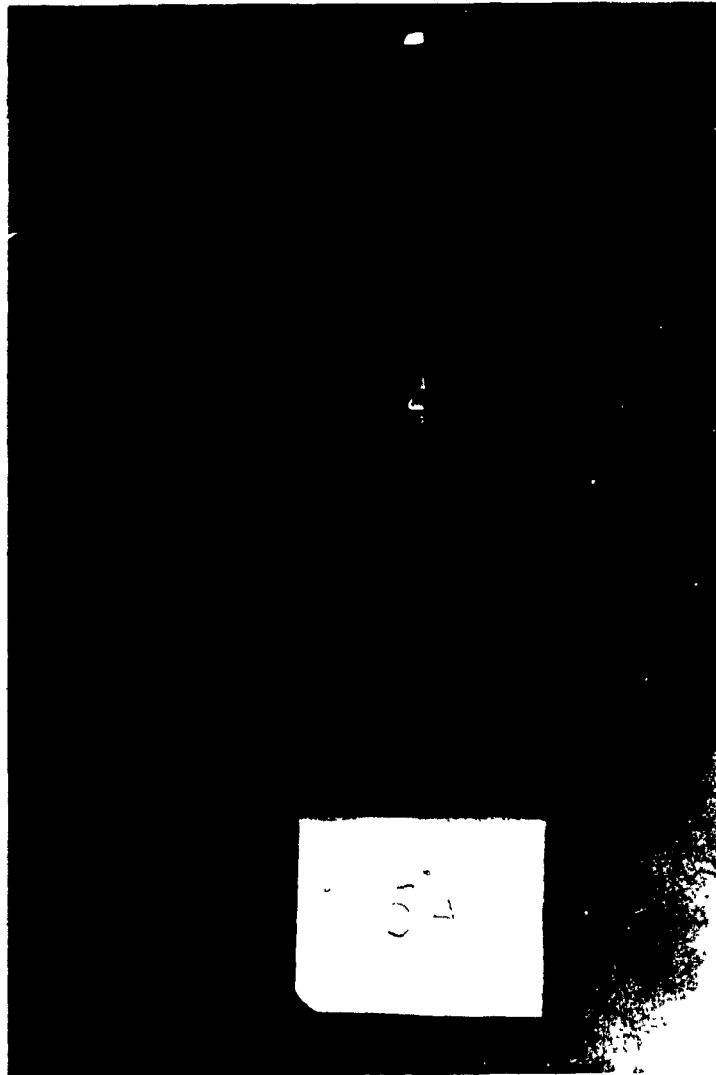


Figure 5.8. Photograph of a sample containing powder no. 5 after it was immersed for 30 seconds at 1400°C.

determine whether the thermocouples would be adequate for the present application.

For the initial test, soda-lime and Pemco powders FM408 and FM907 were used. The steel sheathing was replaced by a 2.1cm O.D. copper sheathing. As was noted in the qualitative tests, the dissolution of the steel was quite slow at 1350°C. In order to show that the protection was provided solely by the glass insulation, copper sheathing was used because the melting point of the copper is less than the hot metal temperature. The thermocouple was embedded at the glass powder/magnesium interface approximately 3cm from the leading end of the composite sample.

Nine samples, three of each powder, were immersed for approximately 60 seconds in a pig iron bath at 1350°C. Two typical temperature traces are shown in Figures 5.9 and 5.10. The thermocouples proved to be adequate for the present application. However, one observation made from the temperature traces was that for a given powder, the temperature traces did not always exhibit the same trend. Consider the trace shown in Figure 5.11. Contrast this with the one shown in Figure 5.9. Both these traces are from samples containing the same glass powder, FM907. However, as can be seen, after 30 seconds of immersion, the temperature of sample FM9073 leveled off whereas that of sample FM9071 rose dramatically. One possible explanation for this is that as the aluminum core softened or melted the composite sample bent upwards. Depending on the location of the thermocouple and the way the composite sample

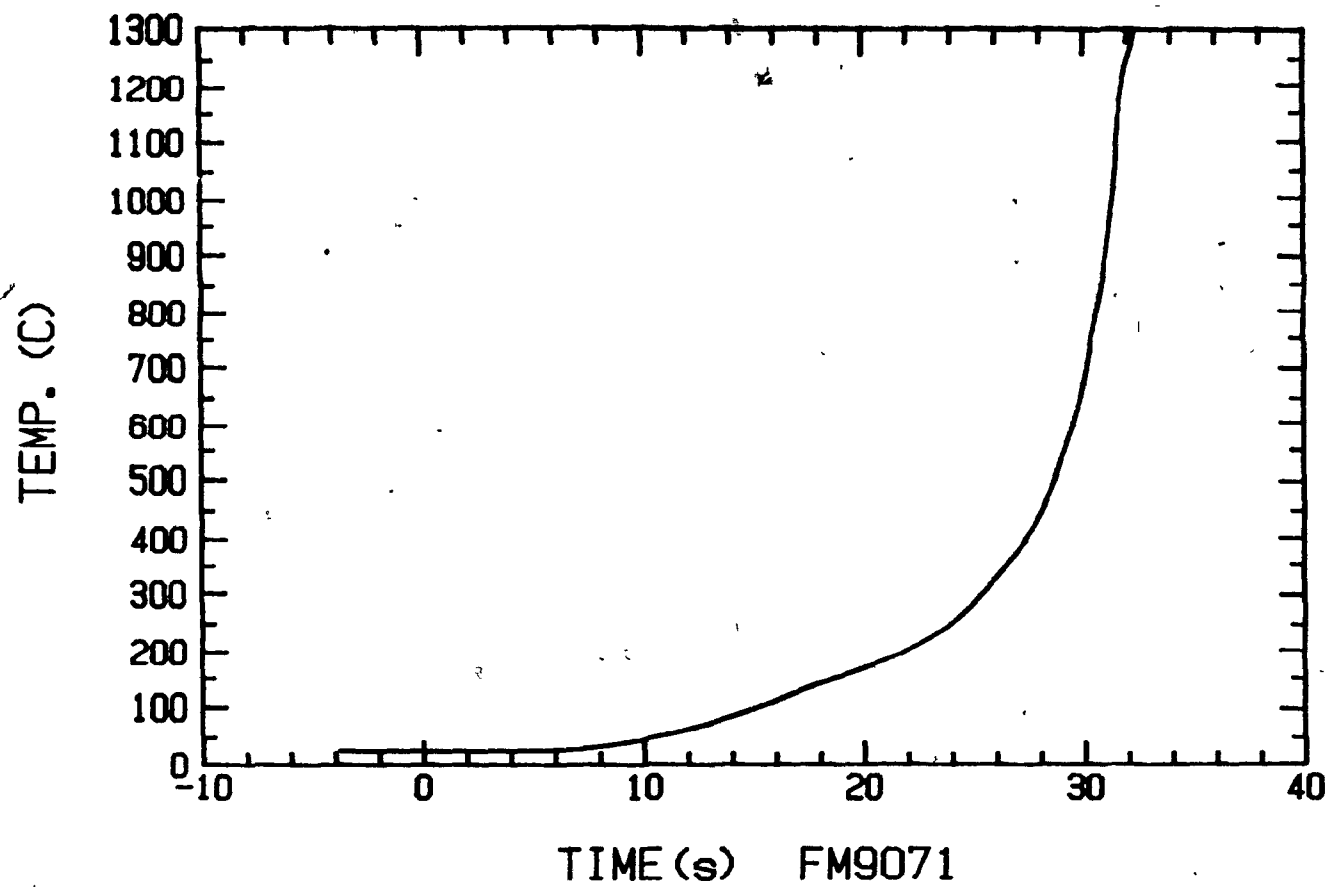


Figure 5.9 Typical temperature trace for a sample containing powder FM907 that was immersed in a bath at 1350°C.

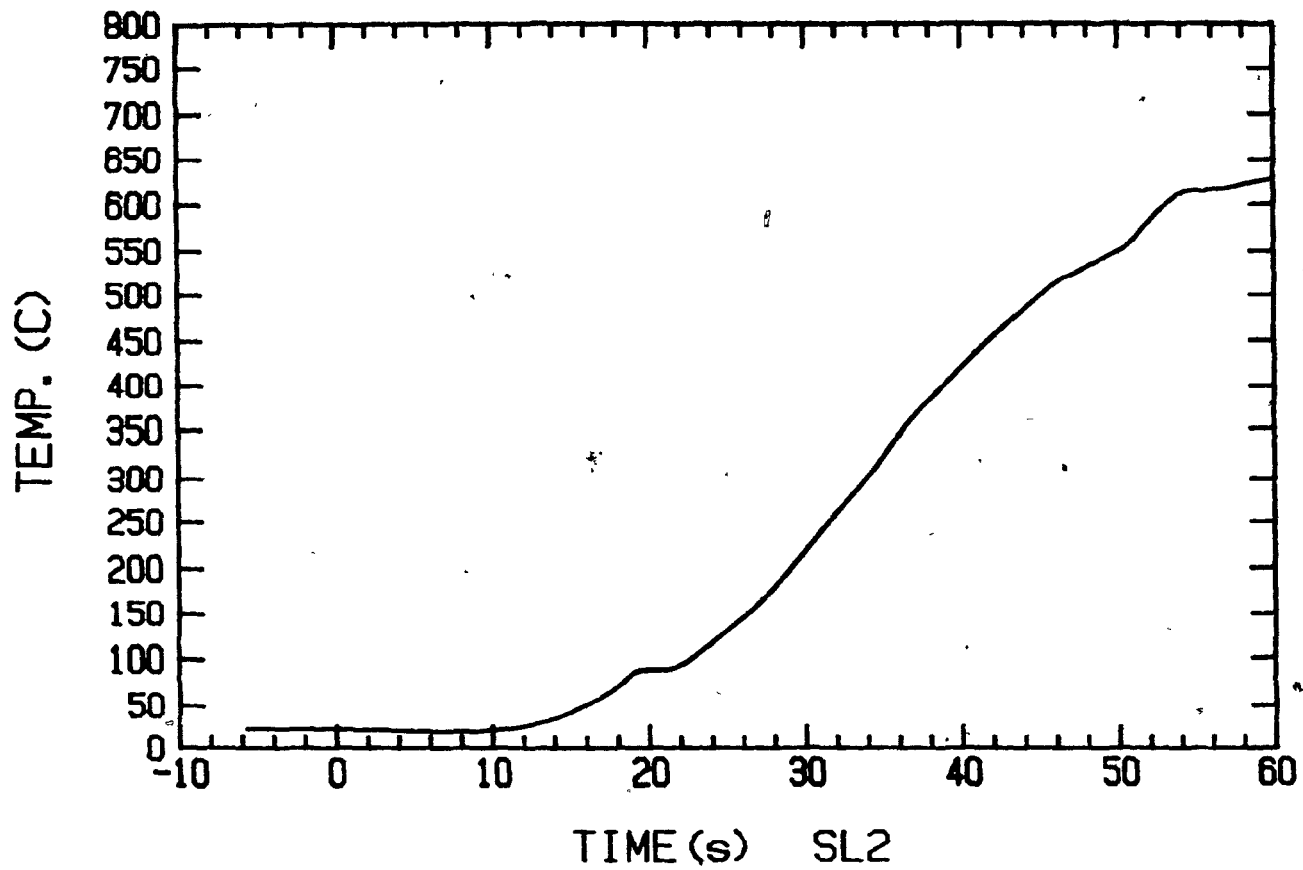


Figure 5.10 Typical temperature trace for a sample containing soda-lime powder that was immersed in a bath at 1350°C.

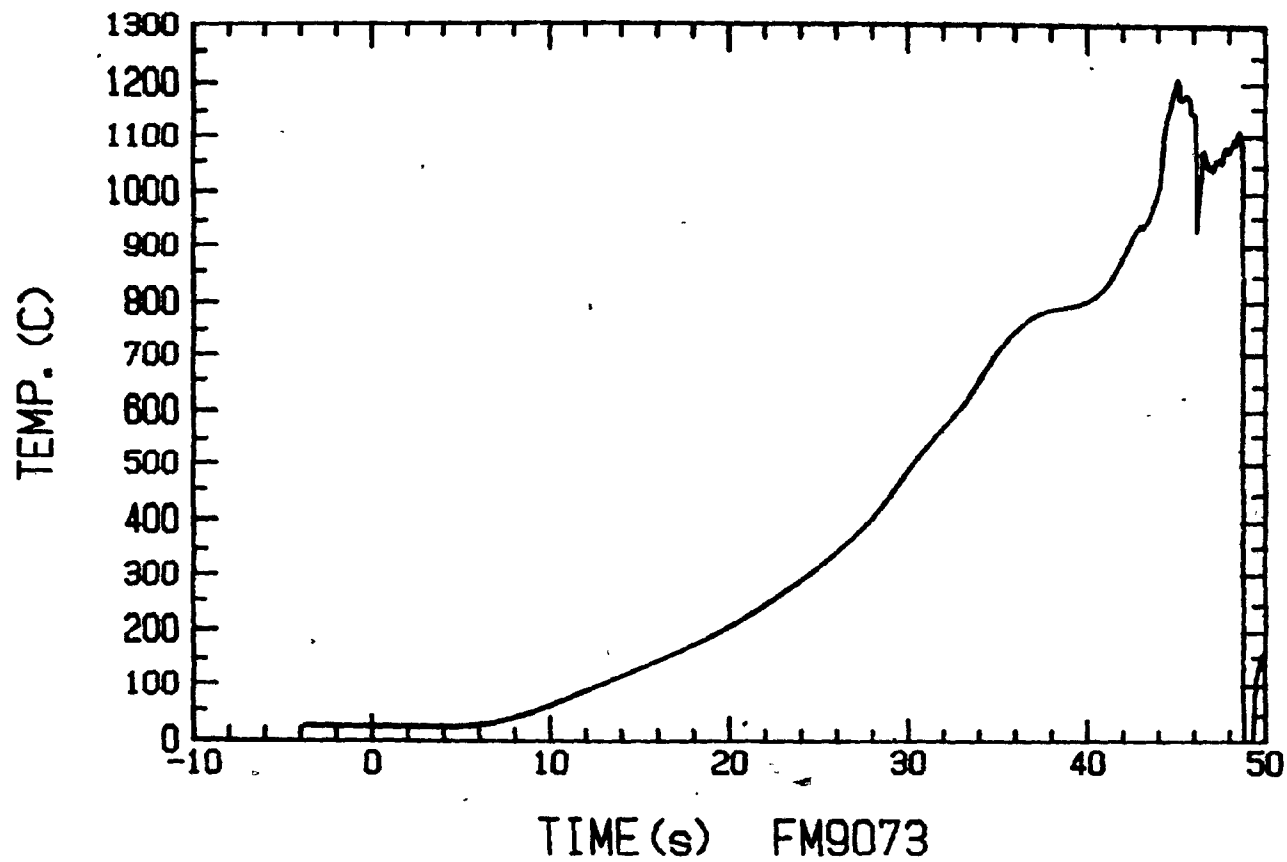


Figure 5.11 Typical trace for a sample containing powder FM907.

bent, the thermocouple was either exposed to the bath or covered up by more glass insulation. It was thought that this set up could hinder the evaluation of the various powders.

Consequently, the aluminum core was replaced by a steel core for subsequent tests. The steel core did not bend thus ensuring that the temperature responses were strictly attributable to the glass insulation.

In the next series of tests, soda-lime powder and Pemco powders FM938 and 1693 were tested. As mentioned previously, powders FM938 and 1693 supposedly exhibited the same characteristics as powders 2, 3, and 4. Figure 5.12 shows the remains of a typical sample containing soda-lime insulation. This sample was immersed for 60 seconds in a pig iron bath at 1350°C . It was evident that essentially none of the insulation had been consumed during this period. Two typical thermocouple traces for the soda-lime insulation are shown in Figure 5.13. These traces show that the core was at approximately 700°C when the sample was pulled out. If the core material was magnesium it would be just melting at this point. Considering that almost none of the soda-lime insulation was consumed, it is conceivable that a large column of liquid may have been entrapped within the glass framework. This was totally undesirable.

A typical sample containing FM938 powder, after it had been immersed for 60 seconds, is shown in Figure 5.14. From the photograph, it is apparent that the insulation was removed gradually. The extent to which it was removed can be assessed

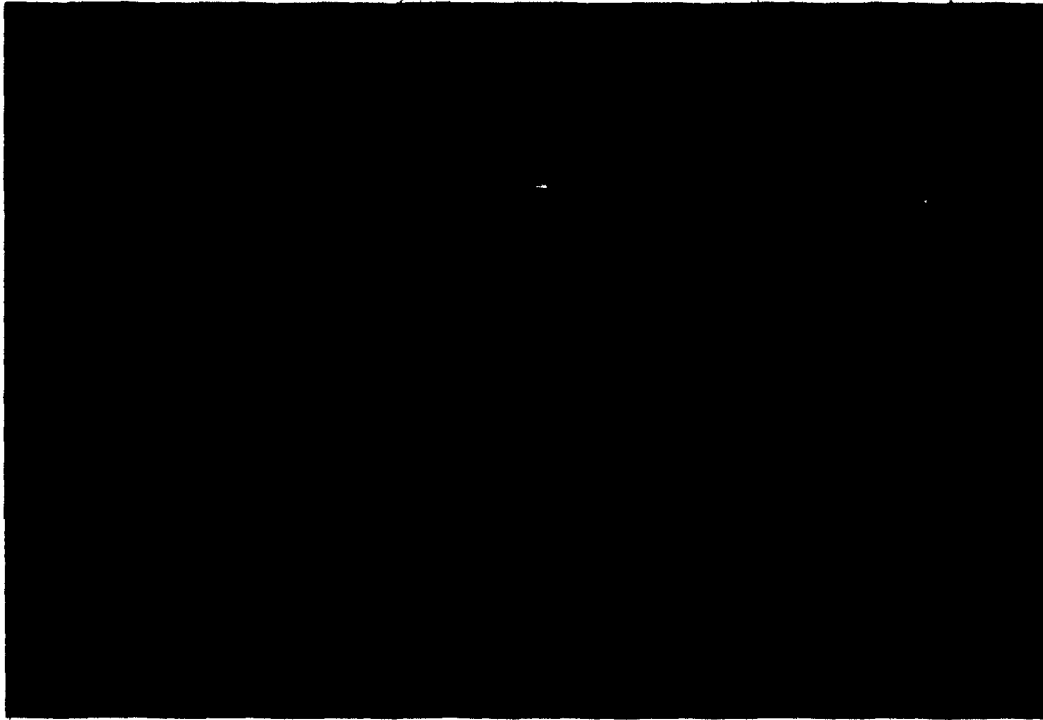


Figure 5.12. This photograph shows the remains of a typical sample containing soda-lime powder.

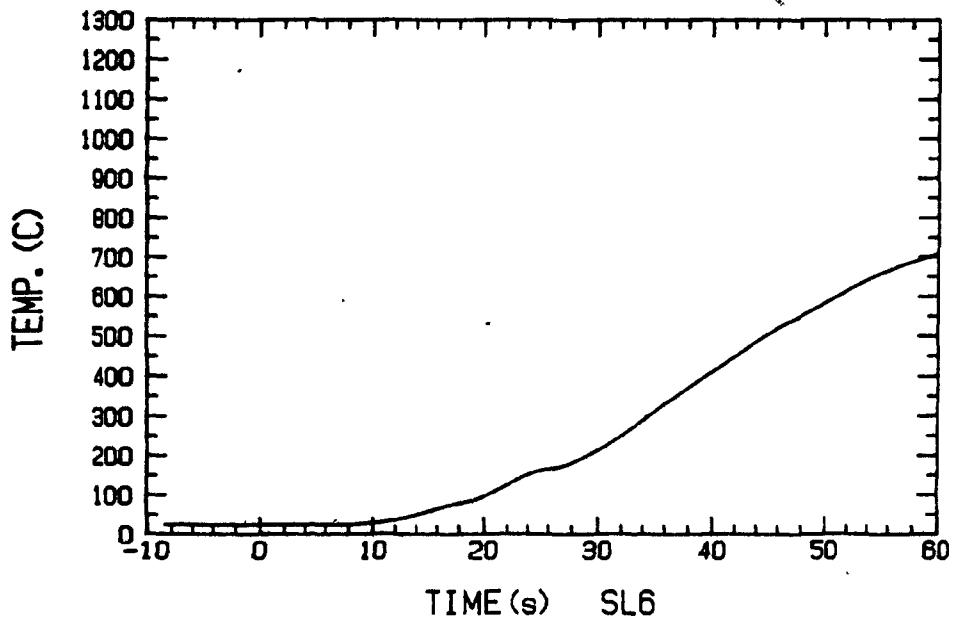
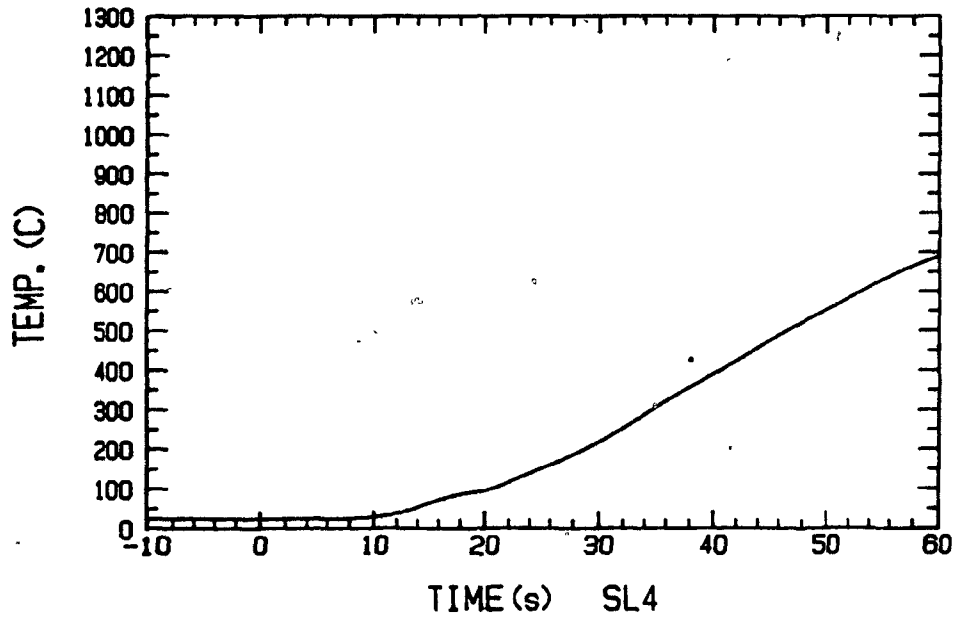


Figure 5.13 Two typical temperature traces for soda-lime powder.



Figure 5.14. Photograph of a typical sample containing powder FM938 after it was immersed for 60 seconds.

from the temperature traces presented in Figure 5.15. The traces show that the powder provided good insulation initially (i.e. the first 25-30 seconds), then the temperature quickly rose to above 650°C (the core melting point) after which the temperature increased at a significantly reduced rate. If magnesium had been used as the core, it was conceivable that a large length of magnesium within the glass framework would be liquid, as in the case with soda-lime glass. This portion of the sample would tend to bend upwards towards the bath surface, and release a large portion of the liquid magnesium close to the bath surface thus causing a violent eruption. Obviously this should be avoided.

Figure 5.16 is a photograph of the remains of a composite sample containing the Pemco 1693 powder. This sample was also immersed for 60 seconds at 1350°C . It is evident from the photograph that almost all the insulation was removed, nonetheless, enough remained to provide some insulation. A typical temperature trace of such a sample is shown in Figure 5.17. It is worth noting that this particular powder was just as good an insulator as was soda-lime in the initial stage. After about 30 seconds the temperature began to rise quickly. Then, once a temperature of 650°C was attained, the remaining insulation was rapidly consumed since the temperature reached the bath temperature shortly afterwards. From these results, one can postulate that if magnesium was used as the core material, the probability of entrapping liquid magnesium within the insulation or redirecting the liquid magnesium back to the melt surface would be minimal.

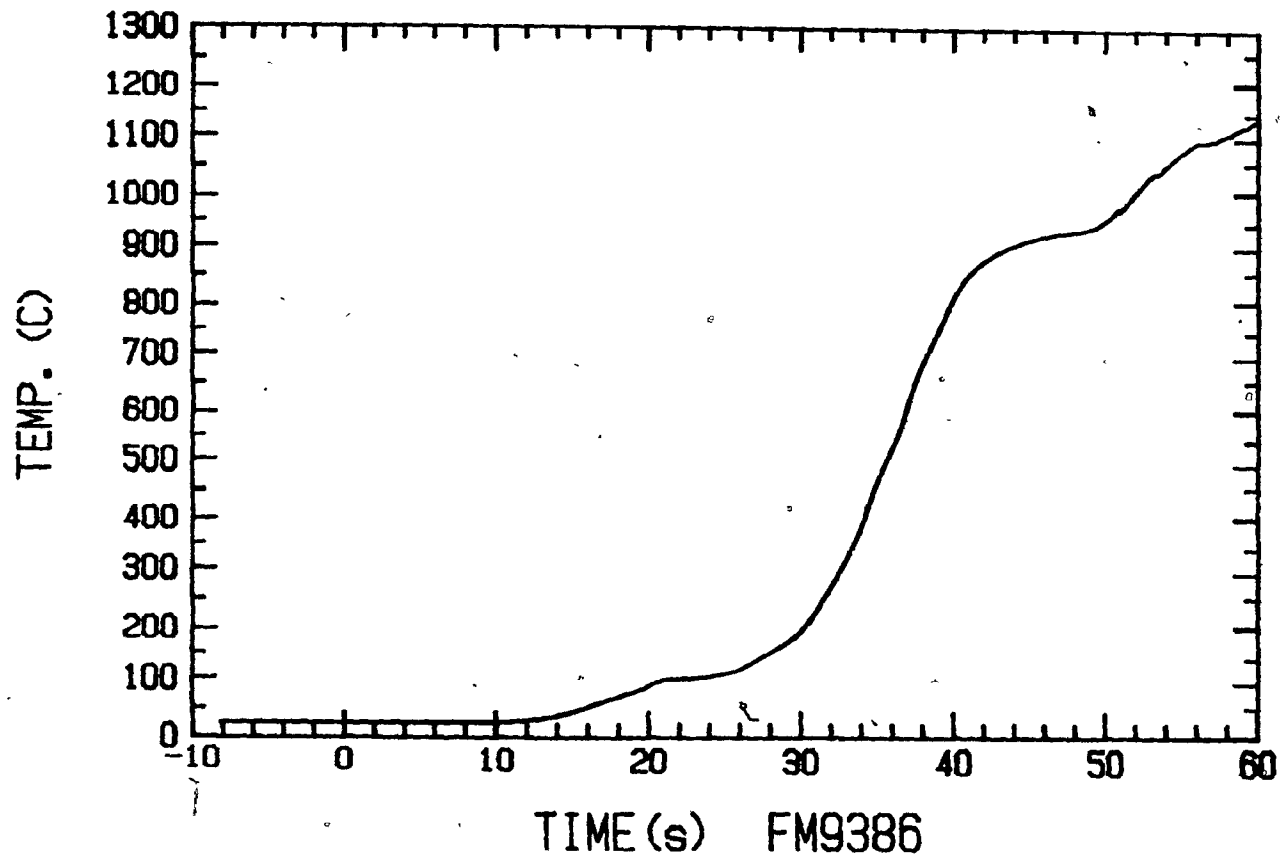


Figure 5.15 Typical temperature trace for a sample containing powder FM938.

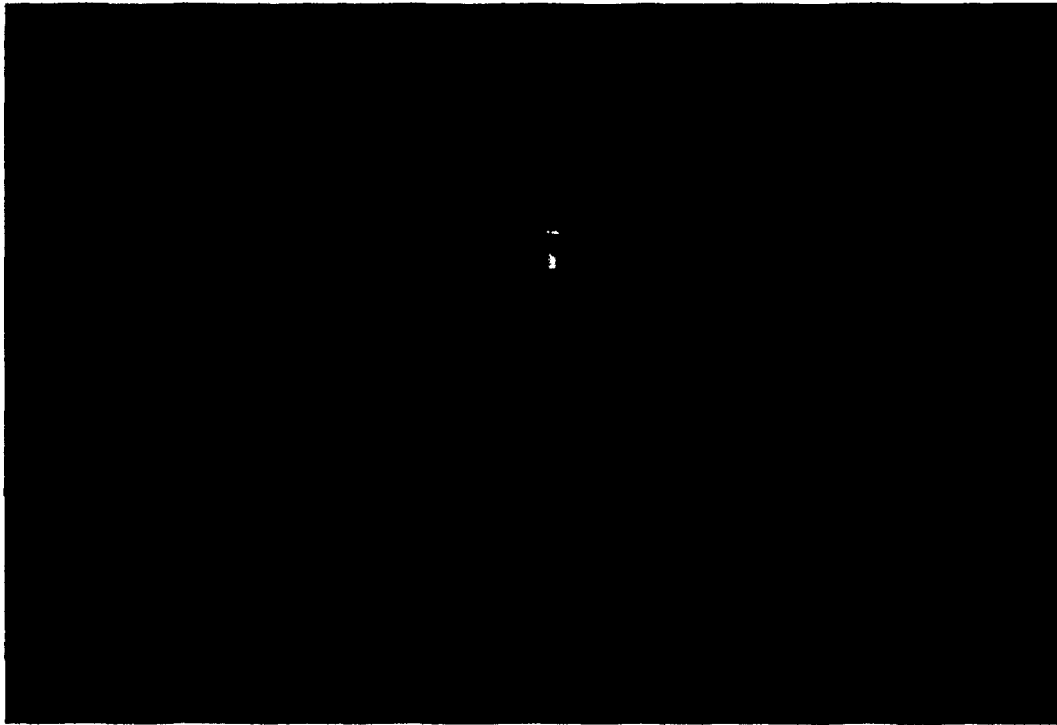


Figure 5.16. Photograph of the remains of a composite sample containing powder 1693.

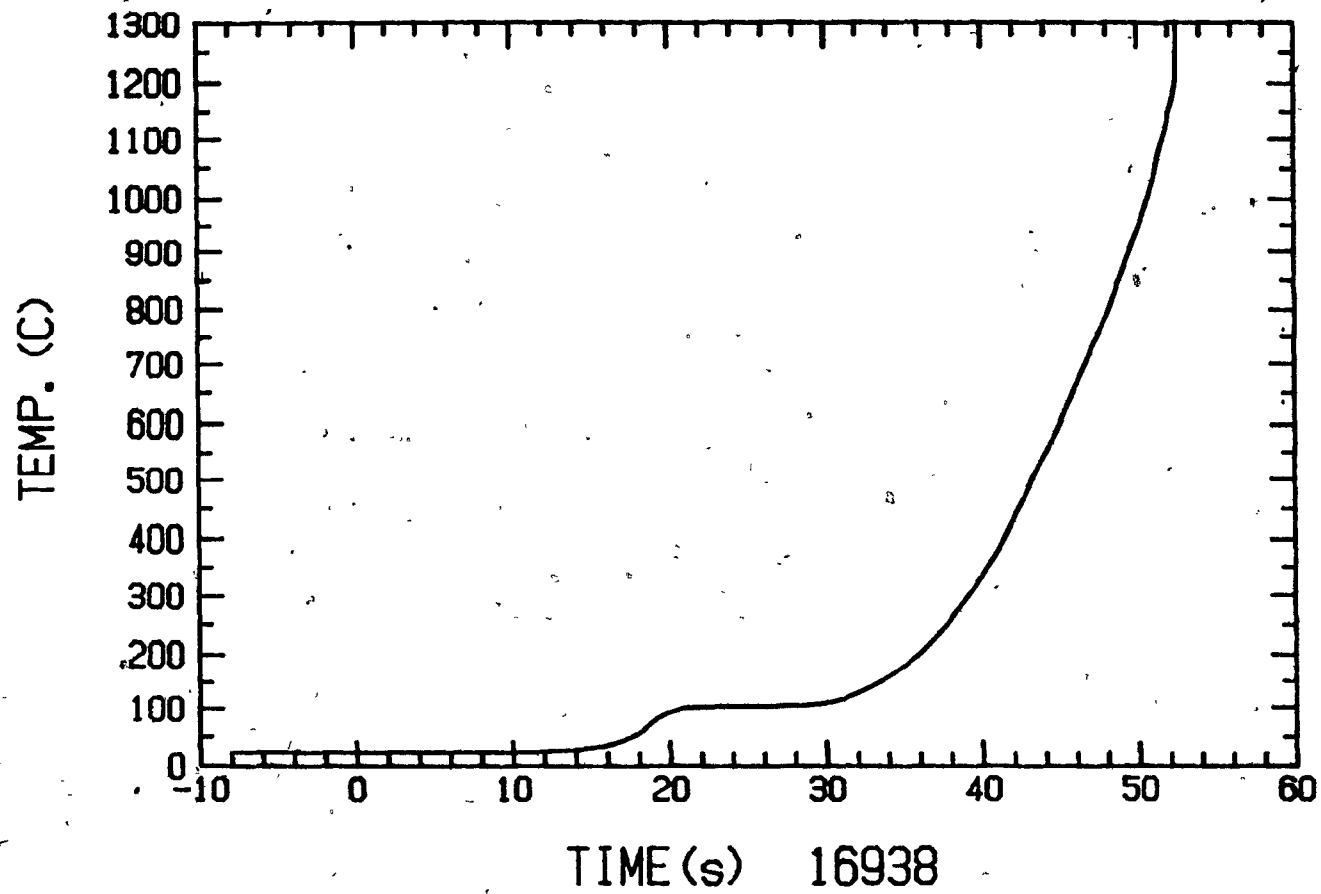


Figure 5.17 Typical temperature trace for a sample containing powder 1693.

The effect of a 5 second immersion on a sample containing powder 1693 is shown in Figure 5.18. This figure shows that the outer surface of the powder fused together as the copper sheath melted. In order for this technique to work the powder must fuse. Otherwise, the powder will be dispersed in the molten pig iron bath as the copper sheathing melts, thus leaving the core material unprotected.

Another point worth mentioning is that most of the temperature traces shown in this section exhibited a kink or a plateau at about 100°C. This was an indication of an endothermic process occurring at this temperature. It was felt that the powders picked up moisture from the air as the samples were being made. In order to verify this hypothesis, additional tests were conducted whereby half the powders tested were dried in a drying furnace for about 18 hours prior to being packed in the metal sheathing. Typical temperature traces from this experiment are shown in Figures 5.19a and 5.19b. Both set of traces were for powder 1693. The traces shown in Figure 5.19b were obtained with dried powder whereas the others were not. Note that two thermocouples per sample were used. Both thermocouples were placed about 3cm from the leading end. As can be seen from the traces, there was no difference between the dried and undried samples. The cause of the temperature arrest is still unknown, although moisture pickup after fabrication is suspect.

5.1.3 Temperature and Pyrotechnic Tests

After it was decided that a suitable powder was found (namely Pemco 1693), tests were conducted on samples containing

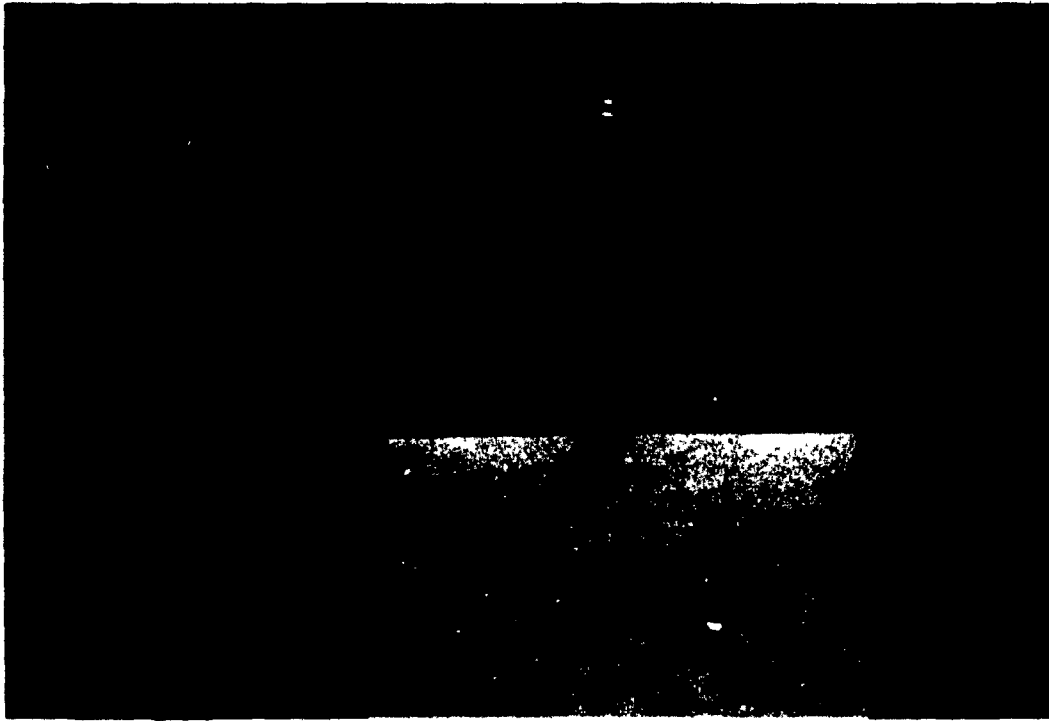


Figure 5.18. The effect of a 5 second immersion on a sample containing powder 1693..

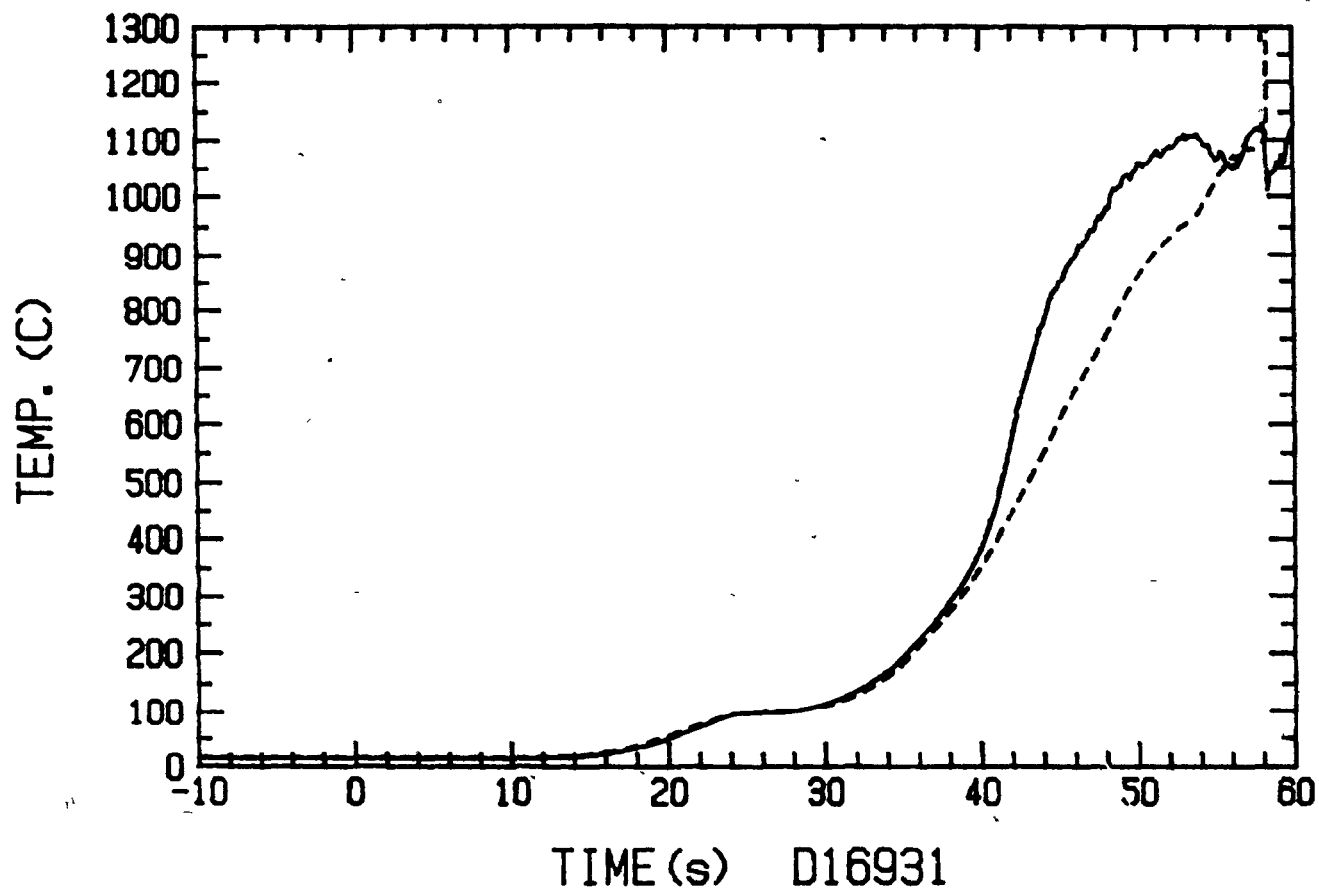


Figure 5.19a Typical temperature traces for a sample containing powder 1693. The powder was dried in a drying furnace prior to being packed in the metal sheathing.

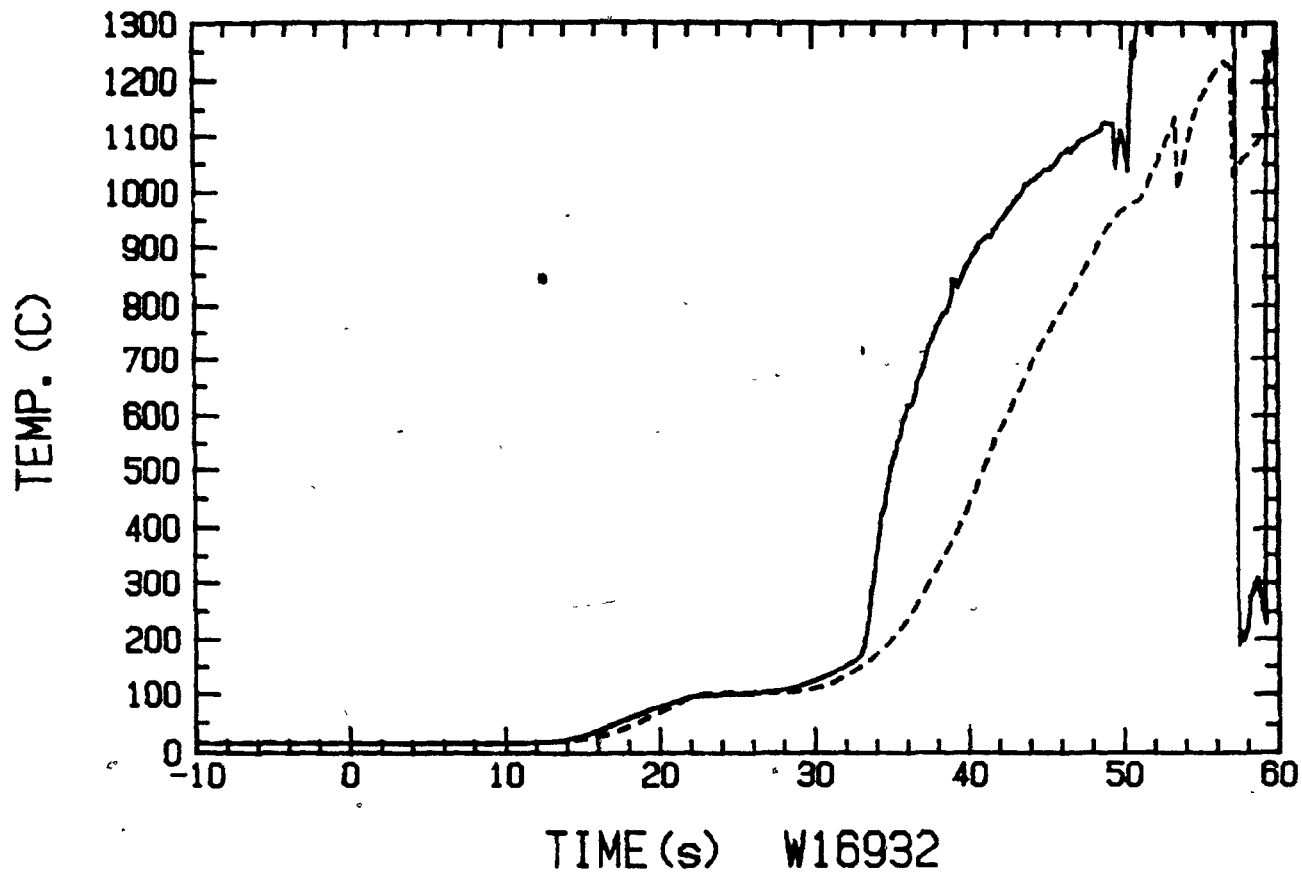


Figure 5.19b

Typical temperature traces for a sample containing powder 1693. The powder was not dried prior to being packed in the metal sheathing.

magnesium cores. The main powder tested was Pemco 1693 powder, however, other powders such as Pemco's FM907, FM408, and FM914 powders were also tested.

The magnesium composite samples were fed into a pig iron bath at 1400°C using a 'plunger' type wire feeder. The composite samples were 45cm in length and the bath depth was 25cm. The magnesium wires measured 3.2mm in diameter and weighed about 4.2g. Two thermocouples were attached to the magnesium core at distances of 10cm and 22cm from the leading end. In addition to using thermocouples, a photocell was also utilized. The photocell was placed about 1m above the crucible so that any flashes or flares that were emitted during an eruption were recorded.

It was found that the samples still exhibited violent and periodic eruptions. The eruptions were indicated by peaks in the photocell readings. Photographs of typical eruptions are shown in Figures 5.20a and 5.20b. As was stated in Chapter 2, it was believed that the violent and periodic explosions in earlier experiments in which soda-lime glass was used, were caused by the sudden release of liquid magnesium that had accumulated within the glass framework. However, this was not the case in these experiments. Consider the temperature and photocell traces shown in Figure 5.21. These traces were for a sample (MG1693) that contained 6.5mm of Pemco 1693 powder insulation encased by copper sheathing. The sample was fed at a velocity of 1.0cm/s. The traces were typical of the tests conducted. There are three points worth noting. First, the initial eruption occurred about

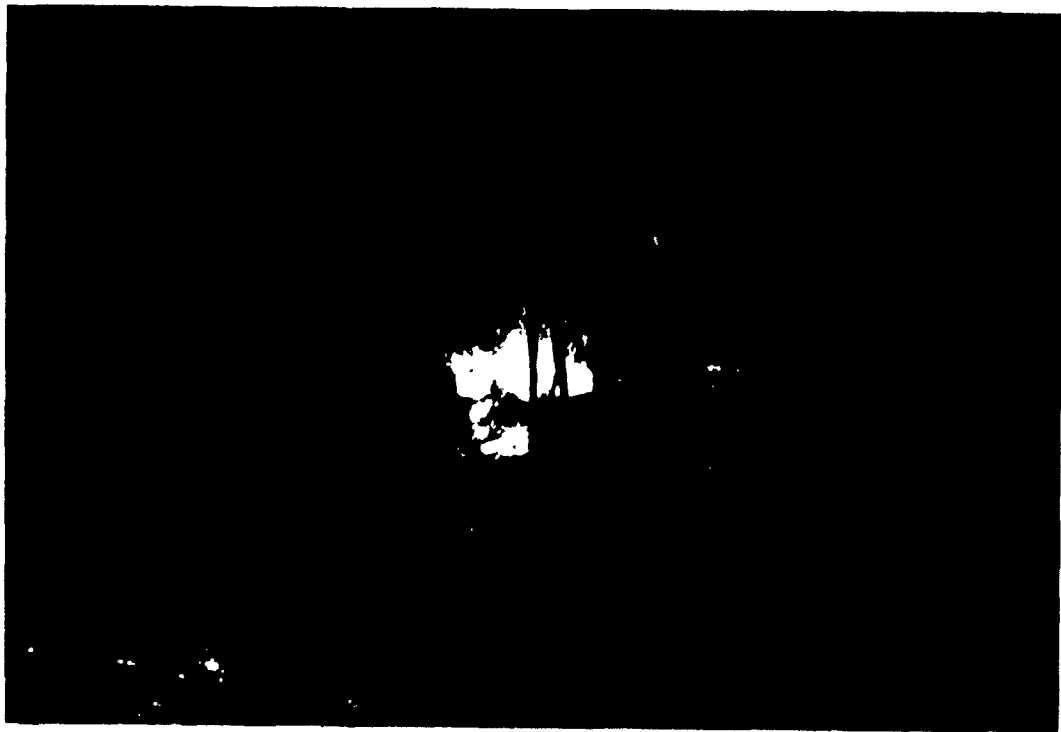


Figure 5.20. Photographs of typical eruptions.

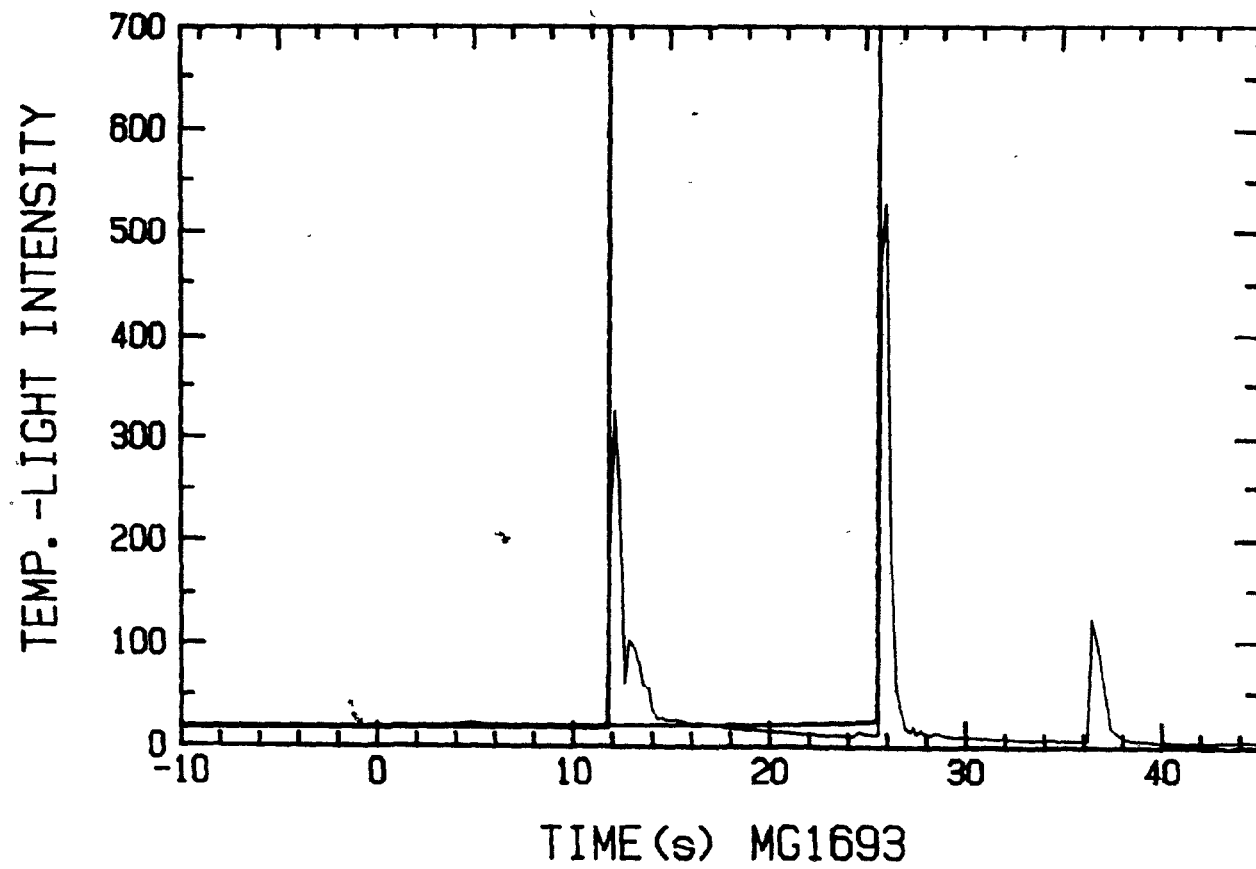


Figure 5.21. Temperature and photocell traces for sample MG1693.

12 seconds after the sample made contact with the surface. Considering that the sample was fed at a velocity of 1.0cm/s, the maximum depth that the sample could have penetrated at the time of the eruption was 12cm. Hence, the sample did not hit the bottom of the crucible. Second, before the eruptions occurred the temperature of the magnesium was essentially at room temperature. Then it immediately rose to bath temperature, thus indicating that the insulation somehow broke off and exposed the 'cold' magnesium wire to the bath. Third, the thermocouple experiments with Pemco powder 1693 indicated that it would take about 30 seconds for an aluminum core to reach a temperature of 650°C. Since the leading end of the composite sample had been immersed for 12 seconds when the first eruption occurred, it was highly unlikely that there was a build up of liquid or gaseous magnesium below the first thermocouple.

As for other examples, consider the traces shown in Figure 5.22-24. Figure 5.22 shows the traces for a sample(LMF3/8) which had a copper sheathing and a glass insulation thickness of about 2.0cm, while Figure 5.23 shows the traces of a sample(M81963) that was the same as sample MG1693, except that it was fed at a velocity of 0.75cm/s. Figure 5.24 shows the temperature traces of sample 1AF3/8. This sample was the same as sample LMF3/8 with the exception that the magnesium was replaced by aluminum. The temperature traces of sample 1AF3/8 show that there was no sudden increase in temperature, thus indicating that the glass insulation remained intact. This suggests that ferrostatic or buoyancy forces were not the cause for the glass breaking or

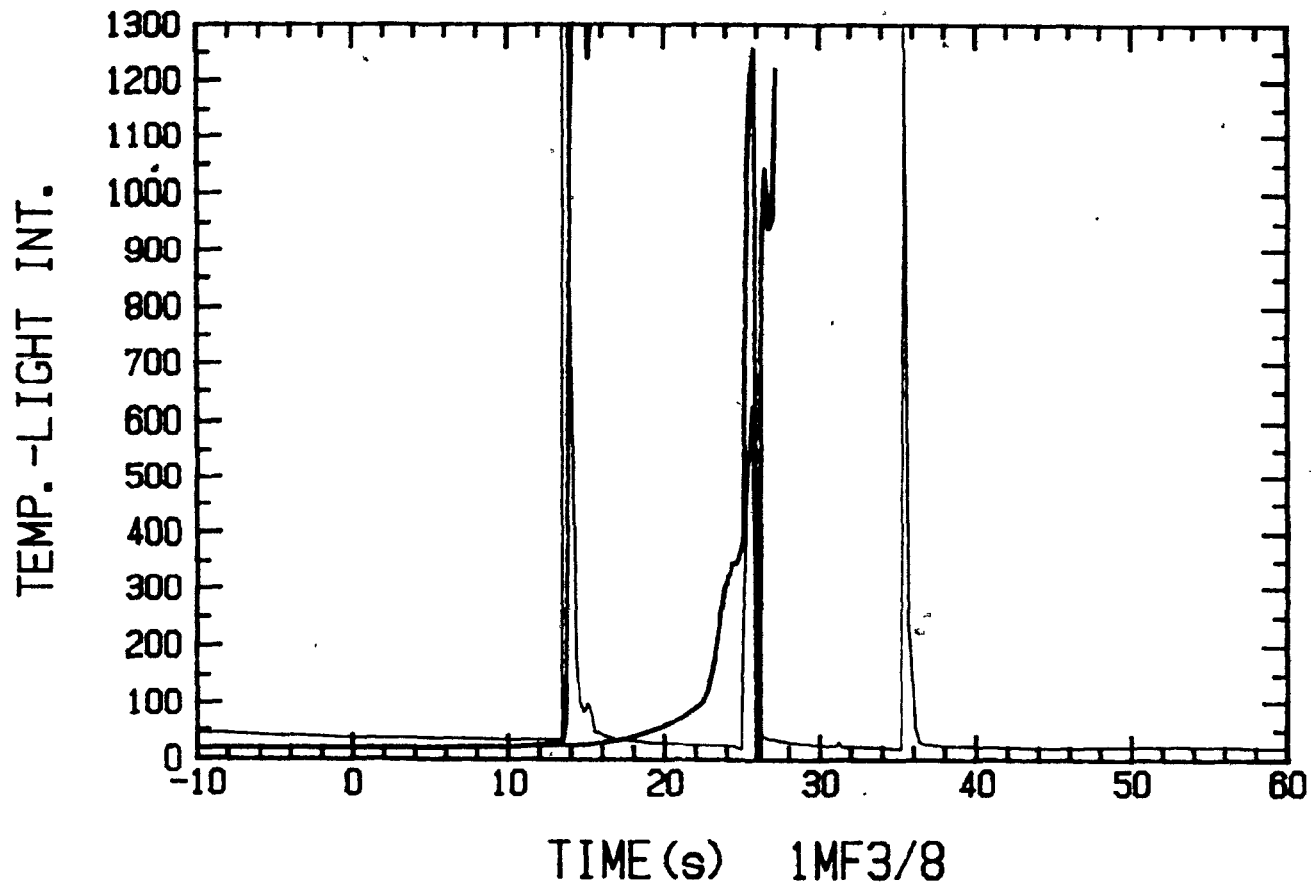


Figure 5.22. Temperature and photocell traces for sample 1MF3/8.

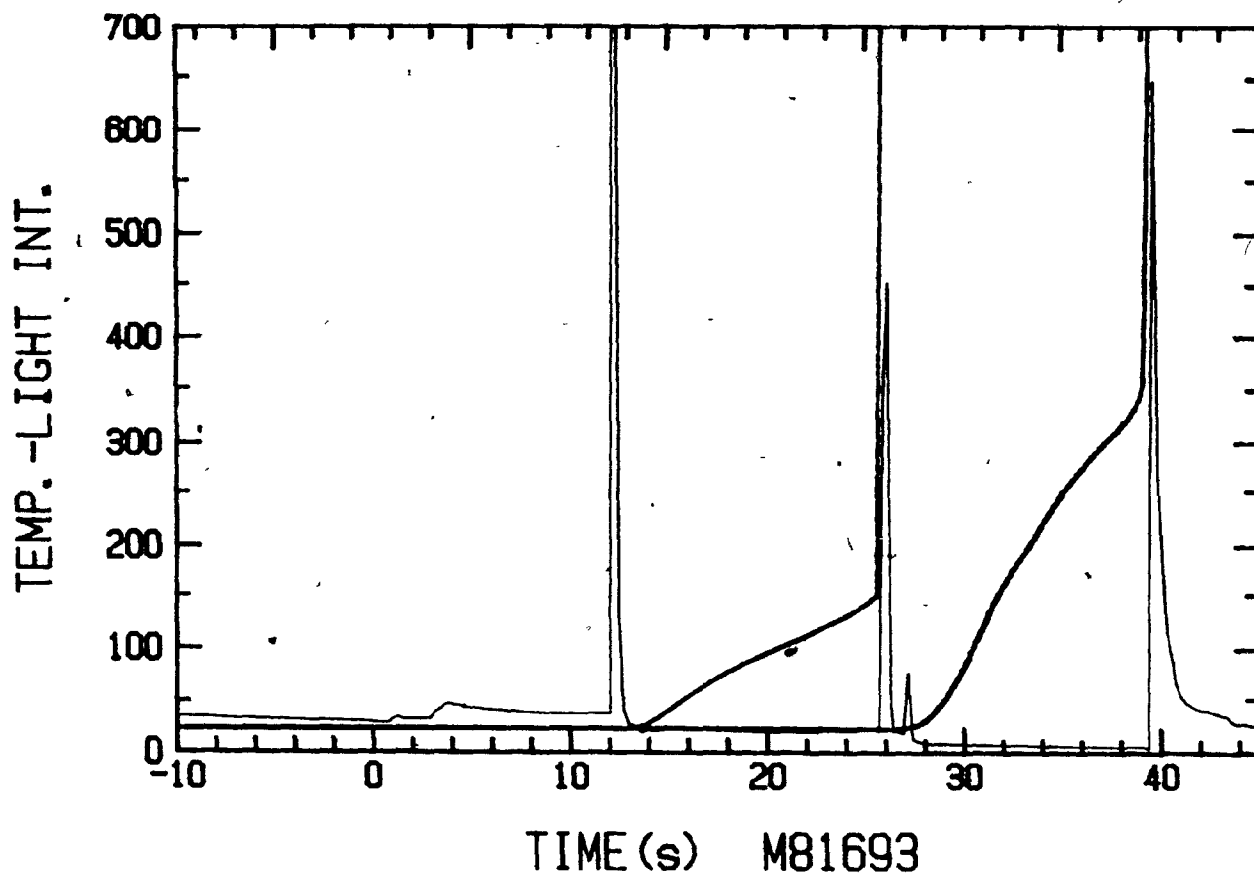


Figure 5.23. Temperature and photocell traces for sample M81963.

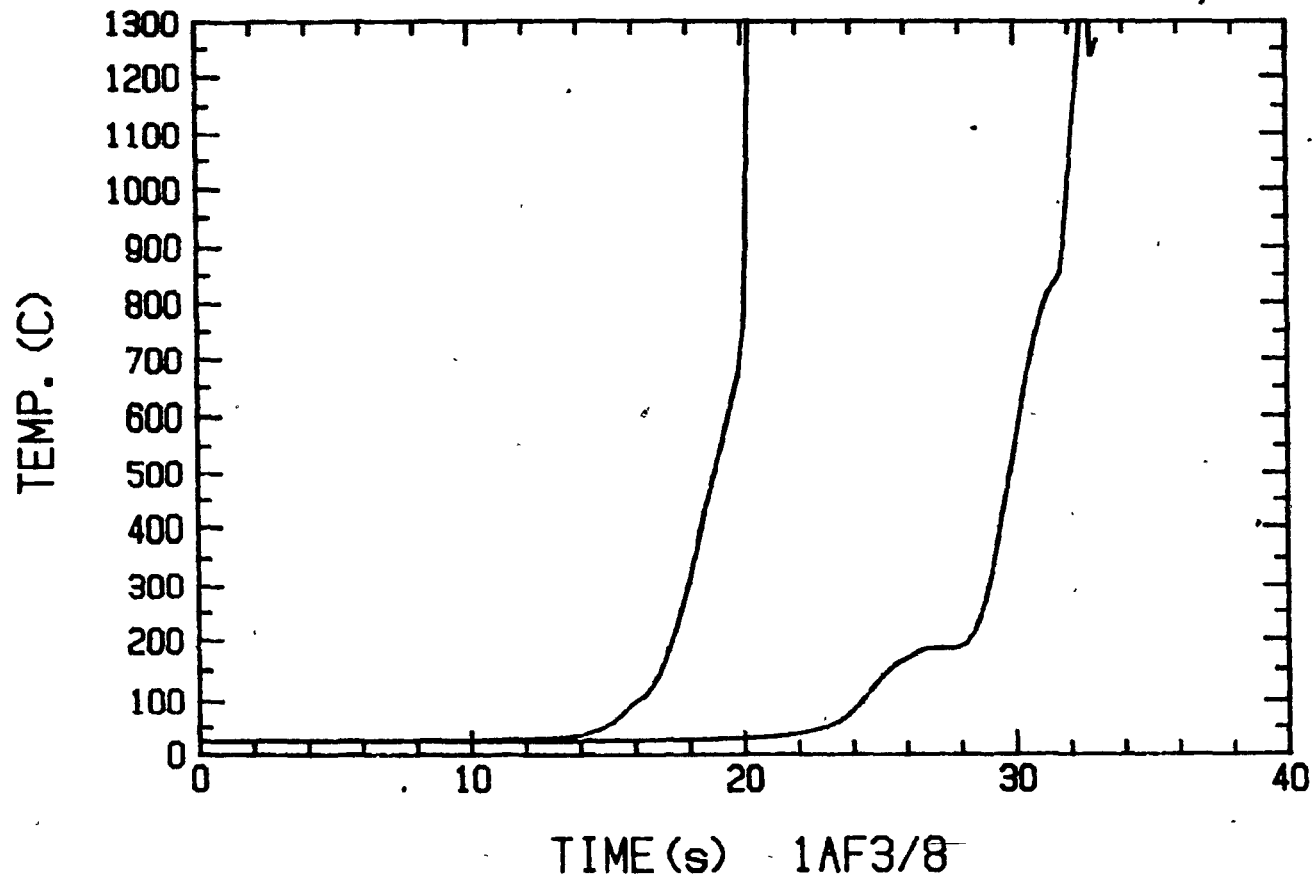


Figure 5.24. Temperature traces for sample 1AF3/8.

peeling off when the magnesium composite samples were immersed. Furthermore, Figures 5.22 and 5.23 show that both magnesium samples exhibited periodic eruptions that occurred 12 to 13 seconds apart. Given that the samples were fed at different speeds and had different insulation thicknesses, it is apparent that the eruptions were not related to immersion velocity, insulation thickness, or penetration depth. The difference between the magnesium and aluminum samples was that magnesium was volatile. Thus it was postulated that once the magnesium started being released at the leading end, it created enough turbulence to destroy the entire length of glass powder that was submerged. As a result, a large length of magnesium would be exposed to the melt causing an eruption with flares and flashes and the possible ejection of hot metal from the crucible.

Referring back to Figure 5.23, it is worth noting that the first eruption did not break the first thermocouple as was the case for the other samples. The reason for this was simply that since the sample was fed at a slower speed, the thermocouple had not entered into the bath when the explosion occurred. This allowed the thermocouple to penetrate the bath for another 12 seconds before the next eruption was initiated.

In Chapter 2, it was mentioned that previous work conducted with soda-lime glass showed that the occurrence of flares and eruptions was almost completely eliminated when the bath temperature was raised to 1600°C. Consequently, it was believed that the problems with explosions were related to the viscosity of the glass. However, the work just presented showed

that reducing the viscosity of the glass did not eliminate the eruptions. In order to attain a fuller understanding of why the process seemed to work at a temperature of 1600°C , an attempt was made to duplicate the previous tests conducted at 1600°C with the exception that this time thermocouples were used. It must be stressed at this point that thermocouples were not used in the previous work. The acquisition of very inexpensive thermocouples made it possible to use them extensively in the present work.

Consider the temperature and photocell traces shown in Figure 5.25. These traces are for sample 34MS2. Sample 34MS2 consisted of 6.5mm of soda-lime insulation encased by a 1.9cm O.D. steel sheath. The sample was fed at a speed of 1.0cm/s into a pig iron bath at 1600°C . It is apparent from the temperature traces that the temperature of the core rose from essentially room temperature to bath temperature almost instantaneously. However, visually the immersion appeared quite calm except for a couple of flares that occurred around the 14 second mark. The large peak in the photocell reading around the 50 second mark occurred as the sample was being pulled out of the bath.

Another example is shown in Figure 5.26. This sample was the same as sample 34MS2. Visually, this test appeared quite calm, except for a couple of flashes around the 16 and 42 second marks. Although these tests appeared much calmer than those conducted at 1400°C , the temperature traces still indicate that the glass insulation may have been breaking off. The reason that the tests seemed calmer may be that at the higher

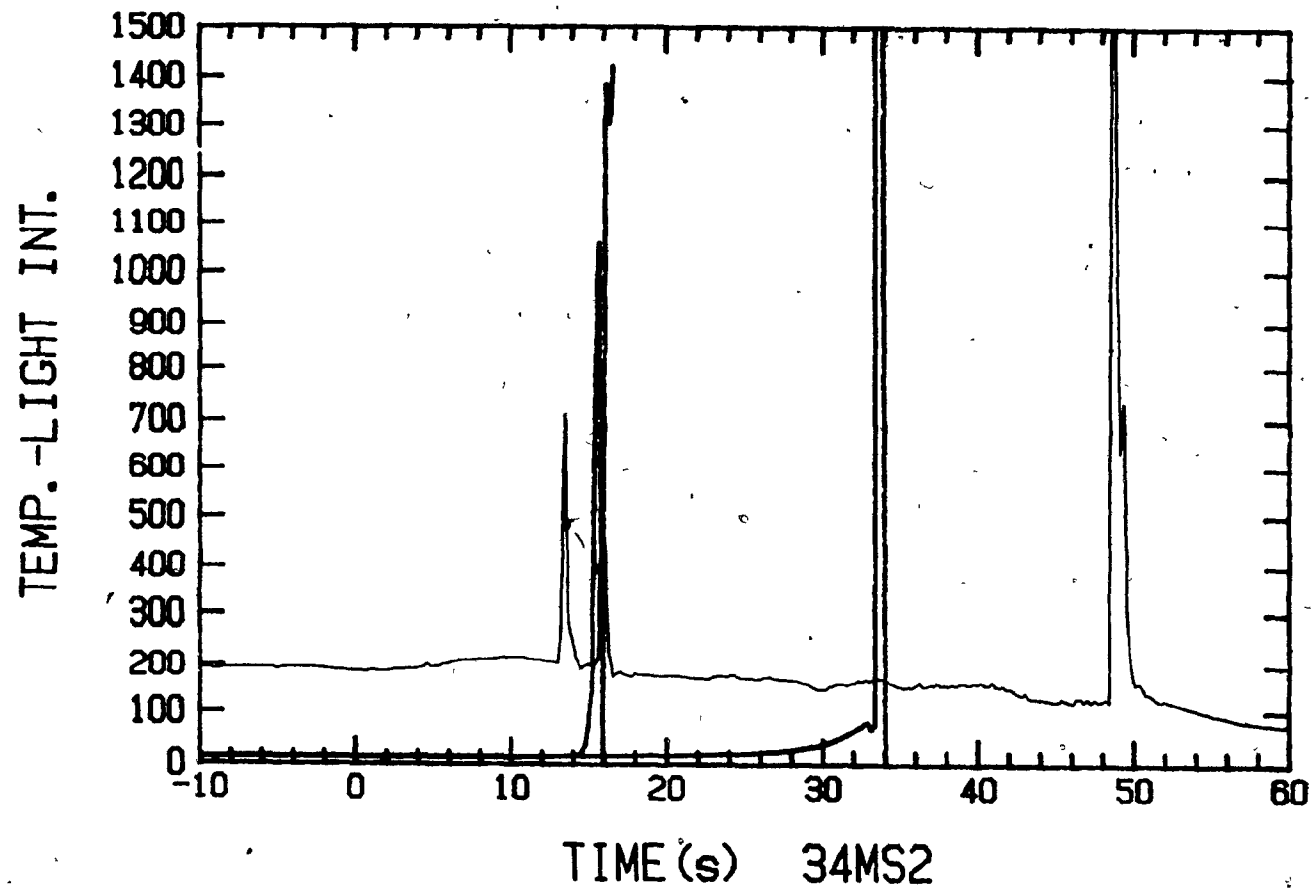


Figure 5.25. Temperature and photocell traces for sample 34MS2.

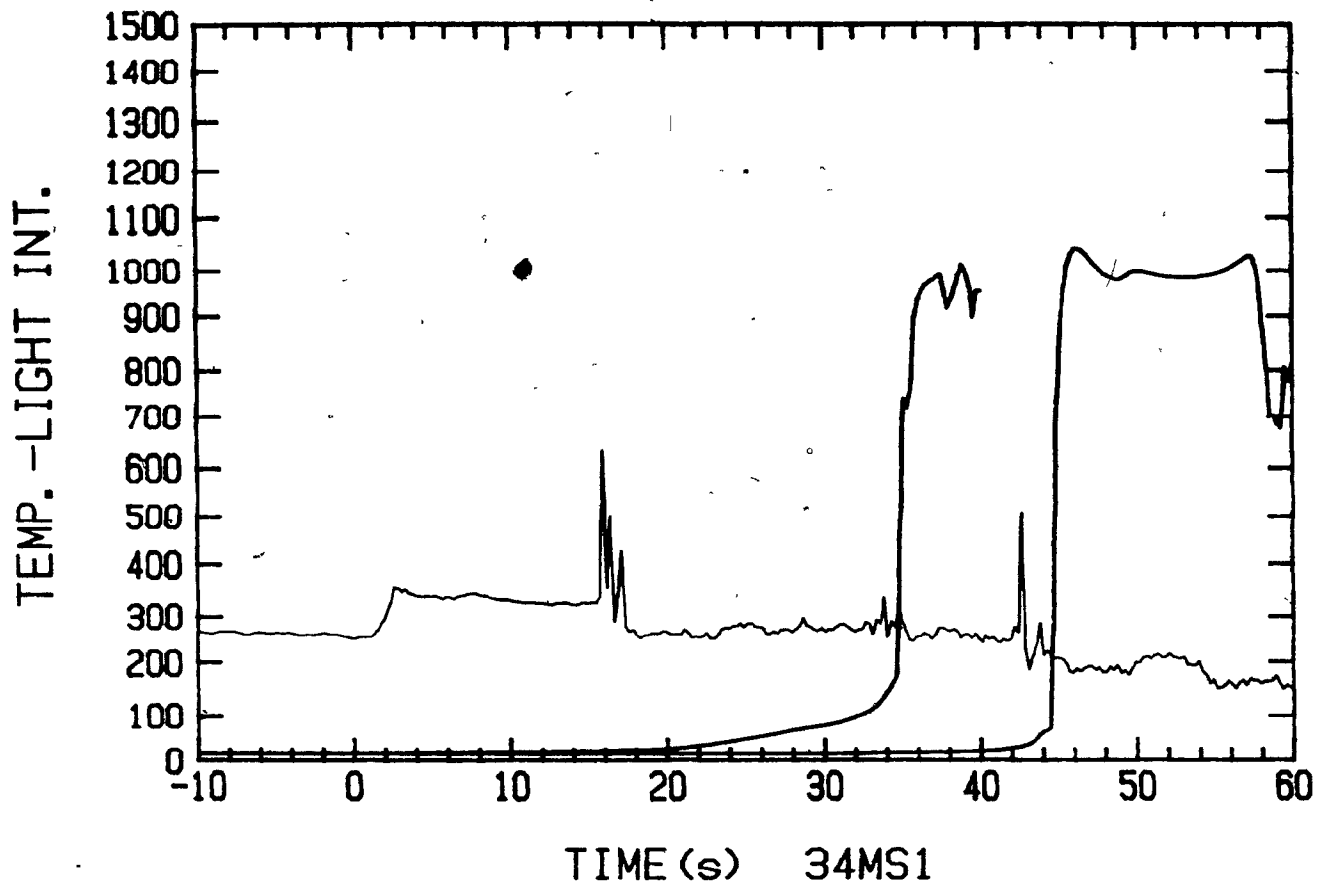


Figure 5.26. Temperature and photocell traces for sample 34MS1.

temperature, the glass insulation fused at a faster rate. This probably provided the glass framework with increased strength. Thus the turbulence at the leading end was probably not strong enough to destroy all the glass that was submerged in the bath and only broke a small portion of the glass. The smaller portion of exposed magnesium was probably not large enough to cause an eruption. Nevertheless, the traces indicated that the glass was still being broken off. This was considered undesirable, even though the immersion of the magnesium samples at 1600°C seemed relatively calm. It was felt at this point that the strength of the insulation had to somehow be increased. Several options were considered. One option was to increase the strength of the powder by mixing the glass with a high temperature binder. This option was rejected because it would complicate an already fairly complicated sample configuration. Other options considered included using other forms of glass such as glass wool, foam glass, or glass tape. It was decided that glass tape would be the most appropriate insulation because it can be easily applied to the magnesium simply by wrapping it on, and, it would obviously provide greater strength than the glass powder. Its use would also eliminate the need for a metallic sheath.

5.2 PART 2- Glass Tape Insulation

Two brands of glass tape were used for the second part of this study. The glass tapes were acquired from Mudge, Watson Inc. and Ajax Magnethermic Inc. A description of the tapes was presented in section 4.2.2.

5.2.1 Heat Transfer Tests

5.2.1.a Aluminum Core

Composite wires containing aluminum cores were tested with 'Ajax' tape at bath temperatures of 1400°C and 1600°C, while the 'Mudge Watson' tape was tested at 1400°C only. Although the Ajax tape was tested at 1600°C, the amount of data obtained was insufficient to make any correlations. Typical temperature traces are shown in Figures 5.27a and b. The vertical displacements of the thermocouples were 10cm and 20cm from the leading end while the feeding velocity was 1.0cm/s. Zero time refers to the instant the leading end contacted the bath surface. A photograph of typical samples is shown in Figure 5.28. Samples with insulation thicknesses ranging from 1.0mm to 5.0mm were tested. From the temperature traces obtained, the 'net time' required to increase the temperature of the thermocouple tip to 650°C (i.e. the approximate melting point of both magnesium and aluminum) was computed. These values are plotted as a function of insulation thickness in Figure 5.29 for both the Ajax and Mudge, Watson tape. It is evident from these results that as the thickness of the tape was increased, the

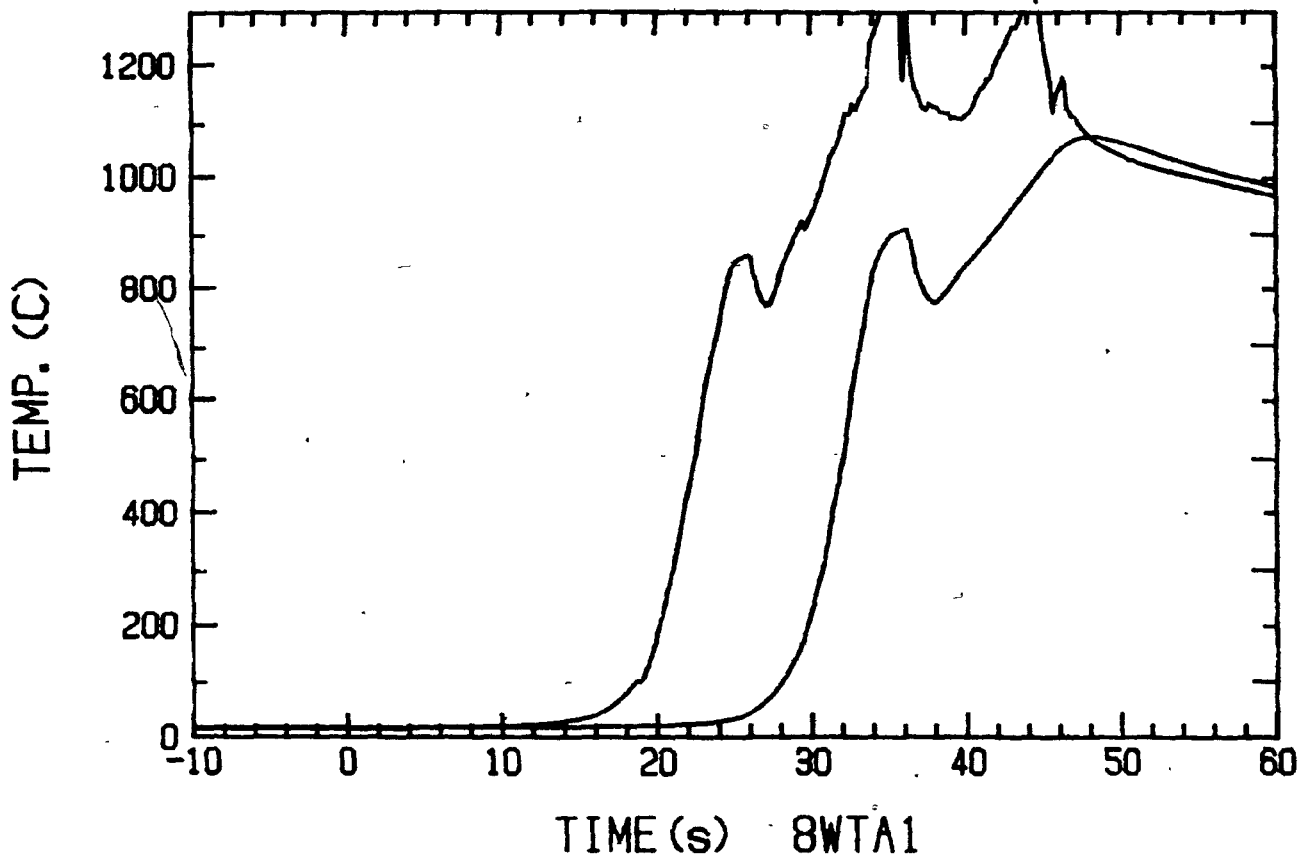


Figure 5.27a. Typical temperature traces for a composite aluminum sample insulated with Ajax tape. The bath temperature was 1600°C.

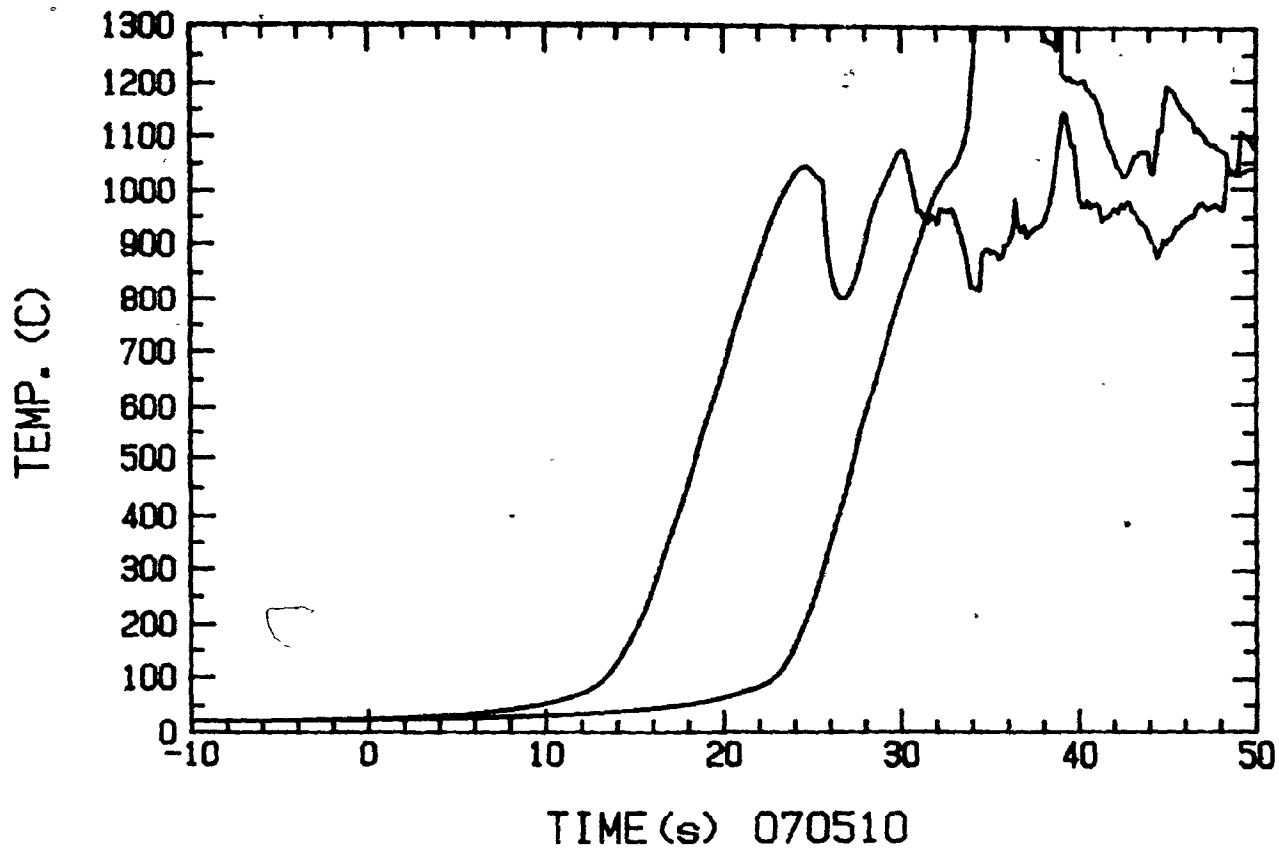


Figure 5.27b. Typical temperature traces for a composite aluminum sample insulated with Mudge, Watson tape. The bath temperature was 1400°C.

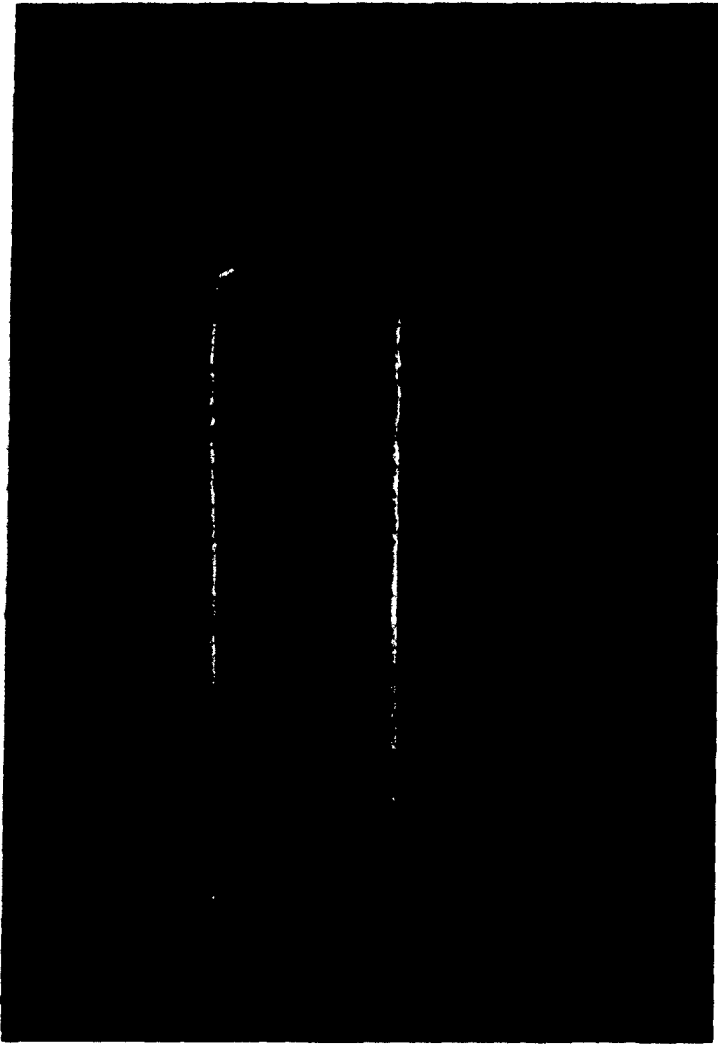


Figure 5.28. A photograph of typical glass tape insulated samples.

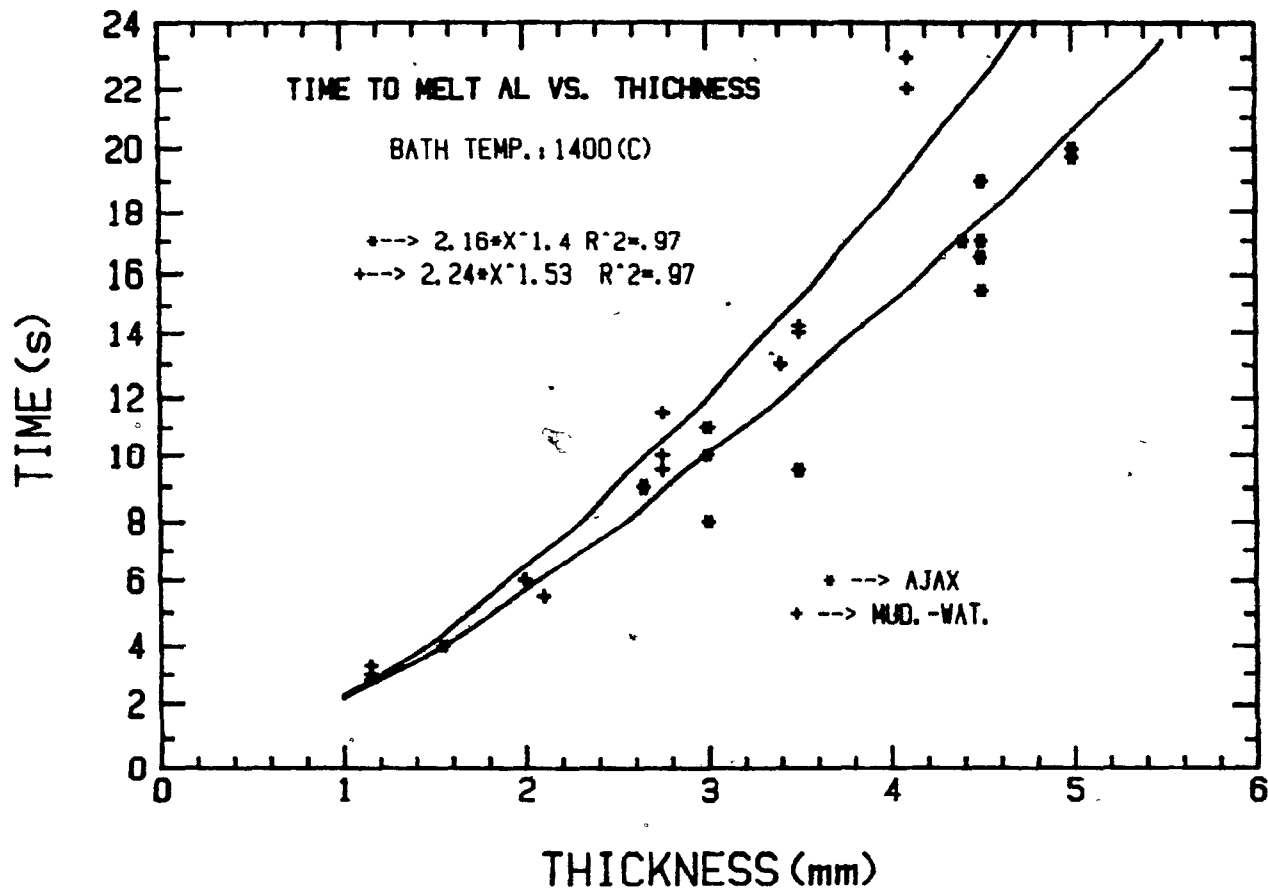


Figure 5.29. A plot of aluminum melting times versus insulation thickness for both Ajax and Mudge, Watson tapes.

average heat flux into the aluminum decreased. Furthermore, it appears that the Mudge, Watson tape was a more effective insulator than the Ajax tape, especially at the larger thicknesses. It was found that the relationship between the aluminum melting time and insulation thickness for both the Ajax and Mudge, Watson tapes can be described as follows:

$$T=2.16X^{1.4} \quad (\text{Ajax}) \quad (13)$$

$$T=2.24X^{1.5} \quad (\text{Mudge, Watson}) \quad (14)$$

where T= time required to melt aluminum (s)

X= thickness of insulation (mm)

The type of curve that would best fit the data was determined by considering a one-dimensional heat transfer model simulating the radial heat flow to a composite cored wire. It should be noted that the model did not take into account the thinning of the glass sheath as it was heated. A description and listing of the program are presented in Appendix A. Heat transfer simulations for typical magnesium samples are also presented. Typical theoretical curves for bath temperatures of 1400°C and 1600°C are shown in Figure 5.30. It was found that from these results that the relationship between melting time and insulation thickness can best be represented by an equation of the form:

$$T=aX^b \quad (15)$$

where a and b are constants.

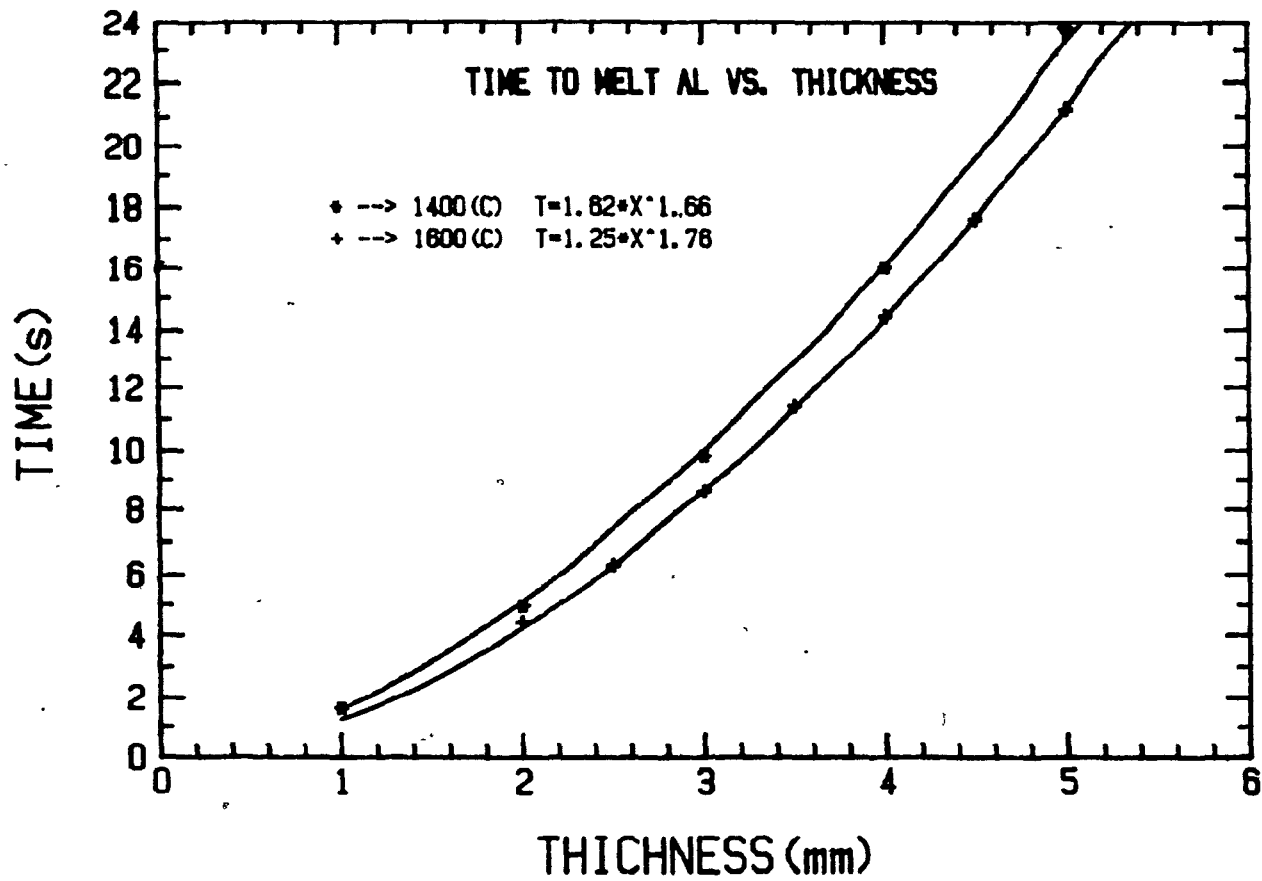


Figure 5.30. Theoretical aluminum melting times versus insulation thickness for bath temperatures of 1400°C and 1600°C.

The reason the 'melting time' versus 'insulation thickness' relationship is important is that it can be quite helpful in determining the depth of penetration of the composite wire in the molten metal bath. It must be stressed at this point, however, that if one knows the melting time, insulation thickness, and immersion speed of a particular sample, it is not necessarily true that one will be able to calculate the depth of penetration accurately. The reason for this is that a composite sample tends to bend upwards towards the bath surface at the point at which it begins to melt. Good examples of this are shown in Figures 5.31 a and b. These figures show photographs of two typical aluminum composite samples fed at a velocity of 1.0cm/s. Notice that large portions of the samples are bent upwards towards the bath surface. For example, Figure 5.26a shows that the sample penetrated 13cm below the bath surface, but, an additional 9cm of the sample had bent upwards. Hence, 22cm of the sample had been immersed in the bath, but, the effective depth of penetration was 4cm (i.e. 13-9cm). It should be noted that the 'bending' problem was more pronounced for larger insulation thicknesses. The insulation thicknesses of the samples shown in Figures 5.31a and 5.31b were 4.5mm and 5.2mm, respectively. It was found that for samples with insulation thicknesses of less than 2.5mm, a small fraction of the sample bent upwards. Hence, the depth of penetration was more easily determined for samples with small insulation thicknesses.

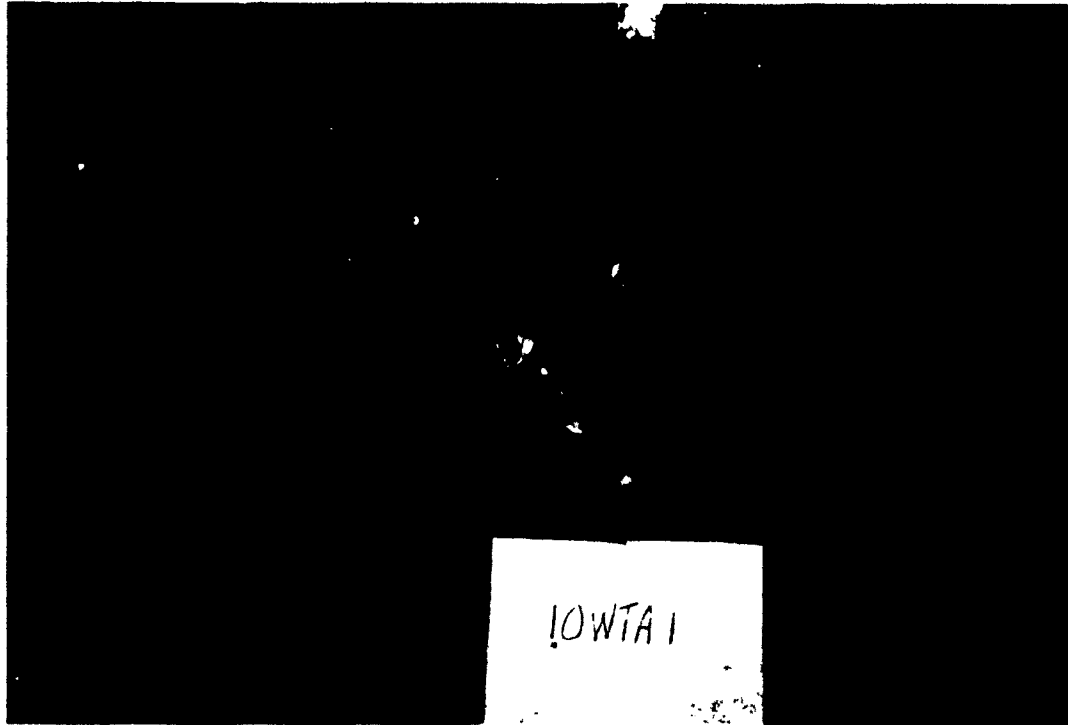


Figure 5.31. These photographs show two typical aluminum composite samples that bent upwards when they were immersed in a pig iron bath.

5.2.1.b Magnesium Core

Composite samples with magnesium cores were tested with both the Ajax and Mudge, Watson tapes at 1400°C. The Ajax tape was also tested at 1600°C. A summary of the melting times obtained at 1400°C is shown in Figure 5.32. The results for both the Mudge, Watson and Ajax tapes were combined on this graph. This graph clearly illustrates the superior thermal insulation characteristics of the Mudge, Watson tape, especially at the larger insulation thicknesses. For example, 4mm of Mudge, Watson insulation would delay the melting of the magnesium core by about 18 seconds whereas the same thickness of Ajax tape would delay the melting by only 12 seconds. The 'melting times' of magnesium and aluminum are compared in Figures 5.33 and 5.34 for both the Mudge, Watson and Ajax tapes. Note that it took a longer time on average to melt the aluminum core than the magnesium. It was stated earlier that aluminum was used as a substitute core because it has a melting point and thermal diffusivity that is similar to that of magnesium. However, their densities and heat capacities are quite different. In fact; it is the product of the density and heat capacity of the core that determines the quantity of energy required to heat the core to the melting point. Therefore aluminum requires about 35% more energy to bring it to its melting point. Hence the difference in melting times between magnesium and aluminum can be totally attributed to the difference in their densities and heat capacities.

Composite magnesium samples were also tested at 1600°C

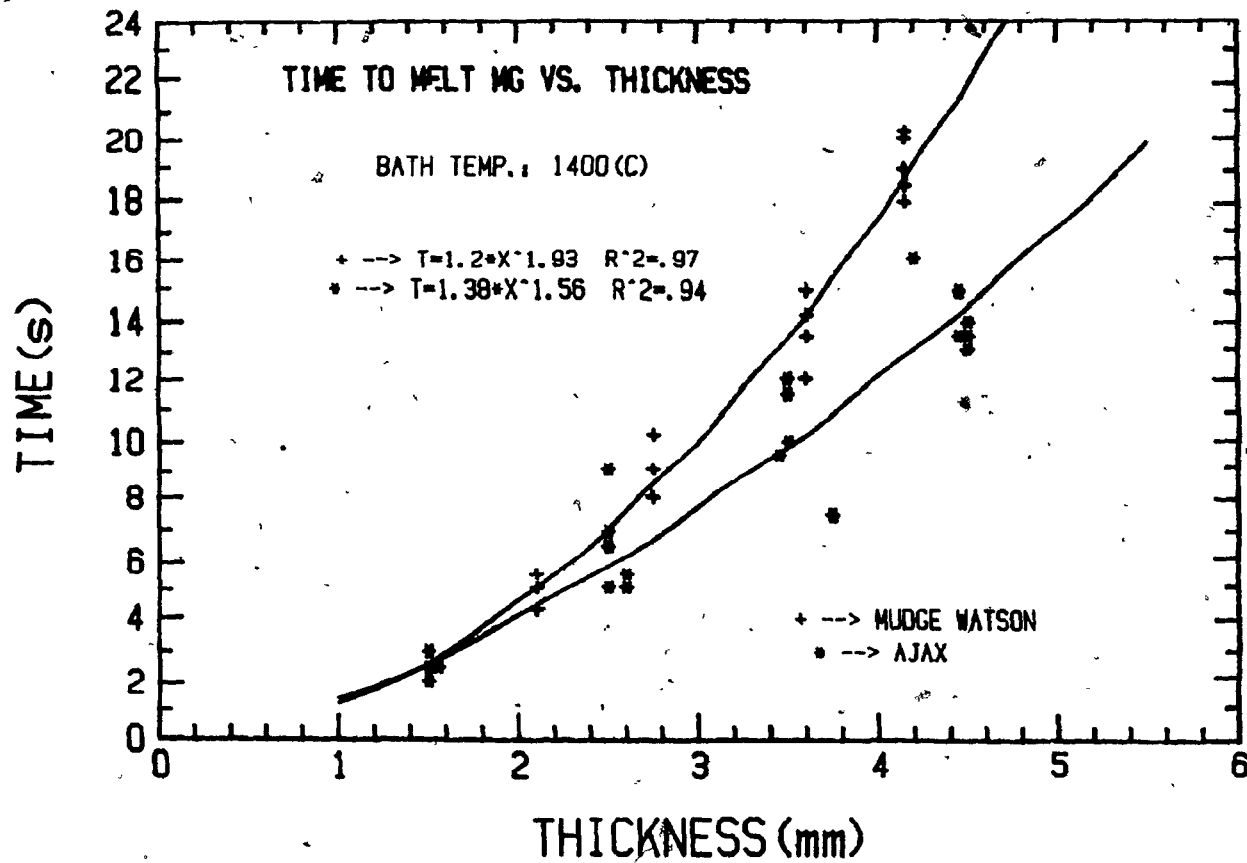


Figure 5.32. A plot of melting times versus insulation thickness for samples containing Mg cores:

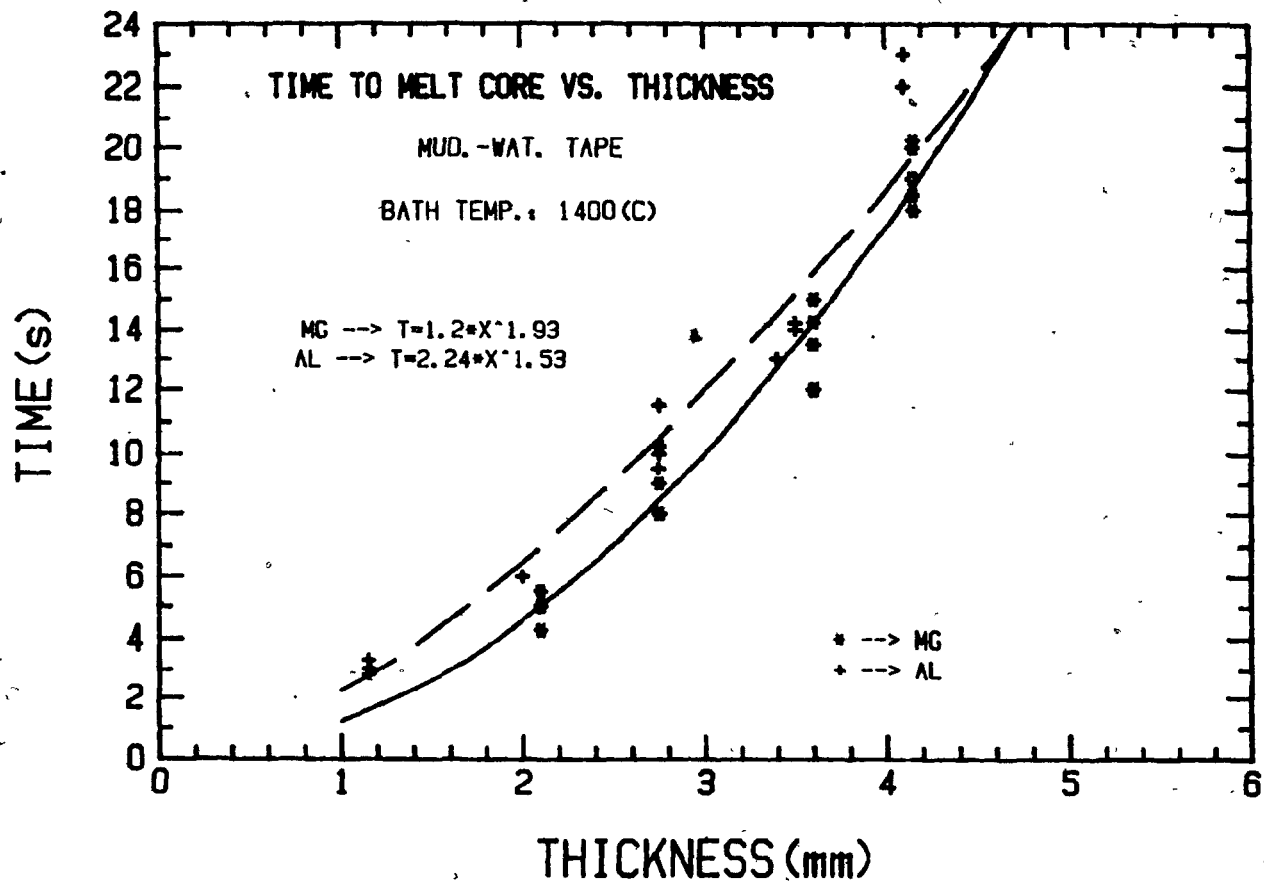


Figure 5.33. Comparison of melting times between magnesium and aluminum samples insulated with Mudge, Watson tape.

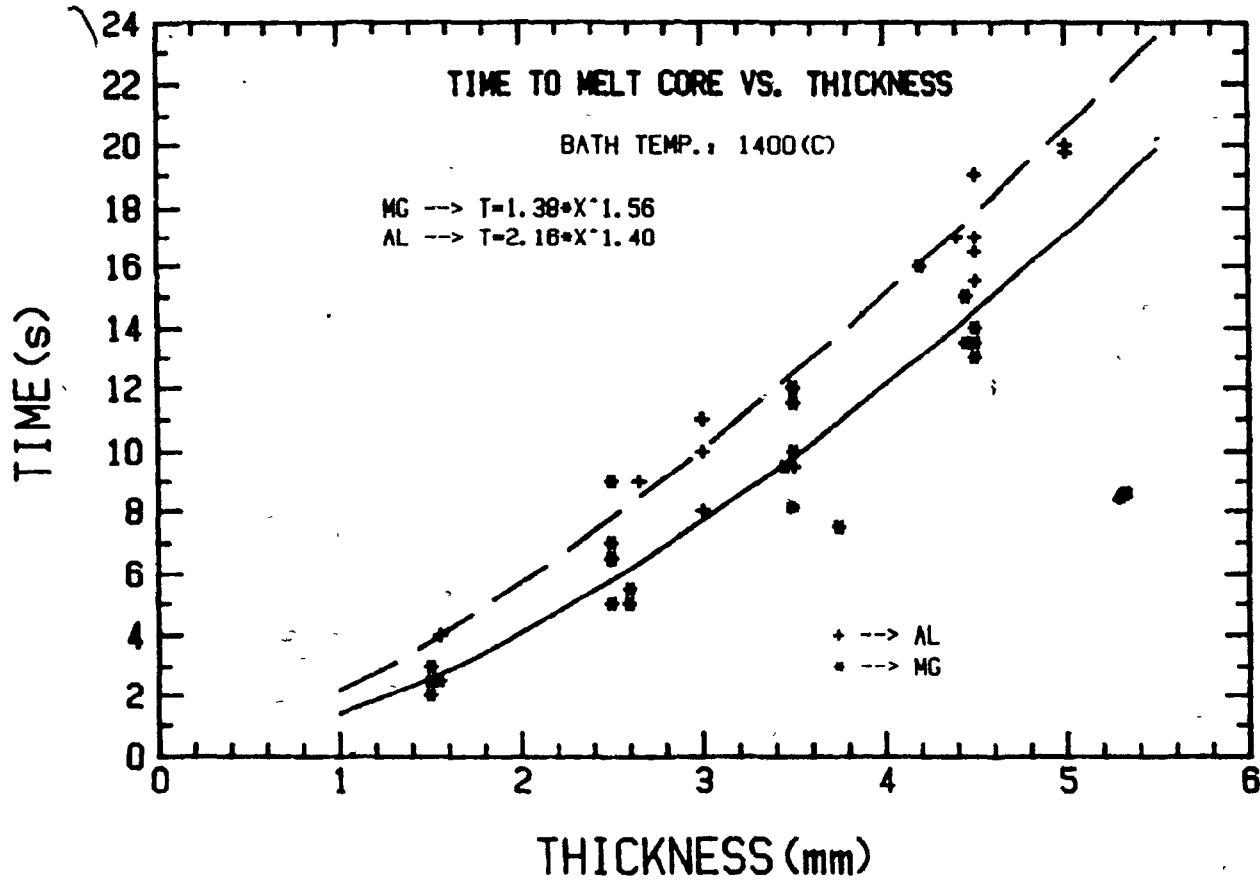


Figure 5.34. Comparison of melting times between magnesium and aluminum samples insulated with Ajax tape.

using Ajax tape only. The insulation thicknesses for these experiments ranged from 3.6mm to 5.4mm. A summary of the melting time results is shown in Figure 5.35. Because of the higher melt temperature, there was a noticeable reduction in the effective insulating potential of the tape. For example a 4mm layer of Ajax tape at 1400°C would delay the melting of the magnesium core by 12 seconds whereas at 1600°C it would be delayed by about 9 seconds. Also note that the 'melting time' versus 'insulation thickness' was found to be essentially linear. However, this relationship is misleading because a narrow range of thicknesses were tested. In order to obtain a more realistic relationship, smaller thicknesses should have been tested. Due to the reduced insulating effectiveness of the tape at 1600°C, there was a reluctance to test the smaller thicknesses since the immersion speed would have to be increased substantially in order to obtain a reasonable depth of penetration. Since an increased immersion speed would also result in an increase in mass flowrate, the turbulence in the bath would probably also increase substantially. Nonetheless these tests should be conducted in the future using Mudge, Watson tape since it is a more effective insulator than the Ajax tape.

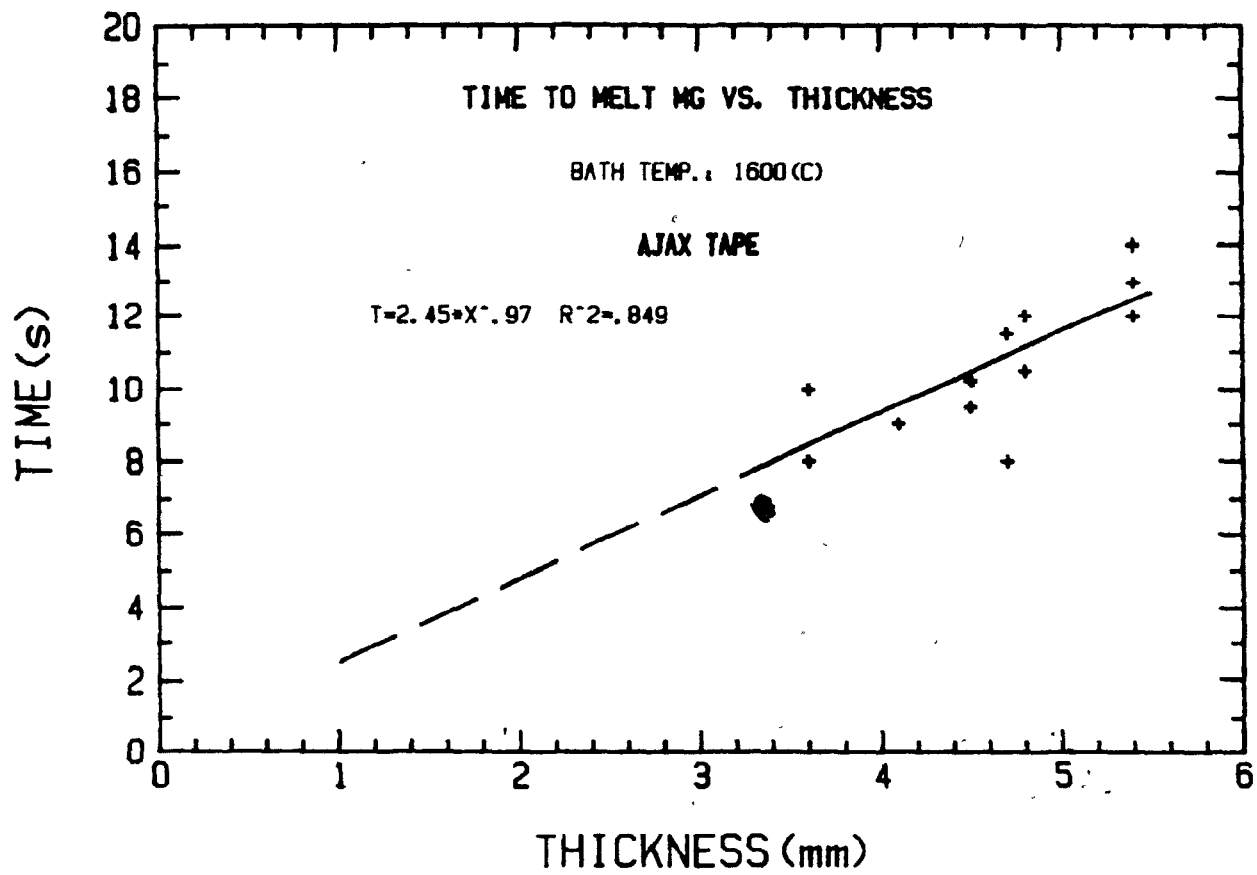


Figure 5.35. Melting time results for Mg composite samples that were immersed in a bath at 1600°C. The samples were insulated with Ajax tape.

5.2.2 Temperature Profile and Pyrotechnic Tests

It would be valuable at this point to examine several typical temperature and photocell traces. Consider the traces shown in Figures 5.36-5.39. These are typical traces of tests conducted at 1400°C with various thicknesses of Ajax tape. Similar trends were observed with the Mudge, Watson tape. The insulation thicknesses were 1.5, 2.5, 3.5, and 4.5mm, respectively. The immersion speed was 1.0cm/s for all tests. Each sample had two thermocouples. One was placed 10cm from the leading end of the sample while the other was placed 20cm away. There are several points worth noting. First, pyrotechnic displays decreased with increasing insulation thickness. The reason for this was simply that the samples with the thicker insulation penetrated deeper into the bath thus allowing sufficient time for the bubbles of magnesium vapor to dissolve as they rose through the melt. For the smaller thicknesses, the magnesium vapor did not have sufficient time to dissolve. As a result, some of the vapor resurfaced and quickly oxidized, producing bright flashes. Second, the thermocouple traces for the two tests appear to be almost identical except that the second thermocouple trace was shifted to the right by 10 seconds. Since the thermocouples were positioned 10cm apart and the immersion velocity was 1.0cm/s, this indicated that steady state was attained. Hence, if one assumes steady state is attained in a given test, the immersion velocity can be calculated from the temperature traces. Third, some traces

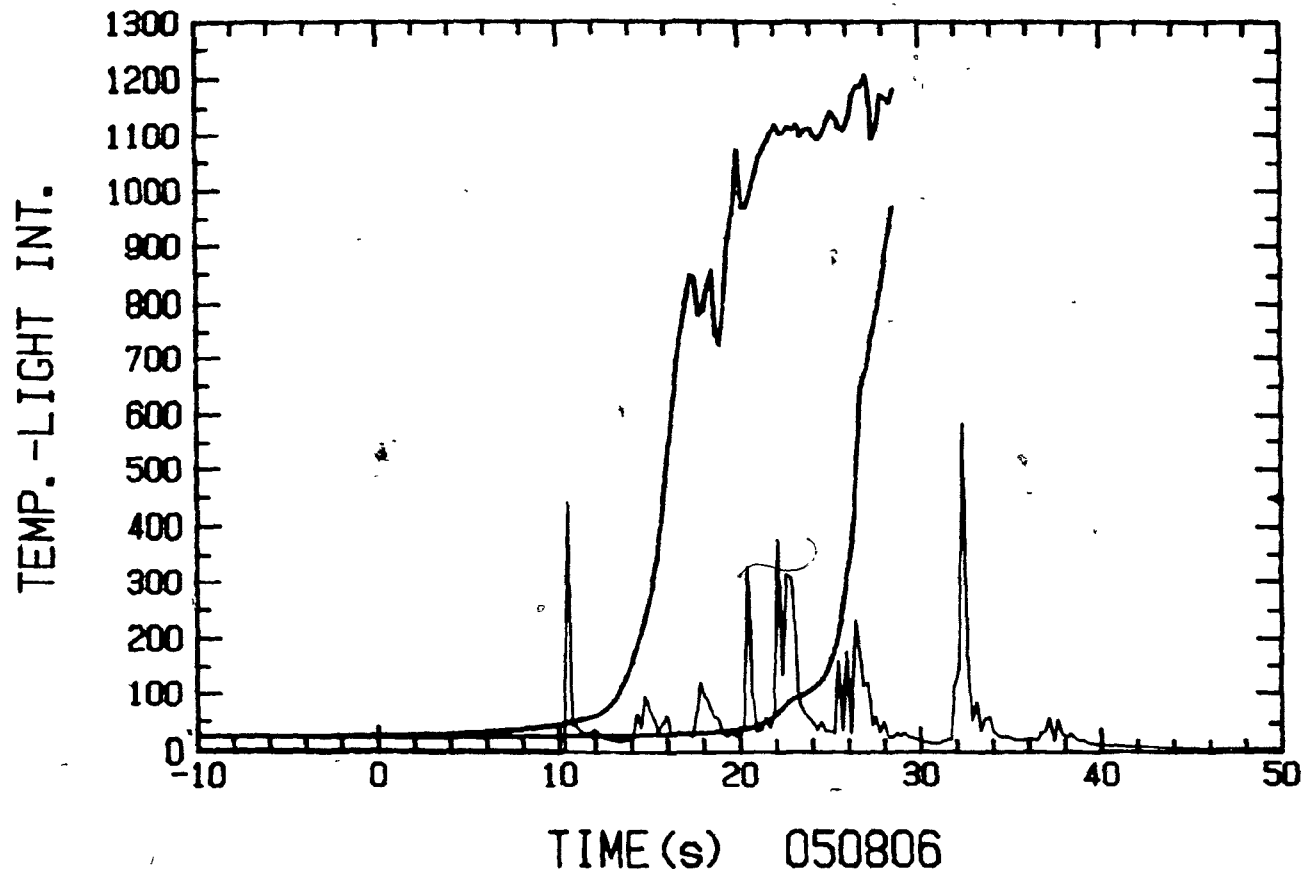
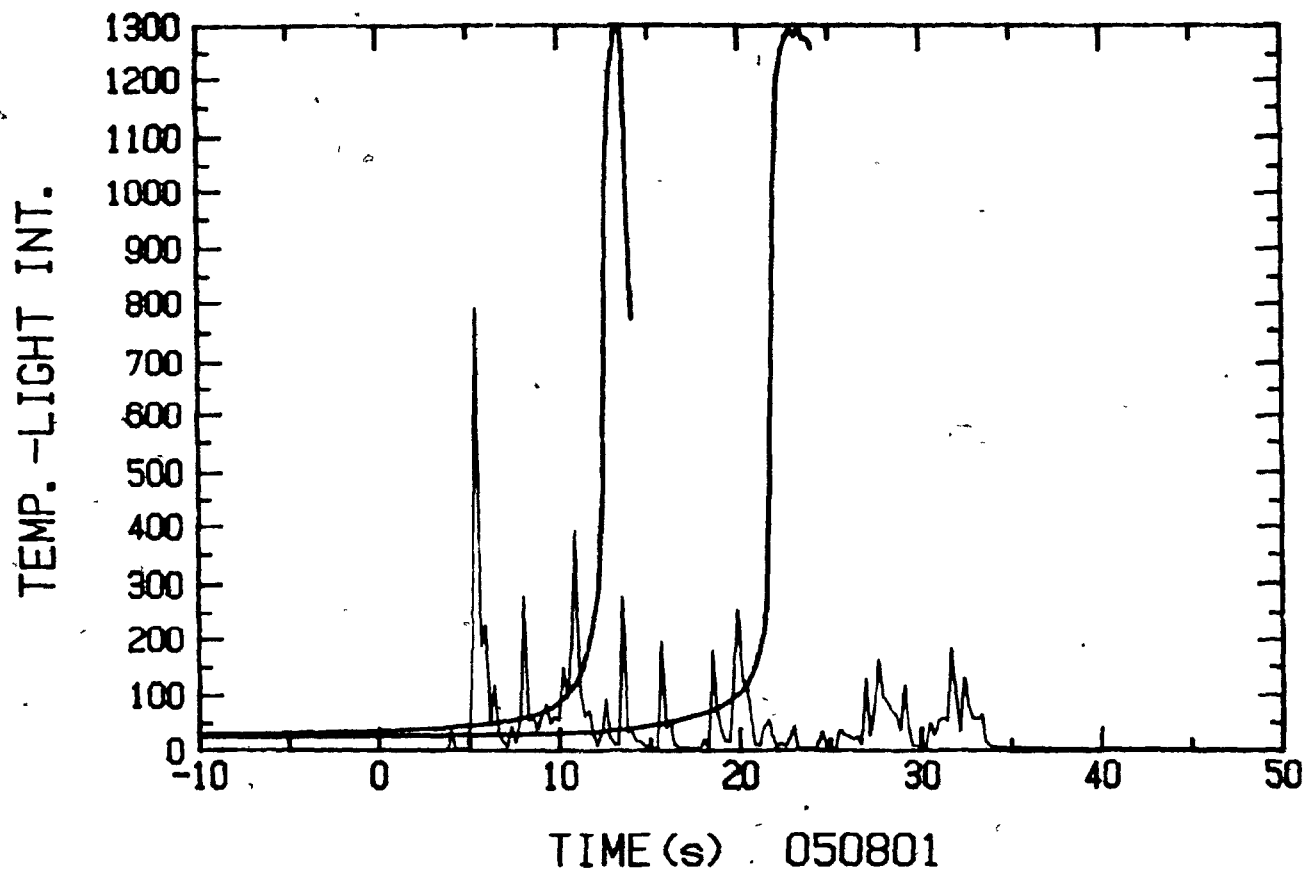


Figure 5.36. Temperature and photocell traces of a 3.2mm magnesium wire insulated with 1.5mm of Ajax tape. The immersion velocity was 1.0cm/s.



U

Figure 5.37. Temperature and photocell traces of a 3.2mm magnesium wire insulated with 2.5mm of Ajax tape. The immersion velocity was 1.0cm/s.

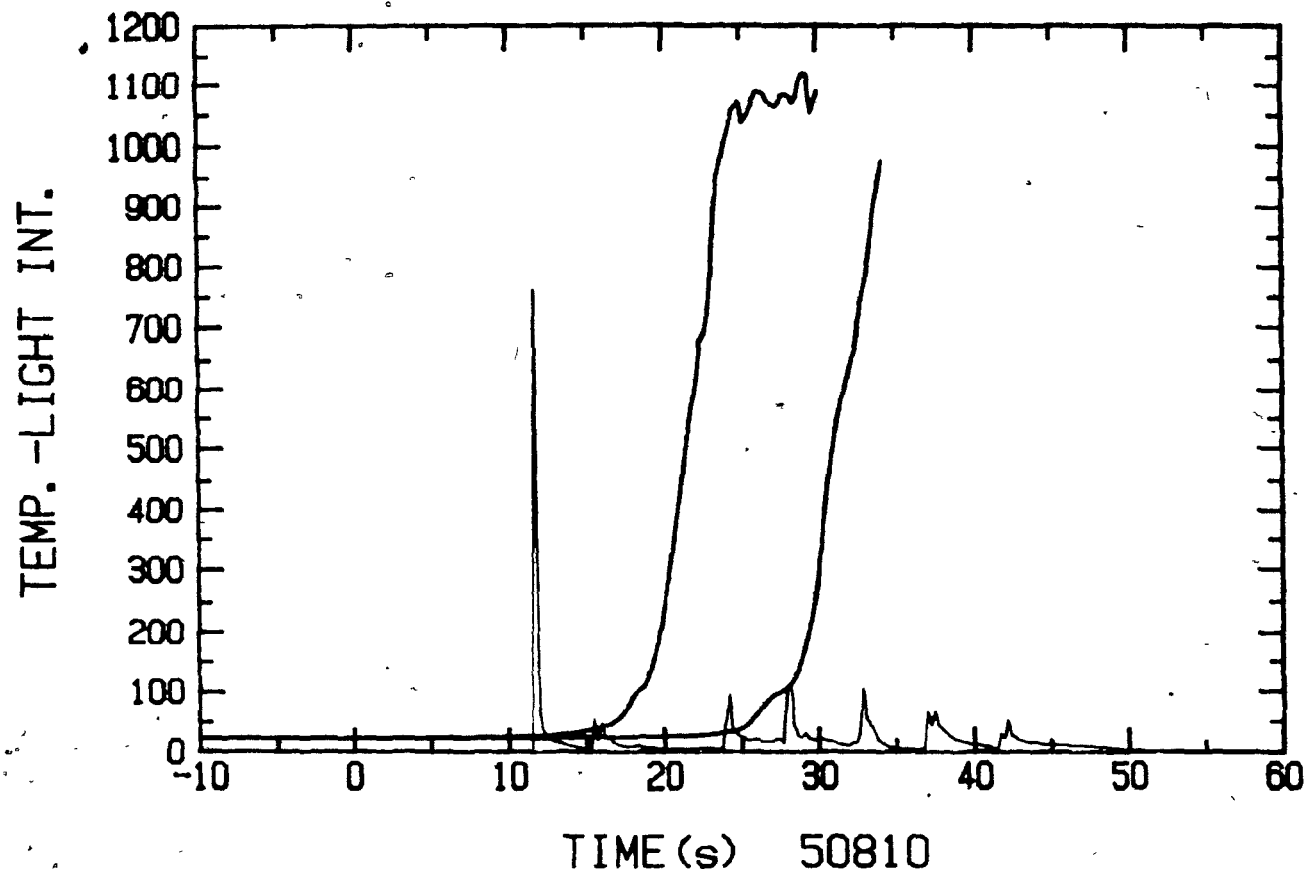


Figure 5.38. Temperature and photocell traces of a 3.2mm magnesium wire insulated with 3.5mm of Ajax tape. The immersion velocity was 1.0cm/s.

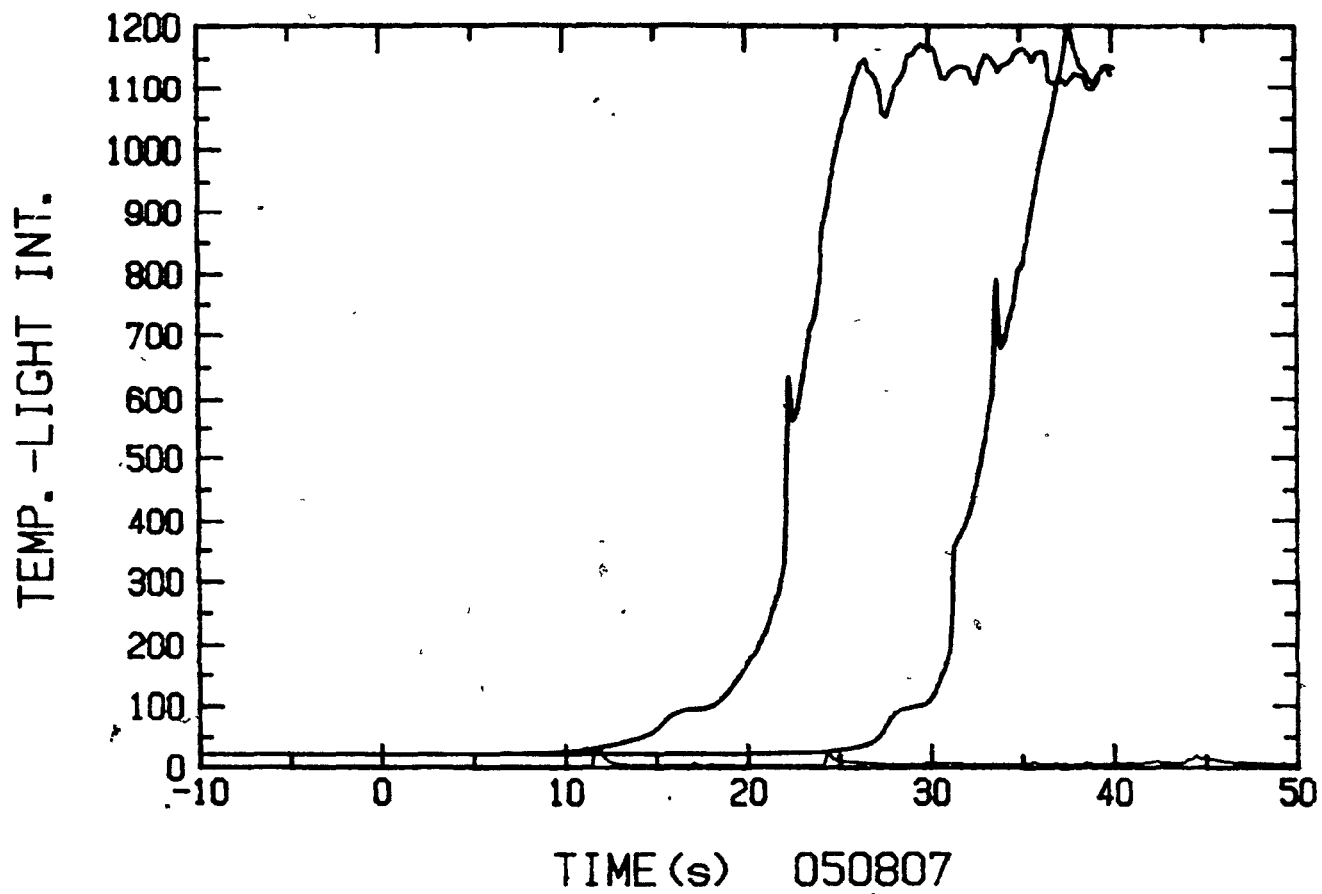


Figure 5.39. Temperature and photocell traces of a 3.2mm magnesium wire insulated with 4.5mm of Ajax tape. The immersion velocity was 1.0cm/s.

showed that the temperature of the first thermocouple stabilized at a temperature of about 1100°C . This value is approximately the boiling point of magnesium (i.e. 1107°C at 1 atm.) From this, it can be postulated that the magnesium was released from the glass sheathing as a vapor. Some of the vapor filled the leading end of the vacated sheath and thus the temperature remained constant. It must be stressed that this event was not always evident and it appeared to be prominent for samples with larger insulation thicknesses.

Consider the traces shown in Figure 5.40. These are typical traces of a magnesium composite sample tested at 1600°C with 5.4mm of Ajax tape insulation. Contrast this with the traces of a typical aluminum sample shown in Figure 5.41. Note that the photocell readings for both tests are essentially the same, except for a few small peaks in the traces for the magnesium sample. Hence this indicates that a relatively quiet immersion can also be obtained in steel, provided that the appropriate insulation and immersion speeds are used.

In section 5.2.1a it was stated that samples with large insulation thicknesses tended to bend upwards towards the bath surface. In doing so, a composite sample containing magnesium would release the magnesium close to the bath surface. An example of this is represented by the temperature and photocell traces shown in Figure 5.42. This particular sample consisted of 4.2mm of Mudge, Watson tape insulation and was fed at a speed of

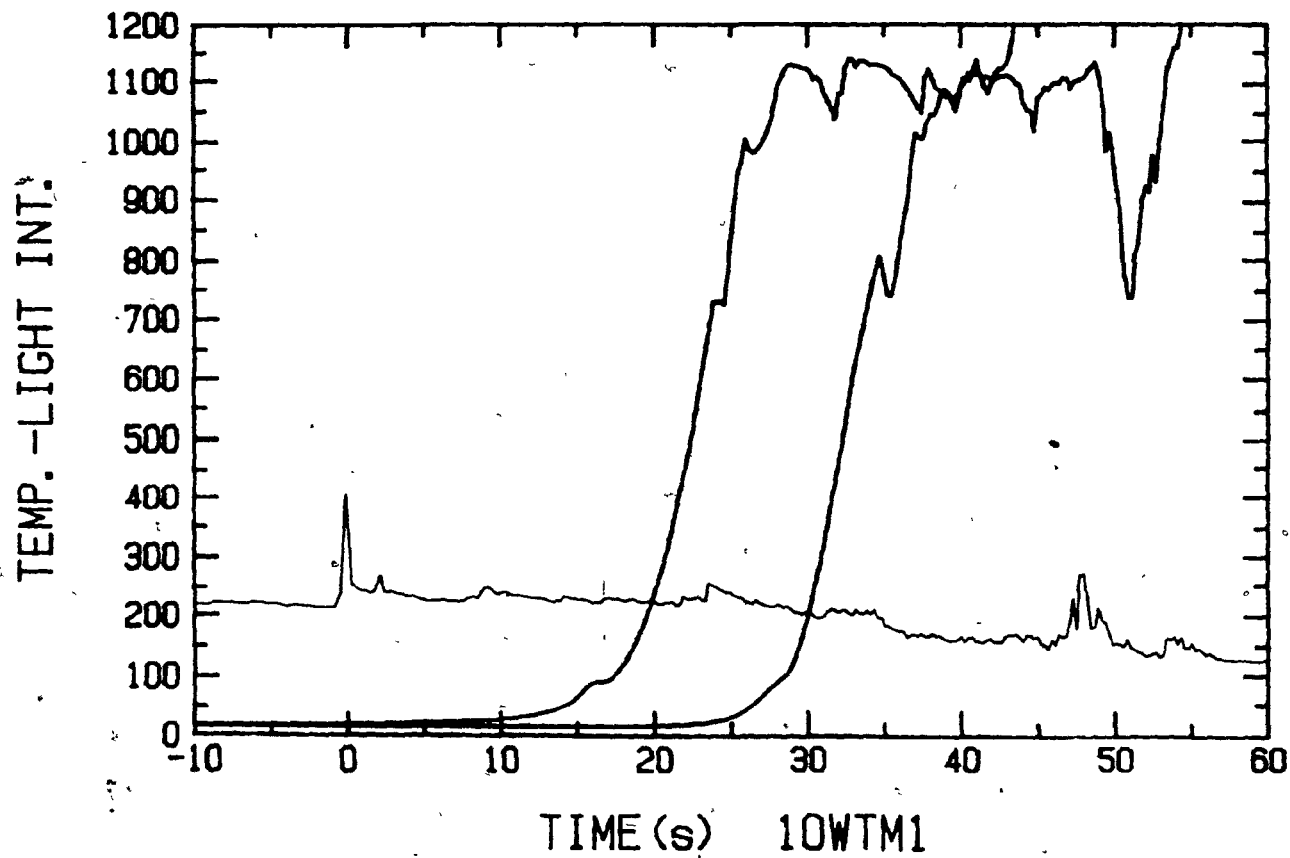


Figure 5.40. Typical temperature and photocell traces for a Mg composite sample tested at 1600°C.

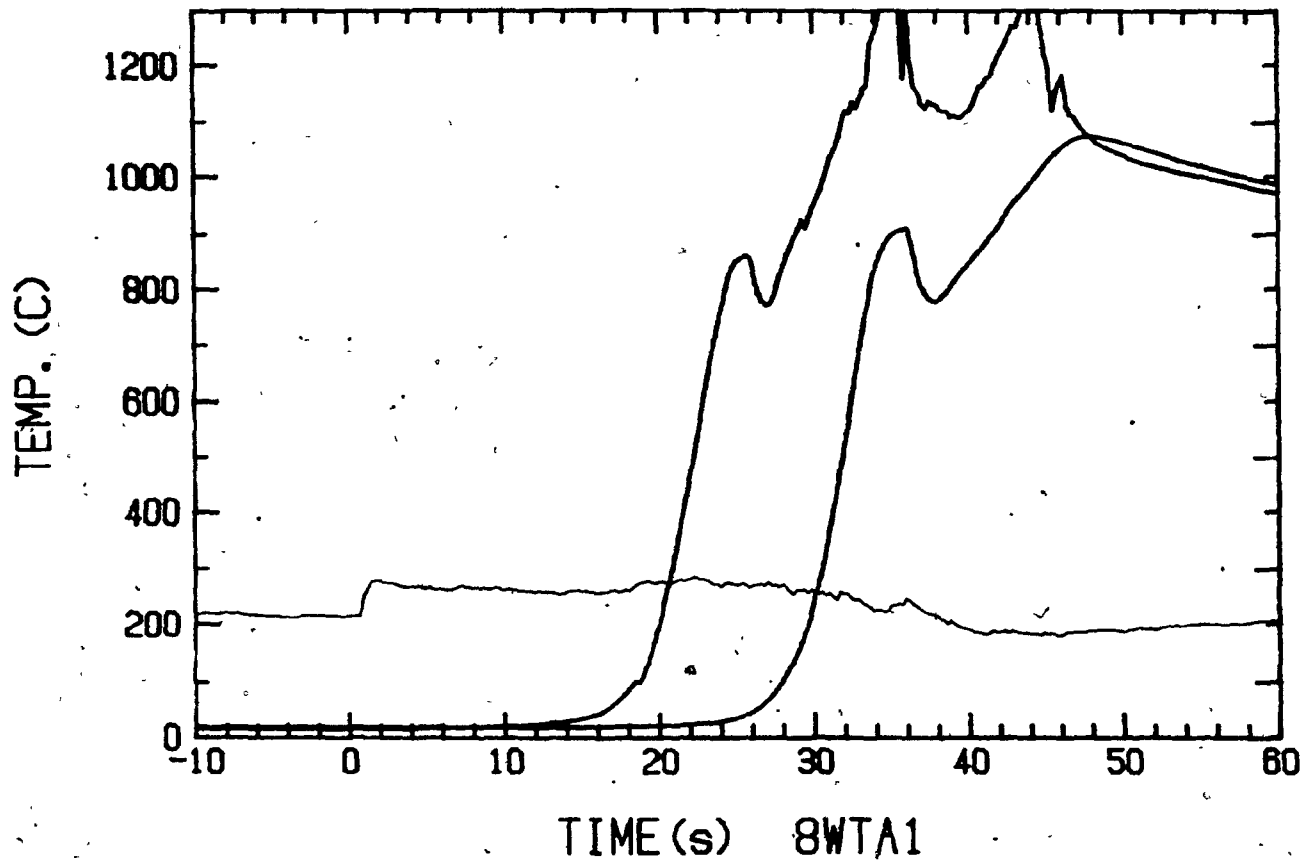


Figure 5.41. Typical temperature and photocell traces for an Al composite sample tested at 1600°C.

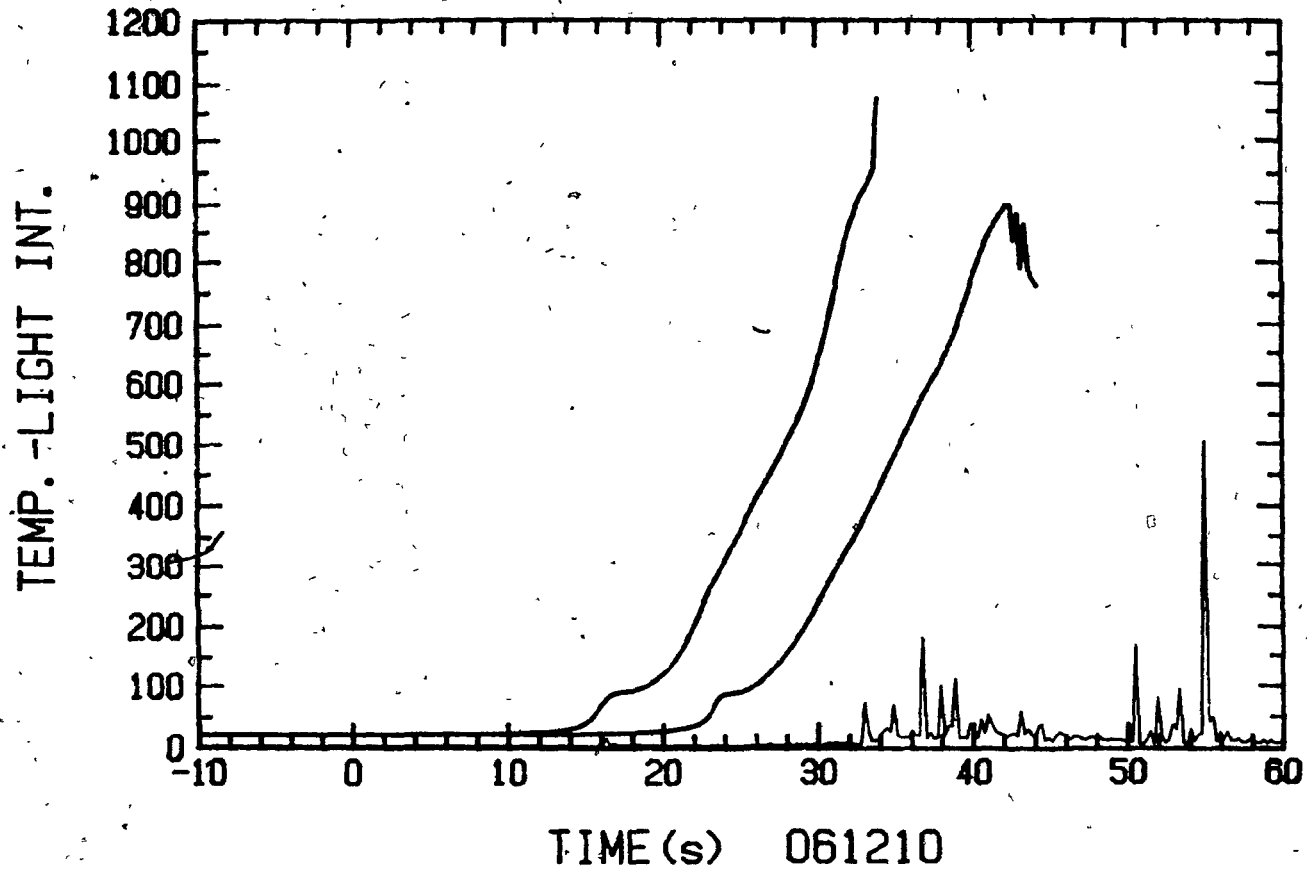


Figure 5.42. Temperature and photocell traces for a Mg composite sample that bent upwards and released Mg close to the bath surface.

1.0cm/s. The length of the magnesium wire was 30cm. In this test, the feeder was stopped after the last portion of magnesium crossed the bath surface (i.e. 30 second mark). Since the last portion of magnesium did not penetrate deep into the bath, the portion of the composite sample that bent released magnesium close to the bath surface, resulting in the emission of bright flashes. This event was prevented in subsequent tests by stopping the feeder after about 10cm of the steel handle penetrated the bath. This allowed the magnesium at the trailing end of the composite sample to penetrate deeper into the bath. The steel handle was also insulated by glass tape.

The results presented up to this point showed that the depth of penetration can be increased by increasing the insulation thickness. It would be instructive at this point to examine the effects of maintaining a constant depth of penetration while varying the immersion speed and insulation thickness. Figures 5.43-5.45 show three typical temperature and photocell traces of samples that were insulated with various thicknesses of Mudge, Watson tape. Sample 091108 had 4.2mm of insulation and was fed at a speed of 1.0cm/s while sample 091109 had 3.5mm of insulation and was immersed at a speed of 1.3cm/s. Sample 091112 was fed at a speed of 2.37cm/s and had an insulation thickness of 2.0mm. The depths of penetration of all three samples, which were estimated from the computed melting times, ranged from 15 to 17cm. Note that the photocell traces for all three samples

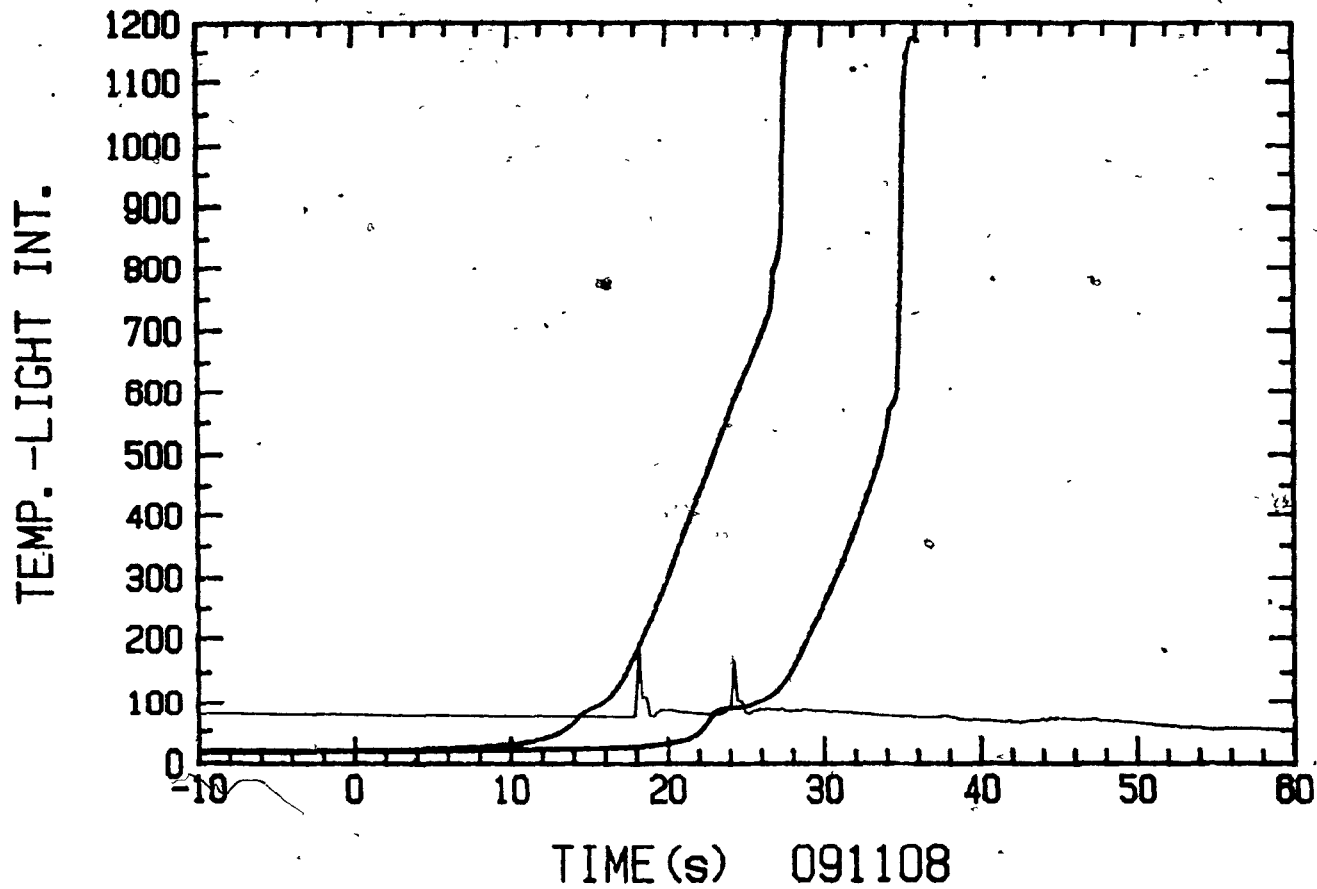


Figure 5.43. Temperature and photocell traces of a 3.2mm magnesium sample insulated with 4.2mm of Mudge, Watson tape. The immersion velocity was 1.0cm/s.

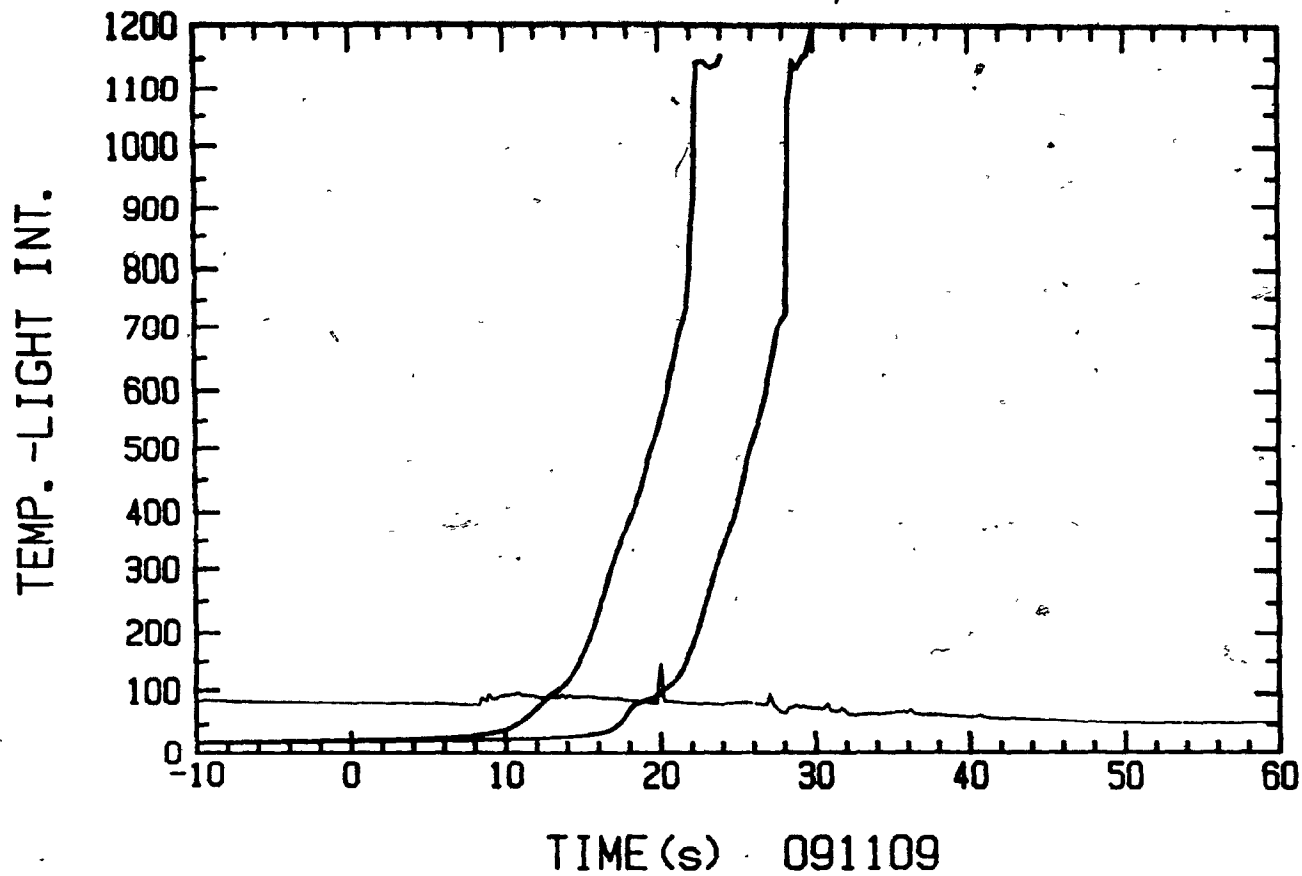


Figure 5.44. Temperature and photocell traces of a 3.2mm magnesium sample insulated with 3.5mm of Mudge, Watson tape. The immersion velocity was 1.3cm/s.

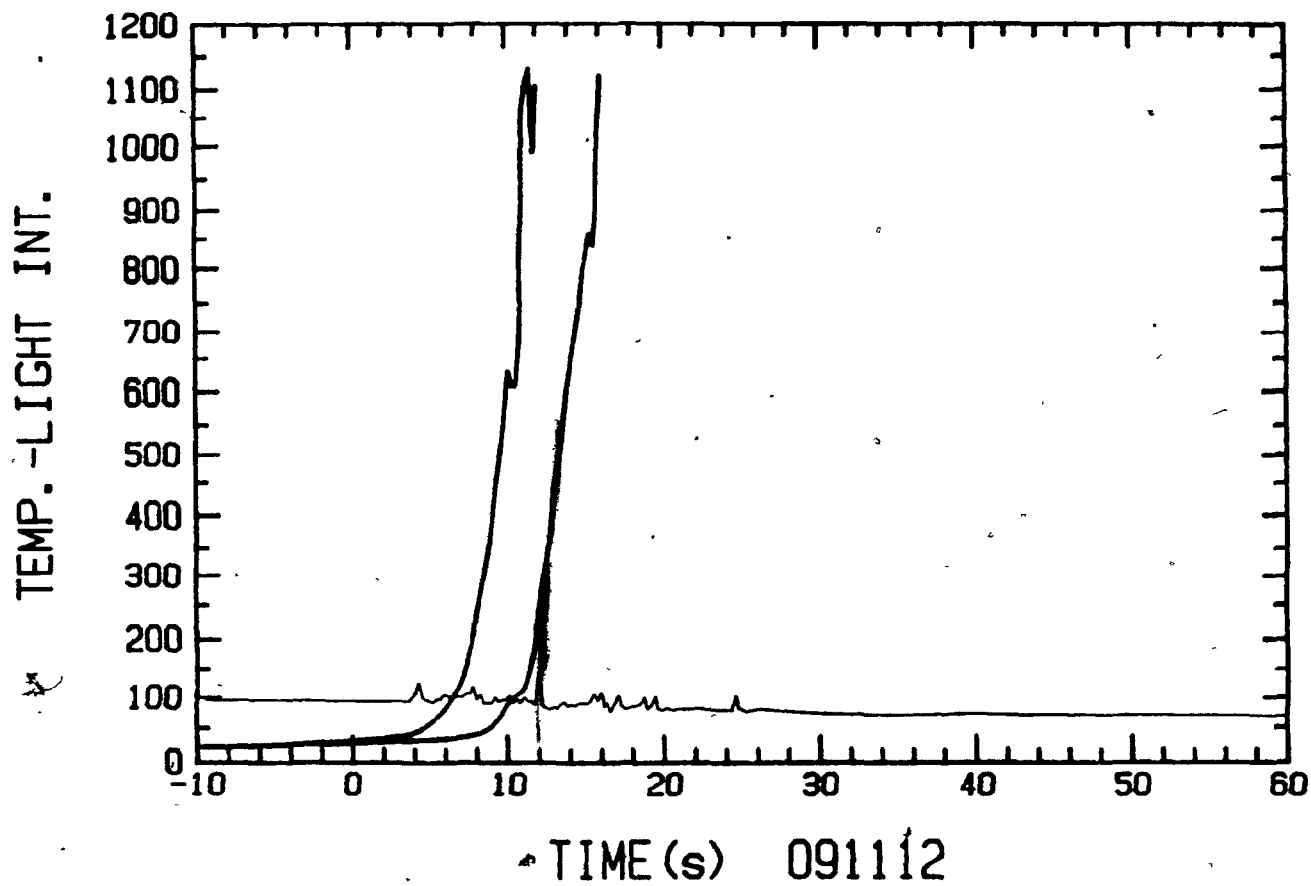


Figure 5.45. Temperature and photocell traces of a 3.2mm magnesium sample insulated with 2.0mm of Mudge, Watson tape. The immersion velocity was 2.37cm/s.

were essentially flat, indicating that very little magnesium resurfaced. Also note that the velocity was increased up to about two and one half times the usual immersion speed and still achieved relatively the same degree of calmness. Putting this into perspective, an immersion velocity of 2.37cm/s would generate 1.6 l/s of magnesium vapor (assuming that all the magnesium vaporizes and none of it dissolves-see appendix B for calculations) in a bath volume of 3.7 litres for a duration of approximately 13 seconds. Since a relatively calm immersion was attained, the magnesium had to dissolve quite quickly. This indicates that increasing the velocity of the immersion does not necessarily increase the turbulence within the bath. The turbulence is largely dependent on the depth of penetration and the size of the magnesium vapor bubbles.

5.2.3 Pyrotechnic and Volatility Tests

For the pyrotechnic and volatility tests, an accelerometer was used to evaluate the volatility of various magnesium samples while pyrotechnic evaluations were based on readings obtained from a photocell.

As was revealed in Chapter 2, one major problem that was encountered in the previous work was that violent and periodic explosions occurred as the samples insulated with glass powder were fed into the molten metal bath. A typical accelerometer and photocell trace of one such sample is shown in Figure 5.46. The line oscillating about the center of the graph represents the accelerometer trace while the line near the bottom of the graph

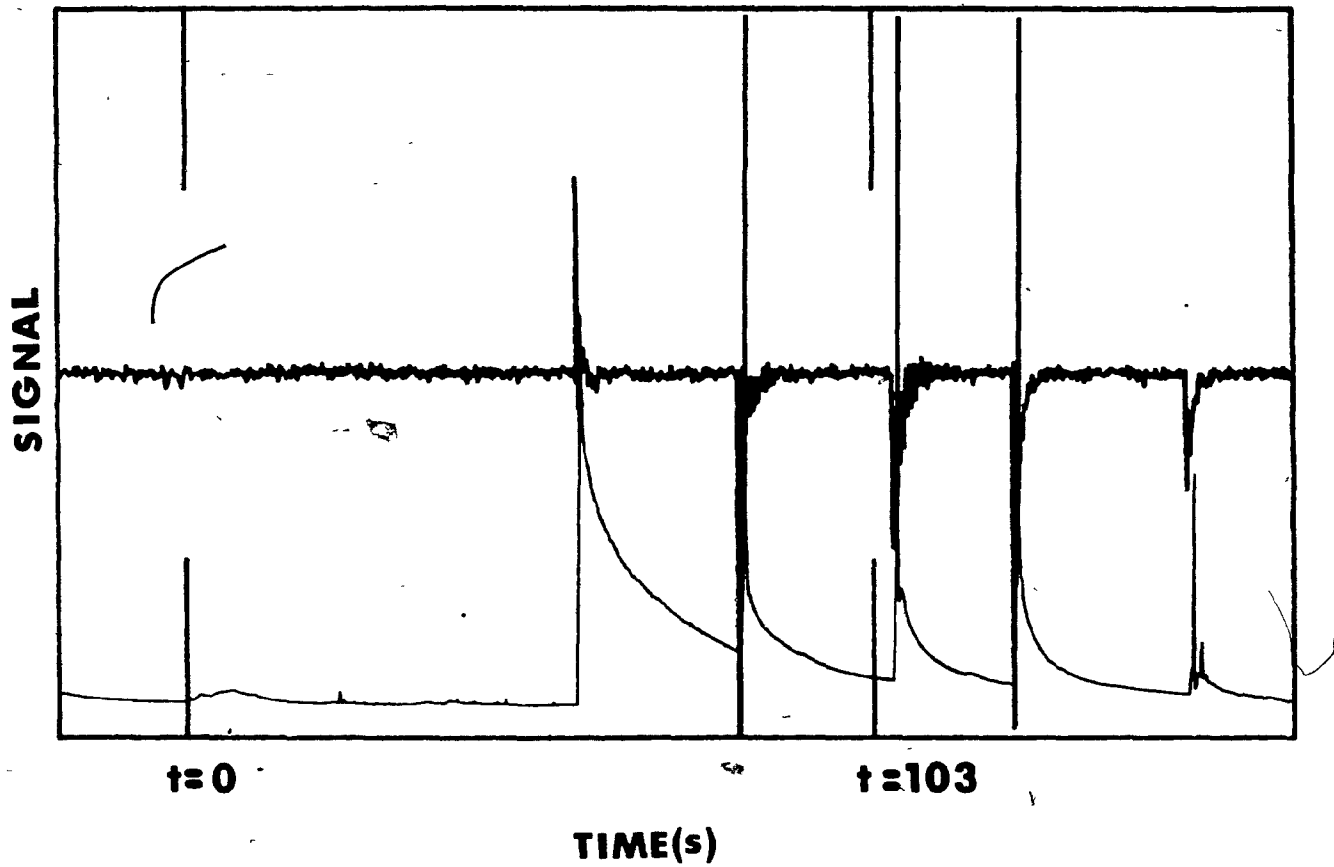


Figure 5.46 . A typical accelerometer and photocell trace showing violent and periodic explosions. These traces were obtained from work conducted previously.

was produced by the photocell. This particular test was conducted with a magnesium wire measuring 36cm in length and was surrounded by 8mm of glass powder. The glass powder was encased by copper sheathing. The sample was fed at a speed of 0.35cm/s. The two large vertical ticks on the left hand side of the graph denote the instant the leading end of the wire contacted the melt while the two vertical ticks on the right side denote when the tailing end of the magnesium wire entered the bath. On an accelerometer trace, the bubbling of magnesium vapor or an eruption is indicated by an increase in the amplitude of the accelerometer reading. One can clearly see from Figure 5.43 that there were a total of five 'explosions' during the test. Furthermore, one can also see that there was no magnesium released between each pair of explosions. An interesting point worth noting is that after each eruption the photocell trace decayed at a very slow rate to the base line. The violence of each eruption caused a significant amount of the hot metal to be ejected from the crucible onto the top of the furnace housing. The ejected metal was contained by the ring of cement that was positioned around the crucible mouth. Because of the newly created radiating surface, the photocell was picking up more light. However, the hot metal on the surface of the furnace housing cooled quickly, and as a result the intensity of the emitted light decayed. Hence, a photocell trace not only shows when bright flashes occurred, it also indicates whether metal was ejected from the crucible.

At the time of the above described test, the causes behind the periodic eruptions were not evident. However, subsequent testing with embedded thermocouples, which were carried out in the first part of the present study, did provide some important clues. Based on this evidence, it was concluded that the turbulence created when the leading end of the magnesium wire began vaporizing was strong enough to destroy the whole length of glass insulation that was submerged, thus exposing a relatively cold magnesium wire. The explosions would consume the magnesium and then the process would repeat itself.

The periodic explosions were eliminated when the magnesium was insulated with glass tape instead of glass powder. An example of a typical accelerometer and photocell trace of a sample insulated with glass tape is shown in Figure 5.47. This sample consisted of 4.6mm of Mudge, Watson insulation and was immersed in the pig iron melt at a velocity of 1.0cm/s. It can be seen from the traces that there was no evidence of pyrotechnic displays during the initial stages of penetration. The magnesium eventually started to melt and vaporize. The traces show that once the magnesium began to vaporize, it was released in the bath in a fairly uniform manner except for an eruption towards the end which resulted in the emission of flares and flashes. The last burst of flashes was the result of the severing of the steel handle used to feed the magnesium wire, thus causing the submerged magnesium to rise to the surface. The steel handle broke as a result of it being pushed

053013

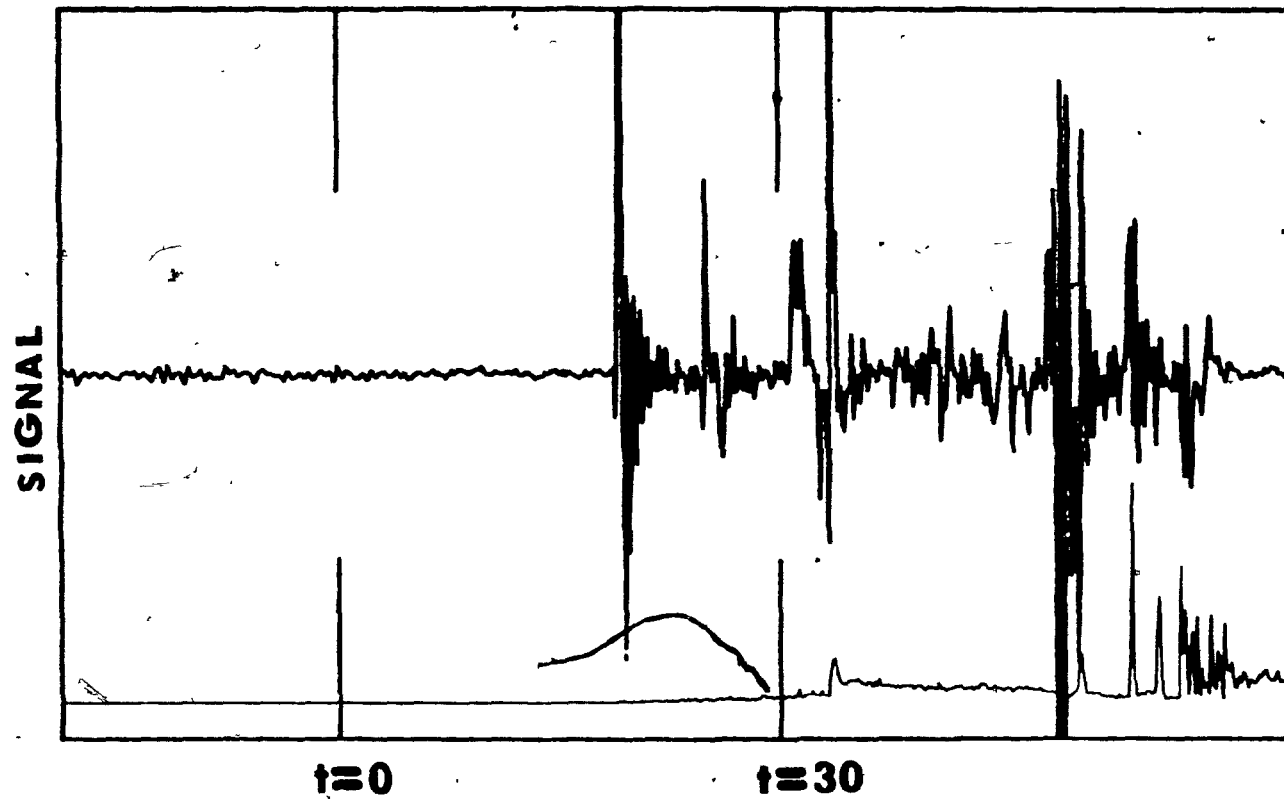


Figure 5.47. Typical accelerometer and photocell traces for a sample insulated with 4.6mm of Mudge, Watson tape.

too deep into the bath, thus, exposing to the bath a portion of the steel handle that was not insulated with glass tape. The portion of the steel handle that broke off was later found floating on the bath surface.

As another example consider the traces shown in Figure 5.48. This graph was produced for the case when two composite samples were simultaneously fed into the bath. Both samples had 4.6mm of insulation and were fed at a velocity of 1.0cm/s. The samples were separated by a distance of 7cm. Notice that the photocell trace shows that there were virtually no flashes or flares. Furthermore, contrast this graph with the one shown in Figure 5.45. If the last burst in Figure 5.45 is excluded, the two graphs are essentially the same, thus indicating that the molten metal bath possibly can accommodate much more magnesium than was originally used. This also suggests that instead of increasing the immersion speed to increase the mass flowrate, the mass flowrate can be increased by increasing the number of wires being immersed. The advantage of using more than one wire is that it allows for better distribution of the magnesium. At present wire feeders that feed more than one wire do exist.

At this point it is worthwhile to consider what happens when a bare magnesium wire is fed into a pig iron melt. Figure 5.49 shows typical traces of a bare 3.2mm diameter magnesium wire fed at a velocity of 0.35cm/s. Note that the accelerometer did not pick up any bubbling of magnesium vapor while the photocell indicated that there was continual burning of magnesium on the

D1415

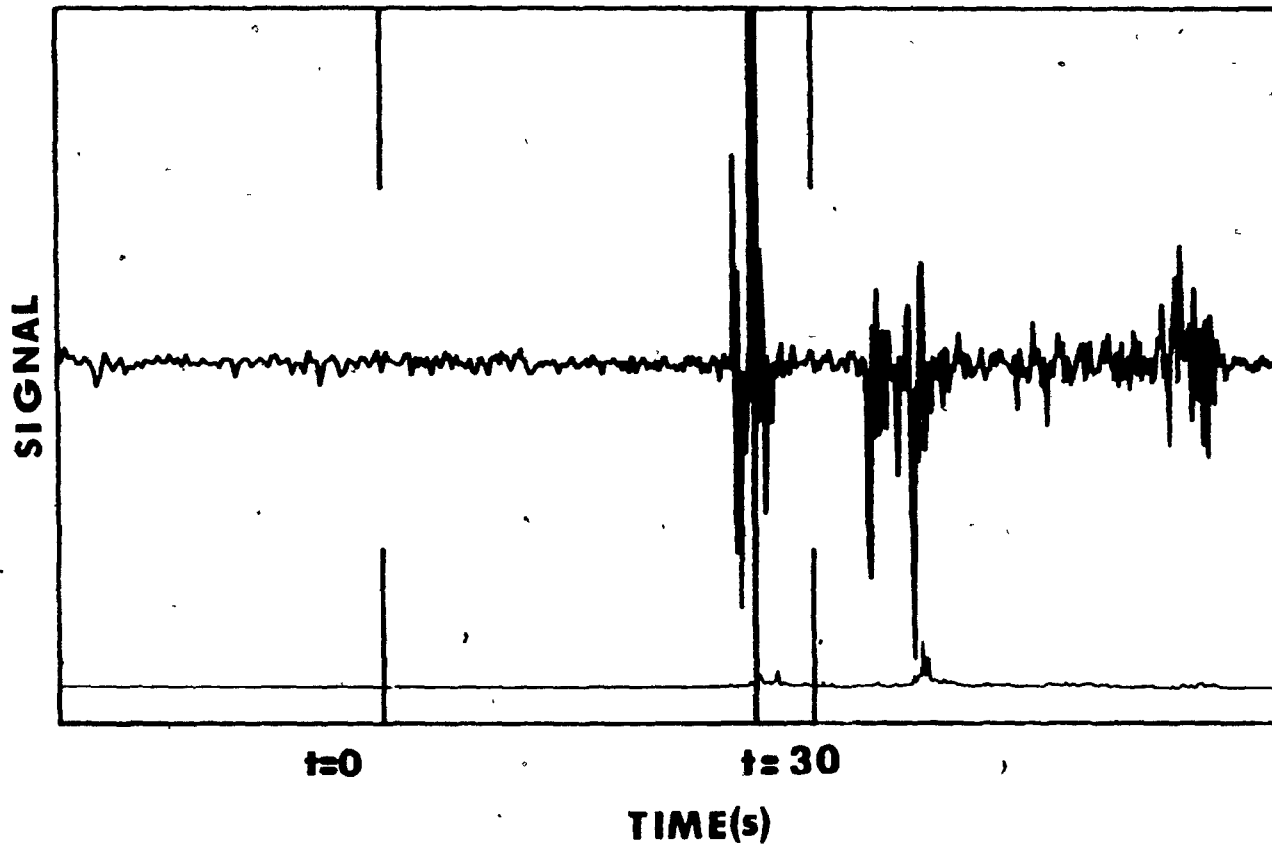


Figure 5.48. Traces for the case when two composite samples were simultaneously fed into a pig iron bath.

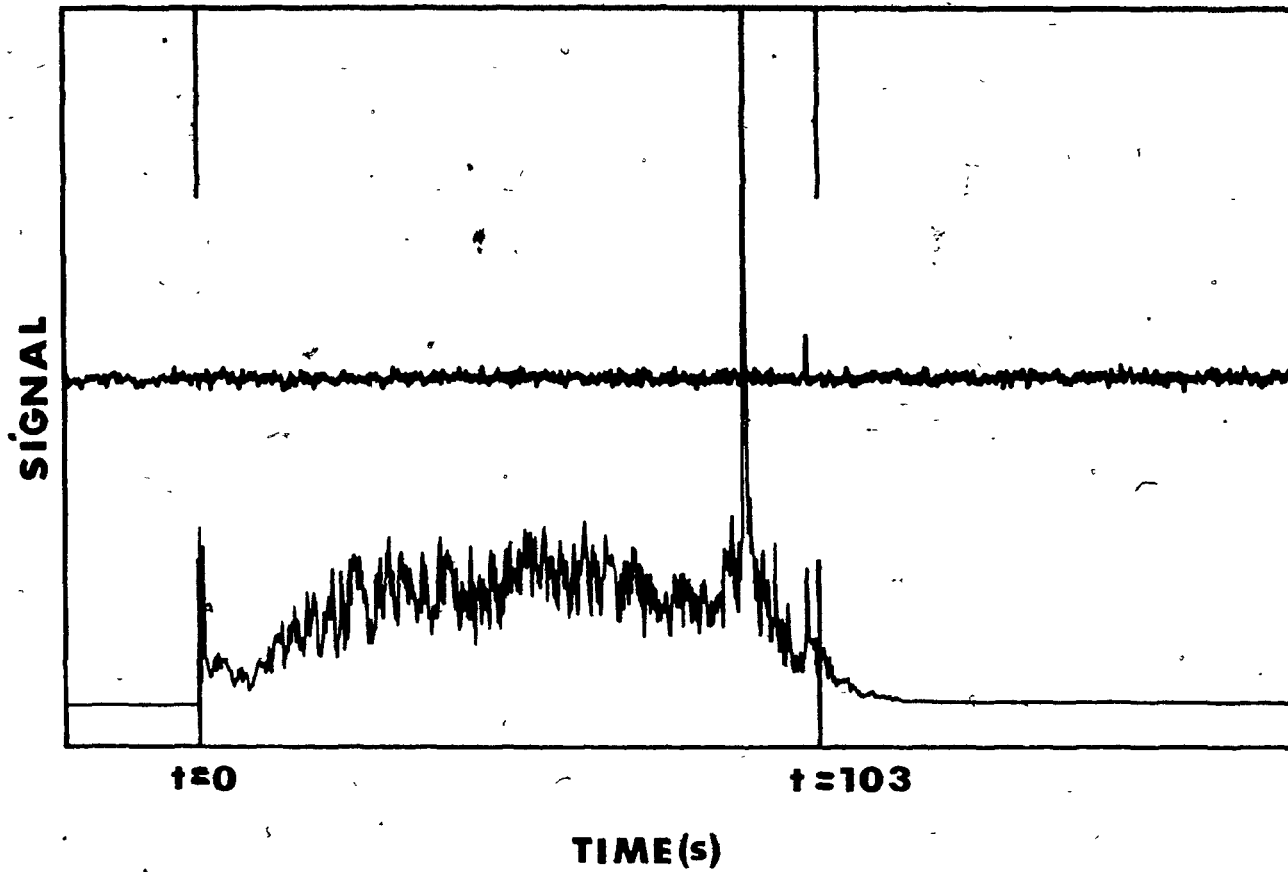


Figure 5.49. Typical photocell and accelerometer traces for a bare magnesium wire.

bath surface. This shows that an uninsulated magnesium wire will not penetrate the surface to any great extent and will as a result burn in the immediate vicinity of the surface.

Consider the trace exhibited in Figure 5.50. This graph shows that the traces for a magnesium sample that was fed at 1.0cm/s and that had a minimal amount of insulation (i.e. 1.45mm). Note that after a brief delay in the initial stage, the magnesium began reacting, as evidenced by the increase in amplitude of the accelerometer reading. At the same time there was persistent burning of magnesium on the bath surface. This indicated that the magnesium did penetrate the bath surface, but, the depth of penetration was not sufficient to allow the magnesium enough time to dissolve completely.

In summary, the photocell and accelerometer traces were useful in determining whether a magnesium wire penetrated the bath surface. When it did, one could estimate to what extent it penetrated by the delay time between the commencement of magnesium bubbling and the bath surface contact time. Furthermore, the accelerometer traces indicated the manner in which the magnesium was released below the bath surface. In other words, they showed whether the magnesium was released uniformly or sporadically.

5.2.4 Desulphurization and Recovery Tests

5.2.4a Desulphurization

The desulphurization tests were conducted in pig iron, however, the bath temperature was raised to 1600°C. The reason for raising the bath temperature to steelmaking temperatures

051513

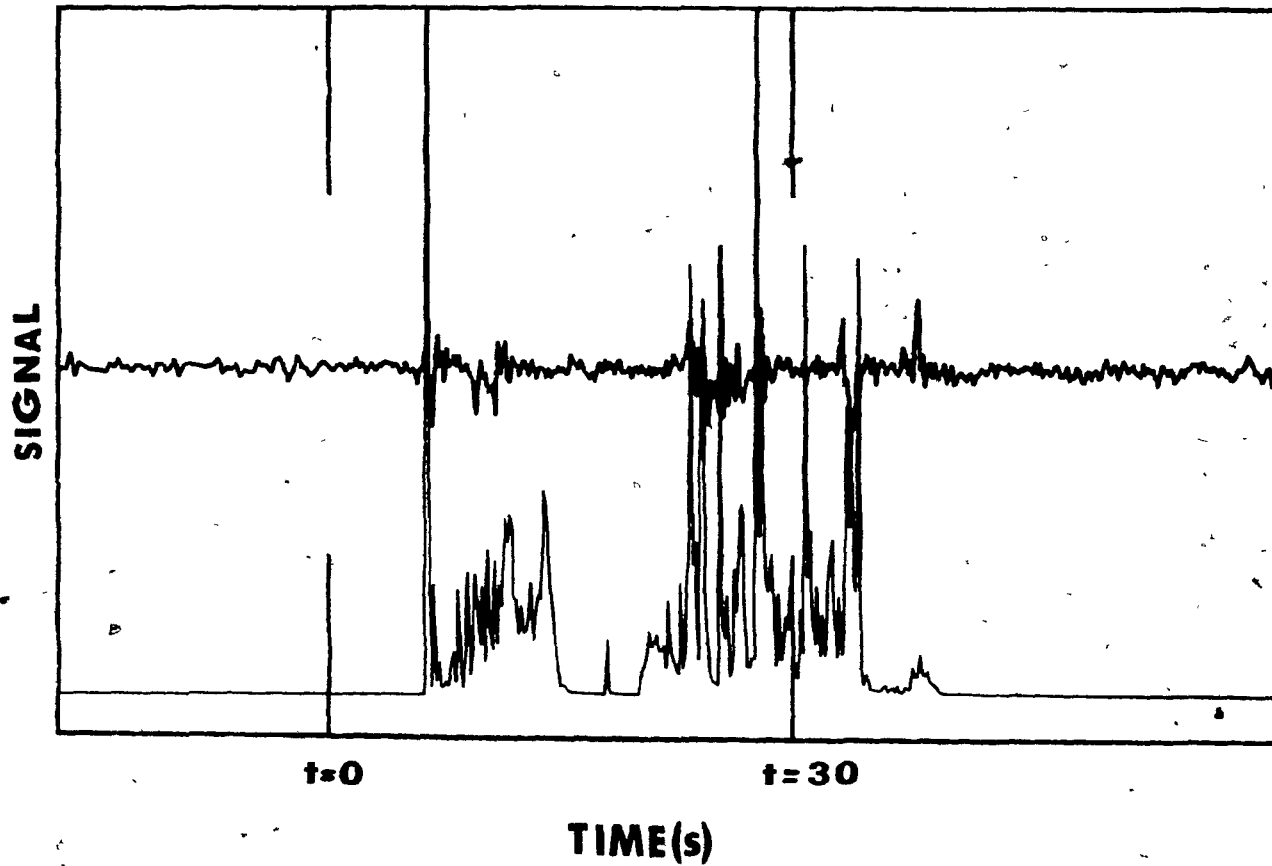


Figure 5.50. Typical photocell and accelerometer traces for a sample that had 1.45mm of Ajax tape insulation.

was to provide a large superheat. The large superheat was needed, firstly, to offset temperature losses during the immersion of the samples since the furnace power was turned off during each test, and secondly, to facilitate melting the slag cover. It was found that at 1400°C it was difficult to obtain a fluid desulphurizing slag. The furnace power was turned off during the immersions to prevent electrical interference with the accelerometer signals.

The weight of the molten metal was approximately 50 kg. About 100 grams of pyrite were added to the bath to raise the sulphur content to about 0.1%. The slag used in these tests was made from a mixture 35% soda-lime (powder glass, 55% lime, and 10% fluorspar. The slag basicity was about 2.2. The composite samples consisted of 3.2mm diameter magnesium wire weighing about 3.61 grams and insulated with 4.5mm of Ajax tape. Bath samples for subsequent sulphur analysis were taken before and after the immersion of each composite magnesium wire sample. The desulphurization results are shown in Table 5.1.

A total of six composite wires were utilized. The desulphurization efficiency (DE) of each test was calculated using the following expression:

$$DE = \frac{\Delta S\% \times HMW \times AW_{mg}}{WT_{mg} \times AW_s} \quad (16)$$

where

- $\Delta S\%$ = change in sulphur content (%)
- HMW = hot metal weight (g)
- AW_{mg} = atomic weight of Mg (g)
- WT_{mg} = weight of Mg utilized (g)
- AW_s = atomic weight of sulphur (g)

TABLE 5.1
DESULPHURIZATION RESULTS

Addition no.	Mg wt. (g)	%S		Efficiency (%)
		before	after	
1	3.61	0.0953	0.0831	125.0
2	3.61	0.0831	0.0844	-
3	3.61	0.0844	0.0930	-
4	3.61	0.0930	0.0890	-
5	3.61	0.0850	0.0845	-
6	3.61	0.0842	0.0842	-

Table 5.1 shows that an efficiency of 125% was achieved with the first immersion. Obviously this value cannot be correct. One reason that may explain this apparently high efficiency is that the slag, by itself, may have contributed significantly to sulphur removal. However what was surprising about the results was that essentially no desulphurization was achieved for subsequent tests. The reason for this was simply that the slag was saturated with sulphur and could not absorb any more. The maximum amount of sulphur that can be accommodated by the slag is largely dependent on the basicity and quantity of slag, although there are other factors that may affect the absorption of sulphur. Knowing the slag basicity, the amount of slag, and the initial sulphur content, the lowest final sulphur content can be determined from the following relationship:⁵¹

$$[S] = [S]_0 \exp(-nY) \quad (17)$$

where $[S]_0$ = initial sulphur content
 $[S]$ = final sulphur content
 n = sulphur partition coefficient
 Y = relative slag amount (slag/metal)

For this particular case approximately 340g of slag was used. This would give a 'Y' value of 0.007. From Figure 5.51, the sulphur partition coefficient for a slag basicity of 2.2 is about 20.⁵² Hence, according to equation (17) the final sulphur content should have been 0.082%. The measured final sulphur content was in fact 0.083%. Therefore, it was obvious that after the first immersion the slag became saturated with sulphur, hence, further sulphur removal from the hot metal was not possible unless the slag was replaced by new slag.

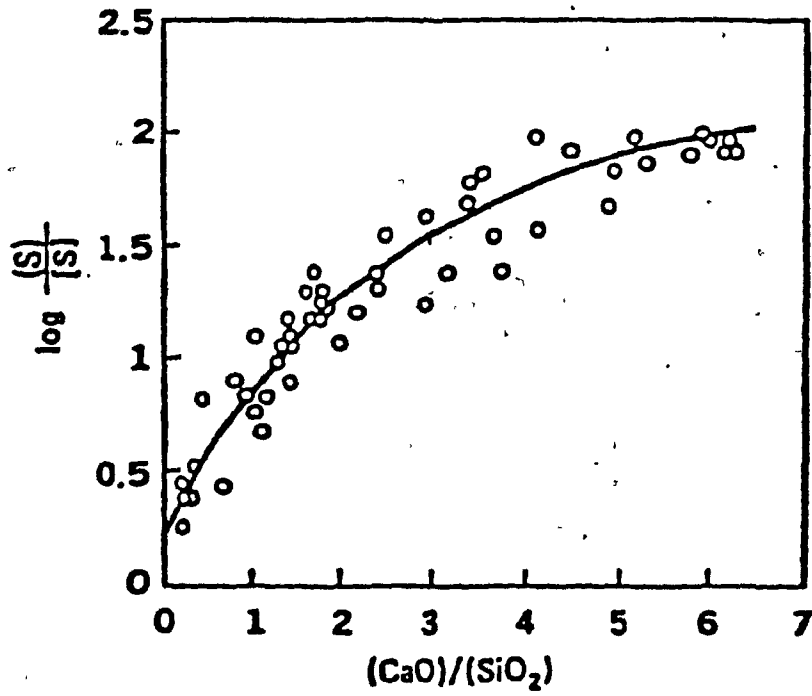


Figure 5.51. Dependence of the sulphur partition coefficient on the slag basicity.

In order to obtain very low sulphur contents for subsequent tests, it was obvious that a larger amount of slag with a higher basicity was required. Due to the problems encountered with the slag in these experiments, it was felt this approach would be impractical. Therefore it was decided that it would be worthwhile to concentrate our efforts in obtaining magnesium recovery results instead of desulphurization efficiencies.

5.2.4.b Magnesium Recovery Tests

The recovery tests were conducted in molten pig iron at 1400°C. The bath weights for the tests ranged between 23 and 26 kg and the initial sulphur contents ranged between 0.02 and 0.024%. In order to prevent the dissolved magnesium from being exposed to the atmosphere, a slag cover was used. The slag consisted mainly of the continuous casting mold powder, Pemco 1693. The reason Pemco 1693 was used was that it was easy to melt and it provided a fluid slag surface.

The magnesium samples used in these tests weighed about 3.6g and all samples were insulated with Mudge, Watson tape. The insulation thicknesses ranged from 1.4 to 4.6mm. The samples were all immersed at a velocity of 1.0cm/s. Bath samples were taken, for subsequent sulphur and magnesium analysis, before and after each immersion. Before the immersion of the samples the furnace power was turned off. After each immersion the furnace power was turned on low power for about 30 seconds. The reason for this was to provide gentle stirring of the bath in order to obtain an homogeneous bath composition. The results are shown in Tables 5.2 and 5.3.

TABLE 5.2
RECOVERY RESULTS OBTAINED WITHOUT STIRRING

Insulation Thickness (mm)	sample	%S		%Mg		Recovery (%)
		before	after	before	after	
1.5	051505	0.024	0.026	0.0011	0.0059	32.0
1.5	051509	0.023	0.022	0.001	0.0202	133.0
1.5	051013	0.008	0.008	0.0291	0.0195	-
2.5	051506	0.020	0.018	0.0174	0.0205	31.9
2.5	051510	0.025	0.023	0.0221	0.0041	-
2.5	051514	0.007	0.006	0.0195	0.024	11.0
3.5	051507	0.020	0.021	0.0195	0.0352	105.0
3.5	051511	0.009	0.011	0.0036	0.028	162.0
3.5	051515	0.006	0.007	0.0204	0.0159	-
4.5	051512	0.011	0.010	0.028	0.0224	-
4.5	051508	0.009	0.009	0.0023	0.0052	19.0
4.5	051516	0.006	0.006	0.0116	0.0164	32.0

TABLE 5.3
RECOVERY RESULTS OBTAINED WITH STIRRING

Insulation Thickness (mm)	sample	%S		%Mg		Recovery (%)
		before	after	before	after	
2.0	053001	0.021	0.022	0.007	0.0039	22.8
2.0	053003	0.018	0.017	0.0126	0.009	4.4
2.65	053007	0.017	0.016	0.0018	0.0038	19.8
2.80	053008	0.022	0.021	0.0027	0.0151	94.0
3.7	053009	0.022	0.021	0.0083	0.0184	77.6
3.6	053010	0.013	0.013	0.0019	0.0125	75.7
3.55	053011	0.014	0.014	0.011	0.0202	65.0
3.6	053012	0.016	0.016	0.0038	0.0142	74.3
4.6	053013	0.015	0.016	0.0141	0.0147	4.3
4.5	053016	0.020	0.020	0.0104	0.0203	70.3
4.6	D1415	0.012	0.011	0.0089	0.0133	18.46

Recovery for these experiments was defined as the percentage of the immersed magnesium that remained dissolved in the bath plus the percentage of the immersed magnesium that was consumed to lower the sulphur content of the bath.

The results shown in Table 5.2 were obtained without any induced stirring (i.e. the furnace power was not turned on immediately after each sample was immersed). The recovery results for these tests ranged from no recovery at all to recoveries well above 100%. Since there was no induced stirring, it was possible that pockets of either magnesium rich or magnesium deficient iron were sampled. For example, consider samples 051513, 051510, 051515, and 051512. The magnesium contents of the bath after the samples were immersed were considerably lower than the magnesium contents before they were immersed, while the sulphur contents did not change significantly. Yet for other samples such as 051509 and 051511, the increases in the magnesium contents after they were immersed were considerably higher than the theoretical maximum increase. These examples tend to support the notion that magnesium rich or magnesium deficient pockets of molten iron were sampled. In order to verify this hypothesis, subsequent tests were conducted with induced stirring.

Table 5.3 shows the recovery results obtained with induced stirring. It is evident that these results were much more consistent than those obtained without any stirring. For samples insulated with more than 2.65mm of glass tape, the recoveries

were quite high (i.e. higher than 60%), with the '3.6' mm samples exhibiting the most consistent recoveries. The samples with less than 2.65 mm insulation exhibited very low recoveries.

Consider sample 053013. This sample was insulated with 4.6 mm of Mudge, Watson tape and it exhibited a very low recovery (i.e. 4.3%). It was observed that when the sample was fully immersed, the sample bent upwards and a portion of it pierced the bath surface. Thus a significant amount of magnesium vapor was exposed to the atmosphere resulting in a display of bright flashes and flares due to the oxidation of the magnesium vapor. Such resurfacing, by way of wire bending, was responsible for some of the low magnesium recoveries when relatively large insulation thicknesses were used.

Test D1415 also exhibited a very low recovery. Test D1415 consisted of two composite samples that were simultaneously fed into the bath. Both samples were insulated with 4.6 mm of Mudge, Watson tape and were fed at 1.0 cm/s. During the immersion of the samples, it was observed that there was vigorous movement of the bath, however, hot metal was not ejected from the crucible and there was no evidence of flashes or flares. Therefore, the reason for the low recovery is not known at this point, although wire bending may have been responsible.

Despite the fact that a couple of the samples with thick insulation showed poor recoveries, the recovery results were encouraging. At present, the most popular magnesium reagent used

in the foundry industry is ferrosilicon (with 4% magnesium). Typical recoveries obtained with this reagent are in the 30-40% range. Moreover, since the ferrosilicon alloy contains only 4% magnesium, a large quantity of reagent must be used. The tests conducted with induced stirring showed that magnesium recoveries of over 70% can be obtained. Hence, due to the fact that the magnesium wire is in pure form and that the magnesium recoveries can be significantly increased, using the present wire feeding technique can result in substantial savings in reagent cost.

CHAPTER 6
SUMMARY AND CONCLUSIONS

In an attempt to develop a novel magnesium wire feeding technique that can be used for both molten iron and steel treatments, the present work was undertaken to find an appropriate insulating material and a viable method of applying it to the magnesium wire surface.

Two types of insulating materials were tested. The first type was powdered glass and the second was glass tape. The glass powders tested were of various chemical compositions and viscosities. The glass tapes were obtained from two suppliers, Ajax Magnethermic Inc. and Mudge, Watson Inc.

From previous work conducted on magnesium wires that were insulated with powdered glass, it was found that the magnesium composite samples exhibited violent and periodic eruptions when immersed in molten iron. It was originally believed that the cause of the eruptions was related to the viscosity of the glass powder. However, the acquisition of very inexpensive thermocouples, along with the use of sensors such as an accelerometer and photocell, made it possible to develop a better understanding of the cause of the violent and periodic eruptions. This led to the development of the glass tape insulated magnesium wire.

The above mentioned sensors also made it possible to determine the effect of parameters such as immersion speed and

insulation thickness on volatility, pyrotechnic display, and depth of penetration.

From the present research work, the following conclusions can be drawn:

1) Although it was previously believed that the cause of the periodic eruptions was related to the viscosity of the glass powder, the internal temperature responses of the powdered glass insulated samples indicated that the primary cause was the inability of the glass powder to remain intact as the samples were immersed in the bath.

2) A more effective method of insulating a magnesium wire is to wrap glass tape around it. The advantages of using glass tape are: 1) it provides greater strength than glass powder, 2) it can be easily applied to the wire, and 3) the insulation thickness can be easily varied by changing the number of wraps of glass tape. Furthermore, it overcomes the problem of centering the magnesium core and it eliminates the need for a metallic sheath.

3) Mudge, Watson tape was a more effective insulator than Ajax tape.

4) Ajax tape effectively insulated magnesium wires that were fed in a molten iron bath at 1400°C. However, the insulation thicknesses had to be significantly increased to attain the equivalent penetration depths as the wires fed into a molten bath at 1600°C.

5) The relationship between the melting time of a core material and its insulation thickness for a core material measuring 3.2mm in diameter can be represented by an equation of the form:

$$T = aX^b$$

where a and b are experimentally determined constants and X is the insulation thickness in mm.

6) The melting time results were used to estimate the penetration depth of magnesium samples. The penetration depth increased with increasing insulation thickness. For small insulation thicknesses (i.e. less than 2.5mm), it can be assumed that the penetration depths were estimated fairly accurately. However for larger thicknesses,

this method was not reliable. The reason for this was that as the insulation thickness increased, the tendency for the magnesium samples to bend upwards also increased. Hence, the calculated depth of penetration may have been significantly different from the effective depth of penetration.

7) As the depth of penetration increased, the degree of pyrotechnic display decreased.

8) The degree of pyrotechnic display decreased as the immersion speed was increased from 1.0cm/s to 2.37cm/s. The insulation thicknesses varied from 4.2mm to 2.0mm, respectively.

9) Photocell and accelerometer traces were useful in determining whether a magnesium wire penetrated the bath surface. The penetration depth can be estimated by the delay time between the start of magnesium bubbling and the bath surface contact time. Furthermore, accelerometer traces indicated the manner in which magnesium was released below the bath surface (i.e. uniformly or sporadically).

10) In order to obtain good magnesium recovery results, it was necessary to gently stir the molten pig iron bath after each composite sample was immersed. This provided the bath with a homogeneous bath composition. Magnesium recoveries of over 65% were consistently obtained for insulation thicknesses greater than 2.65mm when the bath was stirred.

11) The present wire feeding technique need not be limited to the introduction of magnesium for the treatment of molten iron or steel melts. This technique can be used for the introduction of other volatile desulphurizing reagents such as calcium and calcium based reagents. Furthermore, it probably can be used for adding alloying elements such as lead, strontium, and tellurium, or a combination of alloying elements and compounds. These areas are yet to be investigated.

APPENDIX A

The program listed below is a one-dimensional heat transfer model simulating the radial heat flow to a composite cored wire. The composite cored wire can consist of two sections of different materials. Information such as the thickness of each section, number of nodes in each section, the ambient and starting temperatures, melting points, and thermal properties are all input variables. The thermal properties do not vary with temperature, however, different thermal properties can be entered for different states. The program can handle three different states. These include the solid, liquid, and mushy states. The mushy state is a transition phase between the solid and liquid states. The mushy state is included to take into account the heat of fusion for a given section. It is assumed that the transition from solid to liquid occurs over a one degree celsius range. Hence, the mushy state starts at the melting point of a given section and ends one degree celsius above the melting point. Since the transition is assumed to take place over a one degree range, the heat capacity of the state is simply the heat of fusion divided by one degree celsius. The density and thermal conductivity of the mushy state is assumed to be the same as that of the solid state.

Figure A.1 shows the melting time results for 3.2mm diameter composite samples obtained with the heat transfer model. The results were obtained for bath temperatures of 1400°C and

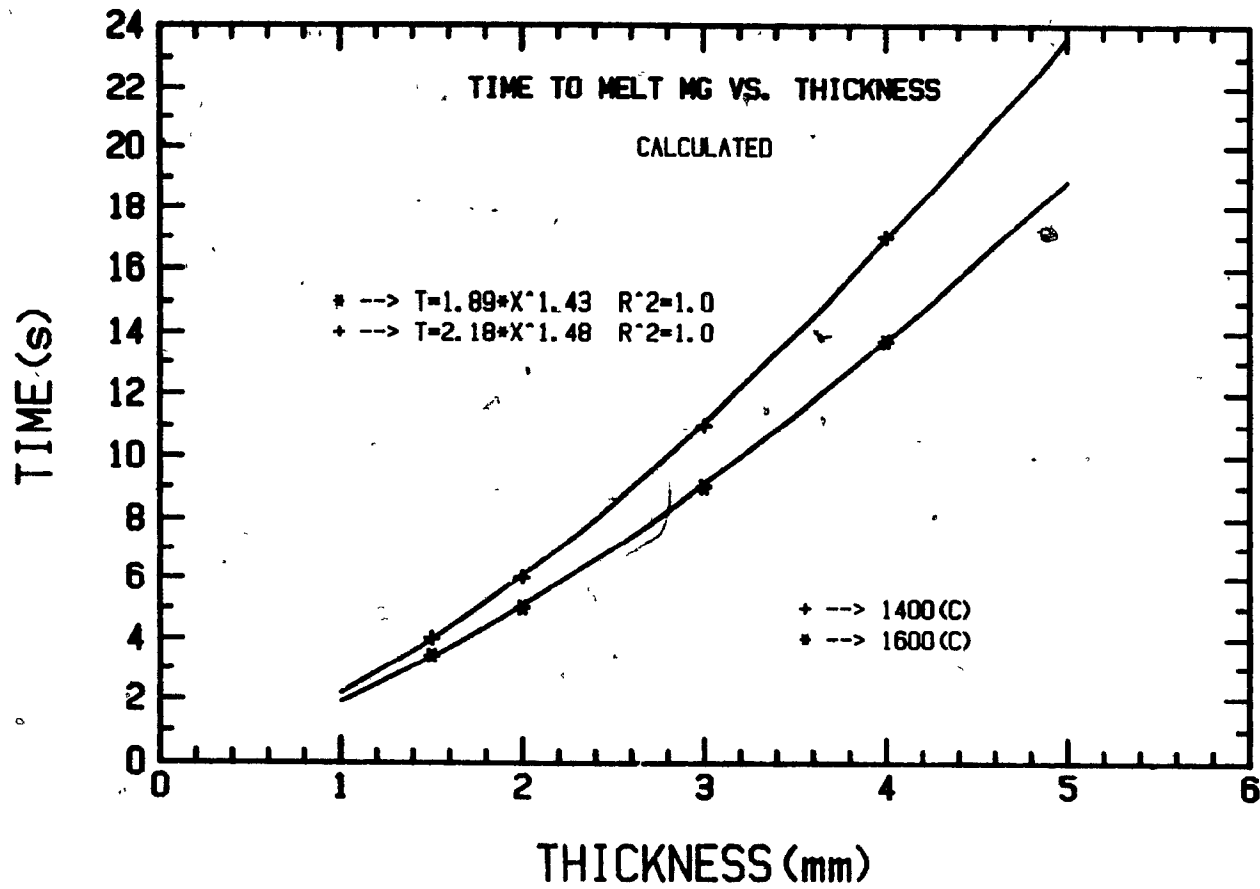


Figure A.1. Plot of magnesium melting times versus insulation thickness for bath temperatures of 1400°C and 1600°C. These curves were calculated using a heat transfer model. The diameter of the magnesium core was 3.2mm.

1600°C.

Figure A.2 shows the melting time results for 15.9mm diameter magnesium composite samples. These results are of particular interest because a joint research project with Stelco was carried out whereby 15.9mm insulated magnesium rods were immersed in a 3 tonne pig iron bath. The research work conducted in conjunction with Stelco is beyond the scope of this thesis. One point worth noting is that if the 'melting time' curve is extrapolated to the 'zero' insulation mark, one will find that it will take approximately 10 seconds to melt the magnesium rod. Because of the size of the magnesium rod, a noticeable temperature gradient exists within the rod. As a result, it would take the center of the magnesium considerably longer to reach the melting point than it would take the surface of the magnesium. Moreover, the melting time versus insulation thickness relationship can no longer be expressed in the form:

$$T=ax^b$$

The melting time versus insulation thickness would be better expressed in the following form:

$$T=ae^{bx} \quad (18)$$

The heat transfer model clearly illustrates the difference between 3.2mm and 15.9mm magnesium rods. Consider Figure A.3 and A.4. Figure A.3 is a plot of the temperature profile of half a composite sample consisting of a 3.2mm diameter magnesium wire insulated with 3mm of glass tape. Figure A.4 is a similar plot of a 15.9mm diameter magnesium rod with the same thickness of insulation.

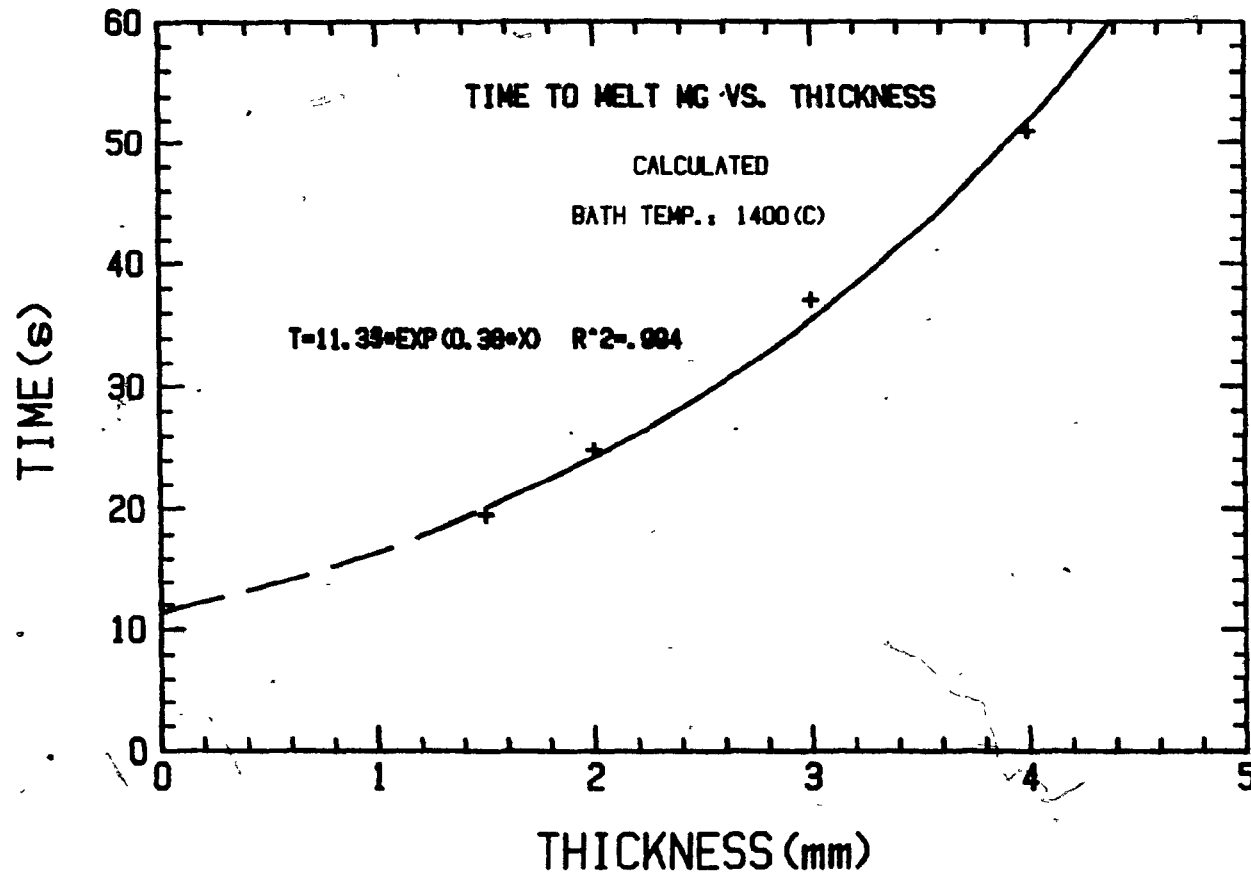


Figure A.2. Plot of magnesium melting times versus insulation thickness for a 15.9mm diameter magnesium rod.

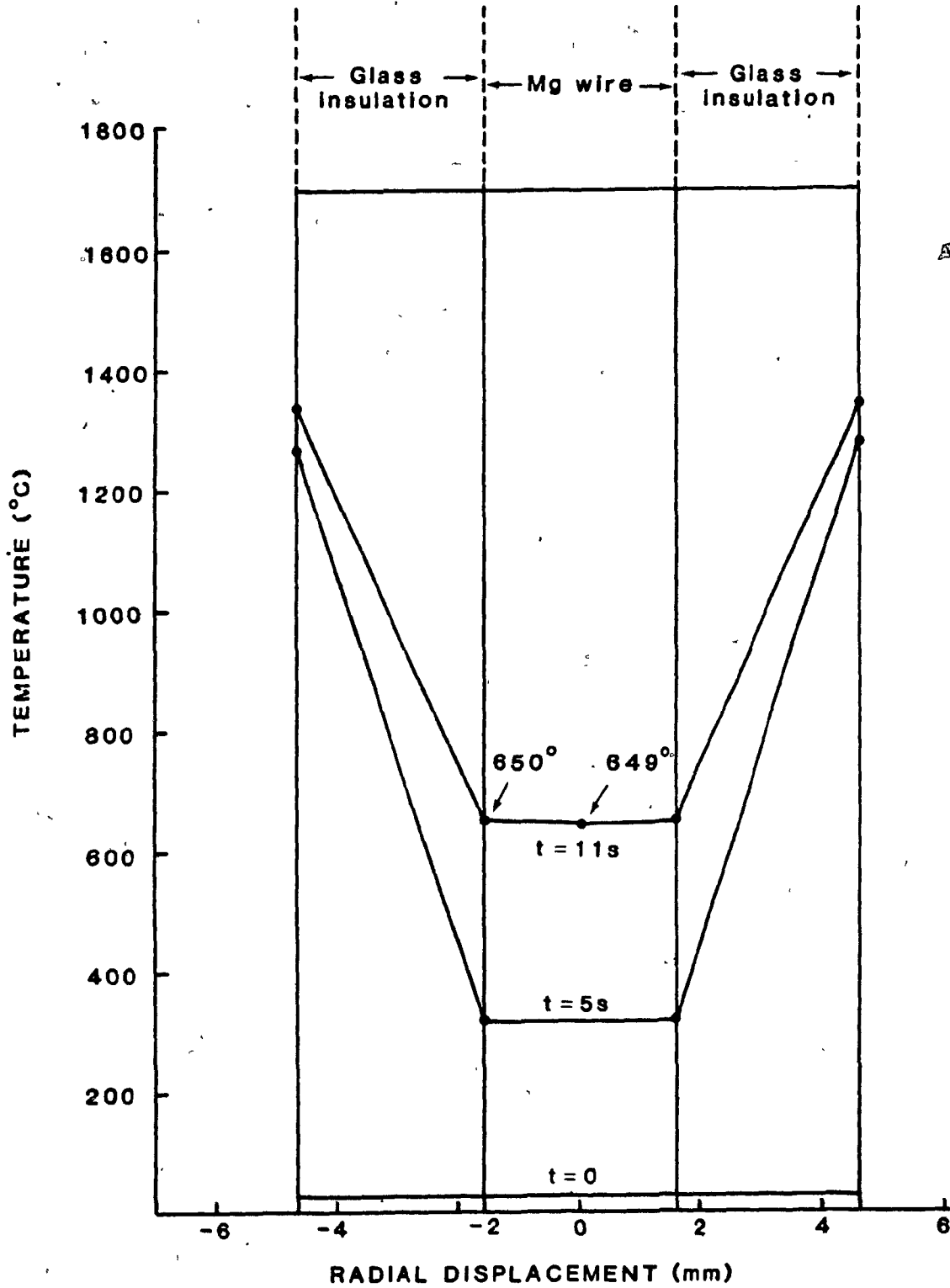


Figure A.3. Schematic of composite sample with temperature profiles. The composite sample consisted of a 3.2mm diameter Mg wire insulated with 3.0mm of glass tape.

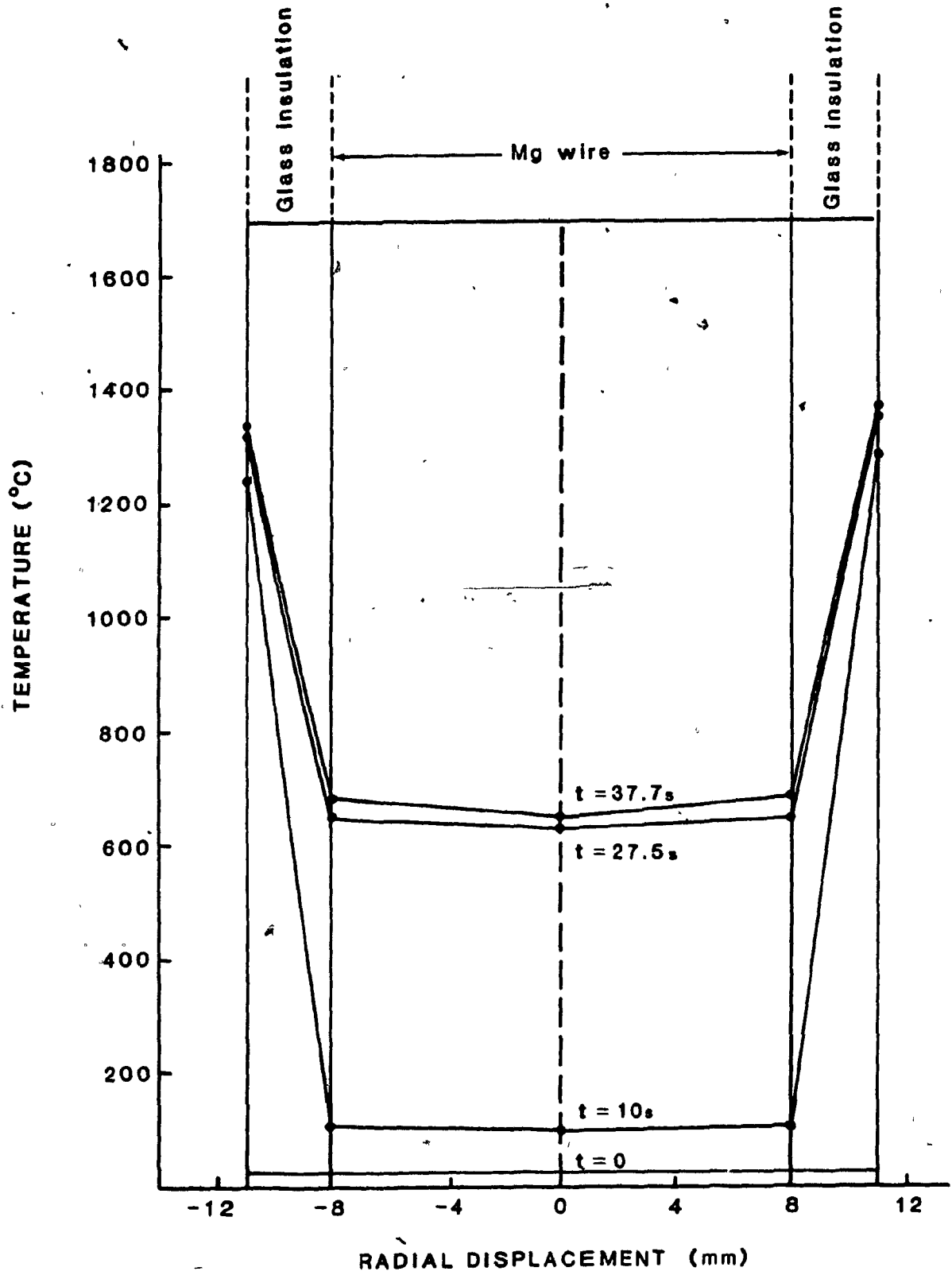


Figure A.4. Schematic of composite sample with temperature profiles. The composite sample consisted of a 15.9mm diameter Mg rod insulated with 3.0mm of glass tape.

Note that the temperature profile within the 3.2mm magnesium wire is essentially uniform whereas a slight temperature gradient exists within the 15.9mm rod. Also note that the surface of the 15.9mm rod reached its melting point about 10 seconds prior to that of the center of the magnesium rod.

In the experiments conducted in the present study, it was assumed that the magnesium wire melted when the thermocouple on the surface of the magnesium rod reached a temperature of 650°C. This was a reasonable assumption since the heat transfer model showed that the temperature of the 3.2mm diameter wire was essentially uniform. However, if 15.9mm magnesium rods were to be used, the melting times would have to be determined by implanting thermocouples in the center of the magnesium rod.

Magnesium rods, 15.9mm in diameter, were not tested in the present study, however, 15.9mm diameter aluminum rods were. In these tests, one thermocouple was placed on the surface of the aluminum while another thermocouple was implanted in the center of the aluminum rod. Consider the temperature traces shown in Figure A.5. These traces were obtained for a composite sample comprising of a 15.9mm diameter aluminum rod insulated with 3mm of Mudge, Watson tape. Note that the center of the aluminum rod took approximately 15 seconds longer to reach its melting point than did the surface of the aluminum rod. It is expected that a magnesium rod would exhibit the same trend, however, the delay time would probably be less since it takes 35% more energy to raise the aluminum to its melting point.

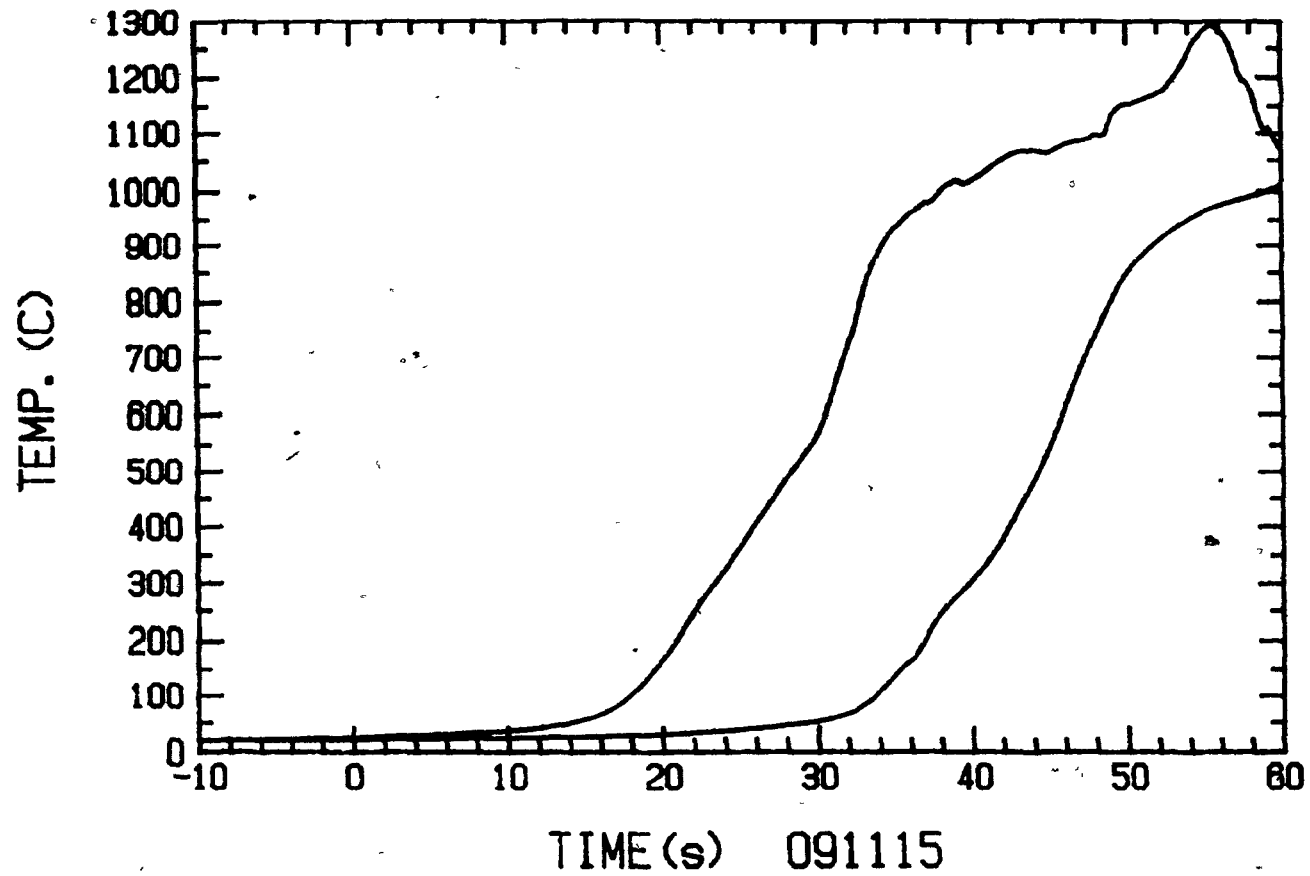


Figure A.5. Temperature traces of a 15.9mm Al rod insulated with 3.0mm of glass tape.

```

*****
*
*           PROGRAM TEMP
*
*****

```

/SYS REG=120

/LOAD WATFIV

```

COMMON AREA(10,2),VOL(10,2),DXN(10,2),TEMP(10,2),DTS,DT
COMMON XTEMP(10,2),NODES(2),THICK(2),ROW(2,3),K(2,3),AS
COMMON CP(2,3),COND(10,2),MPT(2,2),TA,H,XX1,TIME
INTEGER I,J,L,M,COND
REAL K,MPT

```

C
C
C
C
C

```

*****
*   INPUT VARIABLES   *
*****

```

10

```

WRITE(6,10)
FORMAT(' ','ENTER THE THICKNESS OF EACH SECTION AND THE',
&' NO. OF NODES IN EACH SECTION.')
DO 20 J=1,2
WRITE(6,25) J
25  FORMAT(' ','SECTION',I2)
20  READ(9,*) THICK(J),NODES(J)

```

C

30

```

WRITE(6,30)
FORMAT(' ','ENTER THE HEAT TRANSFER COEFFICIENT.')
READ(9,*) H

```

C

40

```

WRITE(6,40)
FORMAT(' ','ENTER THE AMBIENT TEMPERATURE.')
READ(9,*) TA

```

C

50

```

WRITE(6,50)
FORMAT(' ','HOW MANY DENSITY, HEAT CAPACITY, AND THERMAL'
&' CONDUCTIVITY TERMS DO YOU WANT TO ENTER?')
READ(9,*) M

```

C

51

```

WRITE(6,51)
FORMAT(' ','ENTER THE SECTION NO., STATE, DENSITY, HEAT '
&' CAPACITY, AND THERMAL CONDUCTIVITY.')
DO 52 L=1,M
52  READ(9,*) I,J,ROW(I,J),CP(I,J),K(I,J)

```

C

60

```

WRITE(6,60)
FORMAT(' ','ENETR THE SOLIDUS AND LIQUIDUS TEMP. FOR BOTH'
&' SECTIONS.')
DO 65 J=1,2

```

```

63 WRITE(6,63) J
65 FORMAT(' ', 'SECTION ', I3)
65 READ(9,*) MPT(J,1), MPT(J,2)

```

```

70 WRITE(6,70)
70 FORMAT(' ', 'ENTER THE STARTING TEMP. & STATE FOR BOTH',
& 'SECTIONS.')
70 READ(9,*) STEMP, STATE
70 DO 80 J=1,2
70 N1=NODES(J)
70 DO 90 I=1,N1
70 TEMP(I,J)=STEMP
90 COND(I,J)=STATE
80 CONTINUE

```

```

C CALL AVNS
C CALL STABIL

```

```

100 WRITE(6,100) DTS
100 FORMAT(' ', 'TIME INCREMENT MUST BE LESS THAN', F14.7)
110 WRITE(6,110)
110 FORMAT(' ', 'ENTER THE DESIRED TIME INCREMENT.')
110 READ(9,*) DT
110 WRITE(6,120)
120 FORMAT(' ', 'ENTER THE INTERVAL BETWEEN PRINTOUTS.')
120 READ(9,*) TBPO

```

```

C CALL CTEMP(TBPO)

```

```

C STOP
C END

```

```

C *****
C *
C * SUBROUTINE AVNS CALCULATES THE AREAS AND VOLUMES FOR *
C * EACH NODE OF EACH SECTION. *
C *
C *****

```

```

C SUBROUTINE AVNS
C COMMON AREA(10,2), VOL(10,2), DXN(10,2), TEMP(10,2), DTS, DT
C COMMON XTEMP(10,2), NODES(2), THICK(2), ROW(2,3), K(2,3), AS
C COMMON CP(2,3), COND(10,2), MPT(2,2), TA, H, XX1, TIME
C DIMENSION ORAD(2), XIRAD(2), P(10,2), XR(10,2)
C REAL K, MPT
C INTEGER COND

```

```

C ORAD(1) = THICK(1) + THICK(2)
C ORAD(2) = THICK(2)
C AS = 6.28 * ORAD(1)
C DO 10 J = 1, 2
C A = THICK(J) / (NODES(J) - 1)
C N1 = NODES(J) - 1
C DO 20 I = 1, N1

```

```

20      DXN(I,J) = A
      N4=NODES(1)
      N5=NODES(2)
      DXN(N4,1) = 0.0
      DXN(N5,2) = 0.0
C
      XIRAD(J) = ORAD(J) - THICK(J)
      P(1,J) = ORAD(J)
      XR(1,J) = ORAD(J) - A/2.0
      VOL(1,J) = 3.14*(ORAD(J)*ORAD(J) - XR(1,J)*XR(1,J))
C
      N2 = NODES(J)
C
      DO 30 I=2,N2
      XR(I,J) = XR(I-1,J)-A
      IF(I.EQ.N2) XR(I,J) = XIRAD(J)
      P(I,J) = P(I-1,J) - A
      AREA(I-1,J) = 6.28*XR(I-1,J)
      VOL(I,J) = 3.14*(XR(I-1,J)*XR(I-1,J) - XR(I,J)*
&XR(I,J))
30      CONTINUE
C
      AREA(N2,J) = 6.28*XIRAD(J)
      WRITE(6,40)
40      FORMAT(6X,'NODE',6X,'RADIUS',5X,'DELTA',5X,'VOLUME'/
*5X,'POSITION,5X,'OF',7X,'R'/
*15X,'SPACING')
C
      N3=NODES(J)
      DO 50 I=1,N3
      WRITE(6,60) P(I,J),XR(I,J),DXN(I,J),AREA(I,J),VOL(I,J)
60      FORMAT(F9.2,2X,F9.2,2X,F9.2,2X,F9.2,2X,F9.2)
50      CONTINUE
10      CONTINUE
      RETURN
      END
C
*****
C
*
C
* SUBROUTINE STABIL ENSURES THAT THE STABILITY CRITERIA *
C
* ARE MET. IT TELLS YOU THE MAXIMUM POSSIBLE INCREMENTAL *
C
* TIME. THEN YOU CHOOSE A TIME INCREMENT THAT SATISFIES *
C
* THE CONSTRAINT. *
C
*
C
*****
C
SUBROUTINE STABIL
COMMON AREA(10,2),VOL(10,2),DXN(10,2),TEMP(10,2),DTS,DT
COMMON XTEMP(10,2),NODES(2),THICK(2),ROW(2,3),K(2,3),AS
COMMON CP(2,3),COND(10,2),MPT(2,2),TA,H,XX1,TIME
INTEGER I,J,L,COND
REAL K,MPT

```

A=VOL(1,1)*DXN(1,1)
X1=ROW(1,1)*CP(1,1)*A
X2=ROW(1,2)*CP(1,2)*A
X3=ROW(1,3)*CP(1,3)*A

DT1=X1/(H*AS*DXN(1,1)+K(1,1)*AREA(1,1))
DT2=X2/(H*AS*DXN(1,1)+K(1,2)*AREA(1,1))
DT3=X3/(H*AS*DXN(1,1)+K(1,3)*AREA(1,1))

DTS=DT1
IF(DT2.LT.DTS) DTS=DT2
IF(DT3.LT.DTS) DTS=DT3

DO 10 J=1,2
N2=NODES(J)-1
DO 20 I=2,N2
DO 30 L=1,3
DO 31 L1=1,3
DO 32 L2=1,3
X4=ROW(J,L)*CP(J,L)*VOL(I,J)
X5=DXN(I-1,J)*DXN(I,J)
X6=K(J,L2)*AREA(I-1,J)*DXN(I,J)+K(J,L1)*AREA(I,J)
&*DXN(I-1,J)

DT4=X4*X5/X6
IF(DT4.LT.DTS) DTS=DT4

32 CONTINUE
31 CONTINUE
30 CONTINUE
20 CONTINUE
10 CONTINUE

N1=NODES(1)
DO 41 L1=1,3
DO 40 L=1,3
X7=ROW(1,L)*CP(1,L)*VOL(N1,1)+ROW(2,L1)*CP(2,L1)
&*VOL(1,2)
X8=DXN(N1-1,1)*DXN(1,2)
X9=K(1,L)*AREA(N1-1,1)*DXN(1,2)+K(2,L1)*AREA(1,2)
&*DXN(N1-1,1)

DT5=X7*X8/X9
IF(DT5.LT.DTS) DTS=DT5
CONTINUE

40 CONTINUE
41 CONTINUE

N3=NODES(2)
DO 50 L=1,3
X10=ROW(2,L)*CP(2,L)*VOL(N3-1,2)*DXN(N3-1,2)
X11=K(2,L)*AREA(N3-1,2)
DT6=X10/X11
IF(DT6.LT.DTS) DTS=DT6
CONTINUE

50 RETURN
END

C
C
C
C
C
C

```
*****
*
* SUBROUTINE CTEMP CALCULATES THE NODAL TEMPERATURES
*
*****
```

```
SUBROUTINE CTEMP(TBPO)
COMMON AREA(10,2),VOL(10,2),DXN(10,2),TEMP(10,2),DTS,DT
COMMON XTEMP(10,2),NODES(2),THICK(2),ROW(2,3),K(2,3),AS
COMMON CP(2,3),COND(10,2),MPT(2,2),TA,H,XX1,TIME
INTEGER I,J,L,N1,COND
REAL K,MPT
```

C
C
C

```
*****
* SURFACE NODE
*****
```

```
XX1=0.0
TIME=0.0
800 XX=H*AS*DT/(ROW(1,COND(1,1))*CP(1,COND(1,1))*VOL(1,1))
ZZ=K(1,COND(1,1))*AREA(1,1)*DT/(ROW(1,COND(1,1))*
&CP(1,COND(1,1))*VOL(1,1)*DXN(1,1))
XTEMP(1,1)=TEMP(1,1)*(1-XX-ZZ)+XX*TA+ZZ*TEMP(2,1)
```

C
C
C

```
*****
* INTERNAL NODES
*****
```

```
J=1
600 N1=NODES(J)
DO 300 I=2,N1
IF(I.EQ.N1.AND.J.EQ.1) GOTO 500
IF(I.EQ.N1.AND.J.EQ.2) GOTO 700
X=K(J,COND(I-1,J))*AREA(I-1,J)*DT/(ROW(J,COND(I,J))
&*CP(J,COND(I,J))*VOL(I,J)*DXN(I-1,J))
Y=K(2,COND(I+1,J))*AREA(I,J)*DT/(ROW(J,COND(I,J))*
&CP(J,COND(I,J))*VOL(I,J)*DXN(I,J))
XTEMP(I,J)=TEMP(I,J)*(1-X-Y)+X*TEMP(I-1,J)+Y*
&TEMP(I+1,J)
```

300
C
C
C

```
CONTINUE
*****
* INTERFACIAL NODES
*****
```

```
500 W=ROW(1,COND(N1,1))*CP(1,COND(N1,1))*VOL(N1,1)+ROW(2,
&COND(1,2))*CP(2,COND(1,2))*VOL(1,2)
X=K(1,COND(N1-1,1))*AREA(N1-1,1)*DT/(DXN(N1-1,1)*W)
Y=K(2,COND(1,2))*AREA(1,2)*DT/(DXN(1,2)*W)
XTEMP(N1,1)=TEMP(N1,1)*(1-X-Y)+X*TEMP(N1-1,1)+Y*TEMP(2,2)
XTEMP(1,2)=XTEMP(N1,1)
J=2
GOTO 600
```

```

C          *****
C          *                LAST NODE                *
C          *****
700      W=ROW(2,COND(N1,2))*CP(2,COND(N1,2))*VOL(N1,2)*DXN(N1-1,2)
          X=K(2,COND(N1-1,2))*AREA(N1-1,2)*DT/W
          XTEMP=(N1,2)=TEMP(N1,2)*(1-X)+X*TEMP(N1-1,2)

```

```

C
C      CALL STATE

```

```

C      TIME=TIME + DT
          IF(TEMP(N1,2).GE.MPT(2,2)) GOTO 900
          IF((TIME-XX1+1.0E-5).GE.TBPO) CALL PRTOUT
          GOTO 800
900      CALL PRTOUT
          RETURN
          END

```

```

C          *****
C          *
C          *   SUBROUTINE PRTOUT PRINTS OUT THE NODAL TEMPERATURES   *
C          *   FOR THE DESIRED TIME INCREMENTS.                       *
C          *
C          *****

```

```

C      SUBROUTINE PRTOUT
          COMMON AREA(10,2),VOL(10,2),DXN(10,2),TEMP(10,2),DTS,DT
          COMMON XTEMP(10,2),NODES(2),THICK(2),ROW(2,3),K(2,3),AS
          COMMON CP(2,3),COND(10,2),MPT(2,2),TA,H,XX1,TIME
          REAL K,MPT
          INTEGER COND

```

```

C      WRITE(6,10) TIME
10      FORMAT(' ','TIME= ',F9.3)
          DO 20 J=1,2
          WRITE(6,30) J
30      FORMAT(' ','SECTION',I3)
          N1=NODES(J)
          WRITE(6,40) (TEMP(I,J),I=1,N1)
40      FORMAT(1X,20(F8.2,1X))
20      CONTINUE
          XX1=TIME
          RETURN
          END

```

C
C
C
C
C
C
C
C

```

*****
*
* THIS SUBROUTINE DETERMINES THE STATE OF EACH NODE, AND *
* THEN ADJUSTS THE TEMPERATURES ACCORDINGLY BY PERFORMING*
* A ENERGY BALANCE.
*
*****

```

C

```

SUBROUTINE STATE
COMMON AREA(10,2),VOL(10,2),DXN(10,2),TEMP(10,2),DTS,DT
COMMON XTEMP(10,2),NODES(2),THICK(2),ROW(2,3),K(2,3),AS
COMMON CP(2,3),COND(10,2),MPT(2,2),TA,H,XX1,TIME
REAL K,MPT
INTEGER COND

```

53

C

30

C

40

20

10

C

60

50

```

      DO 10 J=1,2
        N1=NODES(J)
          DO 20 I=1,N1
            IF(XTEMP(I,J).GT.MPT(J,1).AND.COND(I,J).EQ.1)
& GOTO 30
            IF(XTEMP(I,J).GT.MPT(J,2).AND.COND(I,J).EQ.2)
& GOTO 40
            GOTO 20
          STARTMELT
          A=ROW(J,1)*CP(J,1)*(MPT(J,1)-TEM(I,J))
          B=ROW(J,1)*CP(J,1)*(XTEMP(I,J)-TEM(I,J))
          C=ROW(J,2)*CP(J,2)
          XTEMP(I,J)=(B-A)/C + MPT(J,1)
          COND(I,J)=2
          GOTO 53
        ENDMELT
          A=ROW(J,2)*CP(J,2)*(XTEMP(I,J)-TEMP(I,J))
          B=ROW(J,2)*CP(J,2)*(MPT(J,2)-TEMP(I,J))
          C=ROW(J,3)*CP(J,3)
          XTEMP(I,J)=(A-B)/C + MPT(J,2)
          COND(I,J)=3
        CONTINUE
      CONTINUE

      DO 50 J=1,2
        N1=NODES(J)
          DO 60 I=1,N1
            TEMP(I,J)=XTEMP(I,J)
          CONTINUE
      CONTINUE
RETURN
END

```

APPENDIX B

CALCULATION OF VOLUMETRIC FLOWRATE OF MAGNESIUM VAPOR

DATA

WEIGHT OF MG WIRE (W_w) : 3.6 g
IMMERSION SPEED (S_i) : 2.4cm/s
VOLUME OF BATH (V_b) : 3.7 litres
LENGTH OF MG WIRE (L_w) : 30 cm
MOLECULAR WEIGHT OF MG (MW_{mg}) : 24.305 g

-IMMERSION TIME(T_i) CALCULATION

$$T_i = L_w/S_i \rightarrow T_i = 12.5_s$$

-FLOWRATE(V') CALCULATION

$$V' = n'RT/P \quad \text{where } n' = \text{molar flowrate}$$

$$V' = (W_w/MW_{mg}/T_i) \times 0.082051\text{-atm-K}^{-1}\text{-mole}^{-1} \times 1673\text{K}/1\text{atm}$$

$$V' = 1.6 \text{ l/s}$$

Hence assuming that all the magnesium vaporizes and none of it dissolves, 1.6 l/s of magnesium would be generated.

REFERENCES

1. The Making, Shaping and Treating of Steel, ed. McGannon, H.E., Pittsburgh: United States Steel Corp., 1971
2. Voronova, N.A., Desulphurization of Hot Metal By Magnesium, Warrendale: The Iron and Steel Society of the A.I.M.E., 1983
3. Agarwal, J.C., "Economic Benefits of Hot Metal Desulphurization with Magnesium", *Iron and Steelmaker*, May 1984, pp.40-44
4. Agarwal, J.C., "Economic Benefits of Hot Metal Desulphurization to the Steelmaking Processes", *Ironmaking Conference Proceedings, I.S.S.-A.I.M.E.*, Vol.40, 1981, pp.146-170
5. Kendrick, V.C., Smillie, A.M., Deeter, R.E., Brown, W.H., "Angular Injection of Magnesium Granules for External Desulphurization of Hot Metal at Armco Inc.", *Developments in Hot Metal Preparation for Oxygen Steelmaking*, ed. Lu.W.-K., McMaster Symposium no.11, May 1983, pp.13-27
6. Goedert, J., Liesch, J.-F., "Experience with the ALT-Process on Desulphurization of Hot Metal at ARBED-BELVAL Steelplant", *Developments in Hot Metal Preparation for Oxygen Steelmaking*, ed. Lu.W.-K., McMaster Symposium no.11, May 1983, pp.119-123
7. Chaussy, J.P., Lecigne, R., Denier, G., Reboul, J.P., "Industrial Experience of Magnesium Injection into Iron: The USIRMAG 2 Desulphurization Process", *Developments in Hot Metal Preparation for Oxygen Steelmaking*, ed. Lu.W.-K., McMaster Symposium no.11, May 1983, pp.148-160
8. Lecigne, R., Senaneuch, D., Sauvage, F., Vachier, R., "Injection Treatment at Usinor Dunkirk Works", *Scaninject III-Part I*, 3rd International Conference on Refining of Iron and Steel by Powder Injection, Lulea, Sweden, June 15-17, 1983, pp.14:1-14:22
9. McGowan, A., Arcangeletti, F., Cheng, A., "Operational Experience at Algoma Steel Using Various Methods of Desulphurizing Iron in the Torpedo Ladle", *Developments in Hot Metal Preparation for Oxygen Steelmaking*, ed. Lu.W.-K., McMaster Symposium no.11, May 1983, pp.163-195
10. Koros, P.J., Petrushka, R.G., Kerlin, R.G., "The Lime-Mag Process for Desulphurization of Hot Metal", *Iron and Steelmaker*, Vol.4, no.6, 1977, p.34
11. Tatsuo, Ohya, et al., "Desulphurization of Hot Metal with Burnt Lime", *Steelmaking Proceedings*, Vol.60, 1977, p.345

12. Wilson, W.G., Mclean, A., Desulphurization of Iron and Steel and Sulphide Shape Control, The Iron and Steel Society of the A.I.M.E., Warrendale, 1980

13. Moore, J.J., "The Case for Rare Earth Desulphurization of Acid Steel in Steel Casting Production", Transactions of the American Foundrymen's Society, Vol.168, 1981, pp.809-828

14. Ashton, M.C., Buhr, R.K., Maguy, J.-G., Davis, K.G., "Use of Magnesium Wire Injection for the Desulphurization of Pig Iron", Ironmaking and Steelmaking, Vol. no.2, 1975, pp.111-114

15. Ashton, M.C., Buhr, R.K., Maguy, J.-G., Davis, K.G., "Use of Magnesium Wire Injection for the Production of Nodular Iron", Transactions of the American Foundrymen's Society, Vol.7, 1975, pp.51-54

16. Smith, J.J., "Pelemag Solves Some Magnesium Problems", Iron and Steel International, August 1982, pp.209-211

17. Seppo Haimi, "Observations About Pig Iron Desulphurization with Granulated Magnesium at the Raake Steelworks of Rautaruukki Oy", Scaninject III-Part I, 3rd International Conference on Refining of Iron and Steel by Powder Injection, Lulea, Sweden, June 15-17, 1983, pp.26:1-26:7

18. Ramon, J.S., "Australian Iron and Steel Pty Ltd. Experience with Ladle Injection", Australasian Institute of Mining and Metallurgy, August 1983, pp.23-29

19. Okamoto, T., Huang, X., Kågawa, A., "Graphite Nodulization and Graphitization of Magnesium Treated Cast Irons Solidified Under Argon Atmosphere Pressure upto 145 Atm.", Metal Science, Vol.18, April 1984, pp.169-176

20. Brown, D.C., "High-Quality, Strand-Cast Steel is Here!", Metal Producing, Sept. 1982, pp.62-66

21. Ototani, T., "Recent Development of Metallic Calcium Core Wire in the Steel Production", Scaninject III-Part II, 3rd International Conference on Refining of Iron and Steel by Powder Injection, Lulea, Sweden, June 15-17, 1983, pp.36:1-36:18

22. Heiber, A.F., Watmough, T., "An In-Ladle Treatment Process for Producing Ductile Iron with Elemental Magnesium", Transactions of the American Foundrymen's Society, Vol.46, 1980, pp.289-300

23. Caruso, V., Coperchini, A., Giaccone, A., Dixmier, J.M., Henry, J.M., Margot, J.L., "Recent Applications of Cored Wire in Continuous Casting", Scaninject III-Part II, 3rd International Conference on Refining of Iron and Steel by Powder Injection, Lulea, Sweden, June 15-17, 1983, pp.34:1-34:27

24. McManus, G., "Ladle Metallurgy Moves to a More Active State", Iron Age, March 19, 1984, pp.30-38
25. Haastert, H.P., "Ladle Metallurgy Processes in Steelmaking. Part 2: Treatment of Steel Heats", Metallurgical Plant and Technology, Vol.2, 1984, pp.48-61
26. Brooks, W.B., Dumas, A.C., Romefelt, B.W., "Treat Steel with Magnesium to Ease Sulphur Problem", The Iron Age, February 11, 1960, pp.148-149
27. Saxena, S.K., "Refining Reactions of Magnesium in Steel At Steelmaking Temperatures", International Symposium of the Physical Chemistry of Iron and Steel Making, Conference of Metallurgists, August 29-September 2, 1982, Toronto, The Metallurgical Society of C.I.M., pp.VII:17-VII:22
28. Moore, W., "The Role of Magnesium in Steel Treatment", 36th Annual World Conference on Magnesium, Oslo, Norway, June 24-28, 1979, pp.35-43
29. Kumar, R.V., Kay, D.A.R., "The Role of Calcium, Magnesium and Rare Earth Additions in Ferrous Ladle Metallurgy", unpublished work
30. Ng, K.L., "Magnesium Wire Desulphurization of Hot Metal", McGill University, Unpublished work
31. Holappa, L.E.K., "Ladle Injection Metallurgy", International Metals Reviews, Vol.27, no.2, 1982, pp.53-76
32. Palumbo, E., Wong, E., "Desulphurization by Magnesium Wire Feeding Technique", McGill University, unpublished work
33. Mucciardi, F.A., "A Wire Feeding Method For Treating Liquid Iron Alloys with Buoyant Volatile Additives", McGill University, unpublished work
34. Mucciardi, F.A., Guthrie, R.I.L., "The Development of a Novel Magnesium wire for the Desulphurization of Hot Metal and Steel", McGill University, unpublished work
35. Riboud, P.V., Larrecq, M., "Lubrication and Heat Transfer in a Continuous Casting Mold", Steelmaking Proceedings, A.I.M.E., Detroit, Vol.62, 1979, pp.78-92
36. Riboud, P.V., Olette, M., Leclerc, J., Pollak, W., "Continuous Casting Slags: Theoretical Analysis of their Behavior and Industrial Performances", Steelmaking Proceedings, A.I.M.E., Chicago, Vol.62., 1978, pp.411-417

37. Esaulov, V.S., Konovalov, G.F., Popel, S.I., Sokolov, V.I., "Viscosity of Slag Melts Used in Continuous Casting of Steel", Steel in the U.S.S.R., Vol.6, 1976, pp.311-313

38. Fuwa, T., Mizoguchi, S., Harashima, K., "Fundamental Aspects of Hot Metal Treatments", Steelmaking Proceedings, Chicago, Vol.67, 1984, pp.257-268

39. Fruehan, R.J., Niedringhaus, J.C., Chan, A.H., "Thermodynamic and Kinetic Considerations in Hot Metal Treatments", Steelmaking Proceedings, Vol.67, Chicago, 1984, pp.269-285

40. Sommerville, I.D., Maeda, M., Weppler, K., "The Effect of Oxygen in Hot Metal on External Desulphurization", Steelmaking Proceedings, vol.67., 1984, pp.285-290

41. Reboul, J.P., Leclercq, F., Grasjean, J.C., Gatellier, C., "Hot Metal Pretreatment with Soda Ash and Lime Based Mixtures", Steelmaking Proceedings, Vol.67, Chicago, 1984, pp.293-300

42. Koros, P.J., Kossler, H.T., "The Effect of Oxygen and Aluminum Contents of Hot Metal on Desulphurization by Lime", Steelmaking Proceedings, Vol.67, Chicago, 1984, pp.341-346

43. Sasaki, K., Nakashima, H., Nose, M., Takasaki, Y., Okumura, H., "A Newly Developed Hot Metal Treatment Has Changed the Idea of Mass Production of Pure Steel", Steelmaking Proceedings, Vol.66, Atlanta, 1983, pp.285-292

44. Budinski, K., Engineering Materials-Properties and Selection, 2nd edition, Reston Publishing Company, Inc., Reston, Virginia, 1983

45. Identification of Textile Materials, 7th edition, The Textile Institute, Manchester, 1975

46. Morey, G.W., Properties of Glass, 2nd edition, Reinhold Publishing Corporation, 1954

47. Shand, E.B., Glass Engineering Handbook, Corning Glass Works, Corning, New York, 1955

48. McMillian, P.W., Glass-Ceramics, Academic Press, New York, 1964

49. Schott Guide to Glass, Van Nostrand Reinhold Company, Inc. 1983

50. Babcock, C., Silicate Glass Technology Methods, John Wiley and Sons Inc., New York, 1977

51. Patankar, S.V., Numerical Heat Transfer and Fluid Flow, Hemisphere Publishing Corporation, New York, 1980
52. Holman, J.P., Heat Transfer, 4th edition, McGraw Hill Book Company, New York, 1976.
53. Davenport, W.G., Peacey, J.G., The Iron Blast Furnace-Theory and Practice, Pergamon Press, New York, 1979
54. Potocic, R.F., Lewis, K.G., "Desulphurization: Sulphur Control Plus More Production", Symposium on External Desulphurization of Hot Metal, McMaster University, Hamilton, Canada, 1975, pp.2:1-2:23
57. Gueussier, A.L., Vachiery, F.V., Tranchant, J.-L., Szesesny, R., "In-Ladle Treatment using a New Cored Wire Technique", Iron and Steel Engineer, Oct. 1984, pp.35-41
58. Robison, J.W., "Ladle Treatment with Steel-Clad Metallic Calcium Wire", Scaninject III-Part II, 3rd International Conference on Refining of Iron and Steel by Powder Injection, Lulea, Sweden, June 15-17, 1983, pp.35:1-35:23
59. "Spheroidizing Treatment for Ductile Iron", Ductile Iron, Number Three of a Series, Modern Casting, June 1983, pp.32-33
60. Kurzinski, E.F., "Desulphurization of Iron-Status and Evaluation", Iron and Steel Engineer, April 1976, pp.59-71
61. Oelschlagel, D., Yamagi, K., Abe, H., "Treating Steel with Ferrokal Wire", Iron and Steel International, Dec. 1981, pp.323-330
62. Leclercq, F., Reboul, J.P., Gatellier, C., Chevallier, A., Gugliermina, P., Defour, A., "Hot Metal Desulphurization by Injection of Lime", Scaninject III-Part I, 3rd International Conference on Refining of Iron and Steel by Powder Injection, Lulea, Sweden, June 15-17, 1983, pp.28:1-28:18
63. Brazzoduro, L., Borgianni, C., Ferretti, A., "Investigation on Mg Behavior Injected as Desulphurizer in Large Pig Iron Ladles", Scaninject III-Part I, 3rd International Conference on Refining of Iron and Steel by Powder Injection, Lulea, Sweden, June 15-17, 1983, pp.27:1-27:19
64. Shestopalov, I.I., et al. "Use of Pig Iron Desulphurization Outside Blast Furnaces at Krivorzhstal' Works", Steel in the U.S.S.R., Vol.13, June 1983, pp.227-229
65. Moncrieff, R.W., Man-Made Fibres, 5th edition, John Wiley and Sons, Inc., New York, 1970